SOCIETY OF
CORE ANALYSTS

33rd International Symposium of the Society of Core Analysts, Pau, France, Aug 26-29, 2019.

Short Course

Interpretation of Pore Scale Experiments - Alternative Descriptions of Porous Media Flow by Topological Means

Ryan T. Armstrong[1] and Steffen Berg[2,3]

[1]University of New South Wales, Australia.
[2]Shell Global Solutions International B.V.
[3]Imperial College London

With key contributions from
James McClure (Virginia Tech), **Steffen Schlüter** (UFZ Potsdam), **Anna Herring** (ANU), **Christoph Arns** (UNSW)

Outline

Why

1. Motivation / necessity for and advantages of a geometric state function
   - 2-phase Darcy = phenomenological extension from 1-phase to 2-phase flow
   - example of having incomplete state variables: ideal gas equation of state

How

2. Introduction:
   - introducing Minkowski functionals
   - Hadwiger’s theorem, Gauss-Bonnet Theorem, Steiner’s formula
3. Description how we found it
   - general background: ganglion dynamics → topological changes
   - beamline data of 2013 experiment: → Hysteresis in Euler characteristic χ
   - proof: (1) Hadwiger’s theorem, (2) 220000 LBM simulations
4. Software: Avizo, FIJI (BoneJ plugin), Matlab, Python, Dragonfly/DeepRocks

What

5. Applications,
   - hysteresis model for relative permeability
   - new route to pc and relative permeability
   - Digital Rock: validation of pore scale simulation techniques
   - wettability: description of contact angle as deficit curvature

Integrated Subsurface Workflow

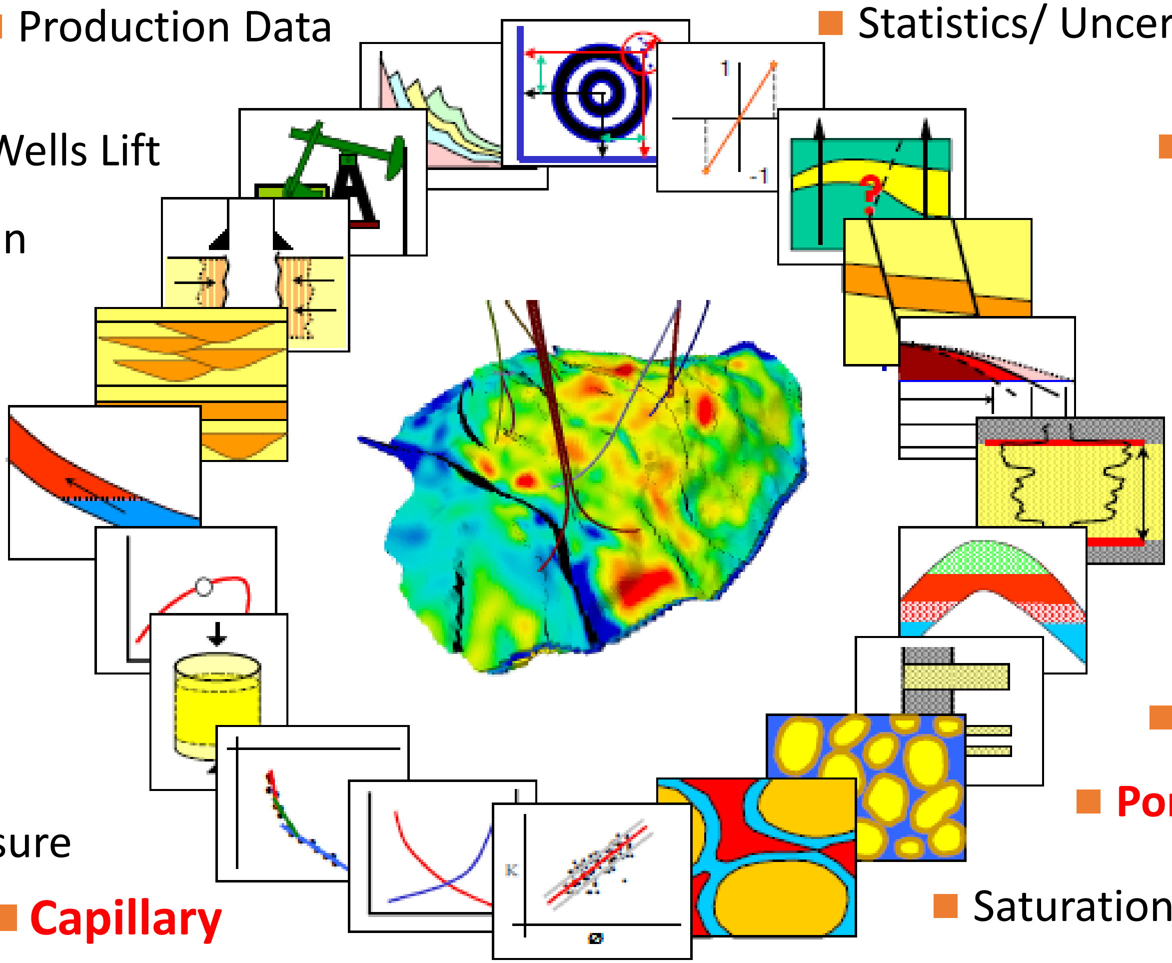

- Production Data
- Statistics/ Uncertainty handling
- Prediction between wells
- Structure
- Reservoir Area
- Gross thickness
- Fluid distribution/contacts
- Net sand
- **Porosity**
- Saturation
- **Permeability**
- **Relative permeability**
- **Capillary pressure**
- Reservoir pressure
- Compressibility
- Fluid PVT
- Aquifer
- Reservoir Connectivity
- Wells: Skin
- Wells Lift

Multiphase Flow in Porous Media at Darcy Scale

Single-Phase

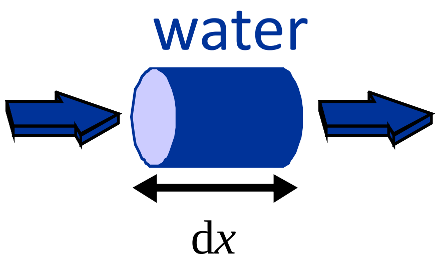

$$v_{Darcy} = -\frac{K}{\mu}\frac{dp}{dx}$$

Darcy's law

μ viscosity
P pressure
K (K_{abs}) absolute permeability

Viscous law (similar to pipe flow) can be derived from upscaling Stokes flow at pore scale by homogenization

Two-Phase

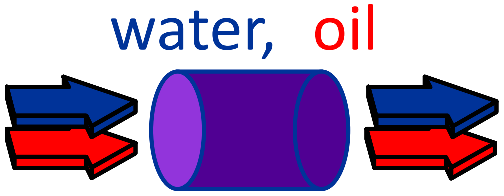

i=w,o

$$v_i = -k_{r,i}\frac{K}{\mu_i}\frac{dp_i}{dx}$$

Phenomenological extension of Darcy's law

relative permeability $k_{r,i} = k_{r,i}(S_w)$

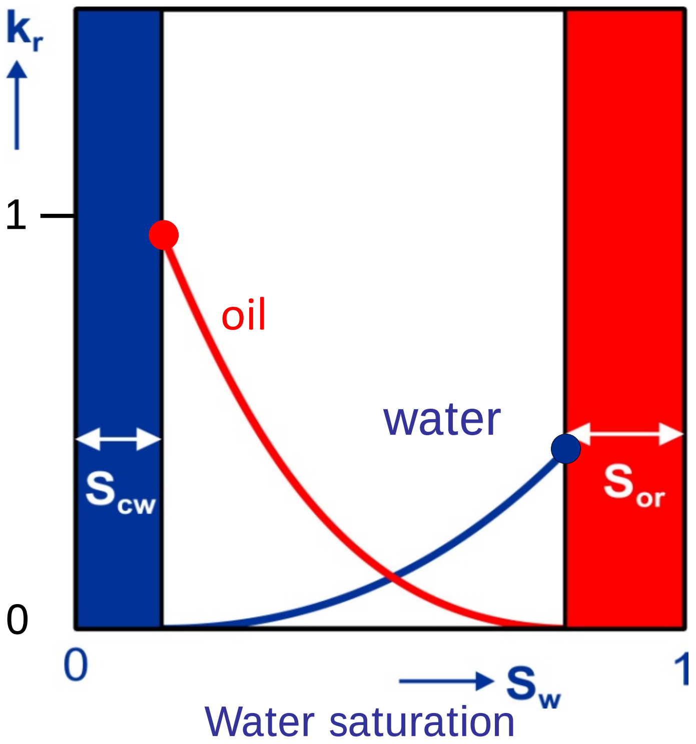

Capillary pressure $p_c = p_o - p_w$

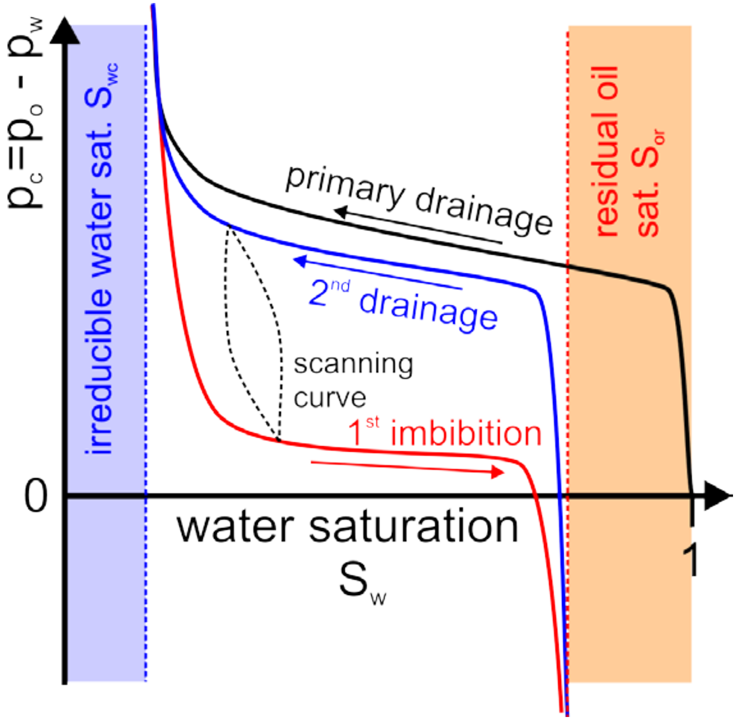

Historical Overview – Classification of the Problem

- 1930s: **flow problem**: mass & momentum balance

  (Wykoff & Botset, Muskat & Meres, Leverett)

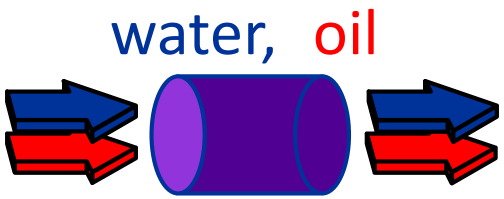

- 1970s: thermodynamics of pore scale displacements

  (Morrow, Swanson & Yuan)

Morrow 1970

$$\Delta F = -S\Delta T - \sum_{\alpha=1}^{2} \boxed{p_\alpha}\Delta \boxed{V_\alpha} + \sigma_{1,2}\Delta \boxed{A_{1,2}}$$

- 1990s: **equilibrium thermodynamics problem**:

  mass, momentum & energy balance (Hassanizadeh & Gray)

  ganglion dynamics in 2D micromodels (Avraam & Payatakes)

- 2000s: **non-equilibrium thermodynamic** problem – no global energy minimum

  TCAT (Gray & Miller)

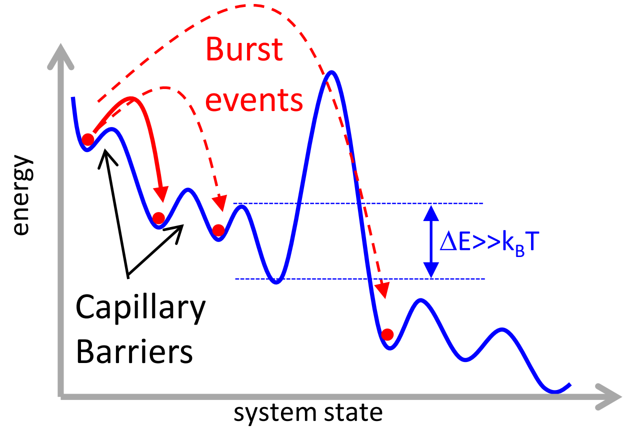

- 2010s: **non-local dynamics**, ganglion dynamics in 3D

  $S_w + A_{nw}$ does not close pc hysteresis

  Armstrong, McClure et al. 2018

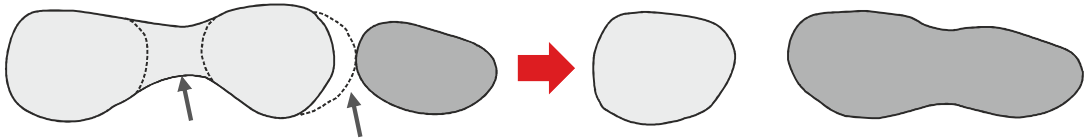

- 2018: **state variables**: S_w, A_{nw}, p_c, χ
- 2019: **wettability** (upscaled contact angle as deficit Gaussian curvature)

Unresolved Issue: Capillary Pressure - Hysteresis

Capillary pressure function of saturation only $P_{nw} - P_w = P_c = f(S_w)$

But: hysteresis

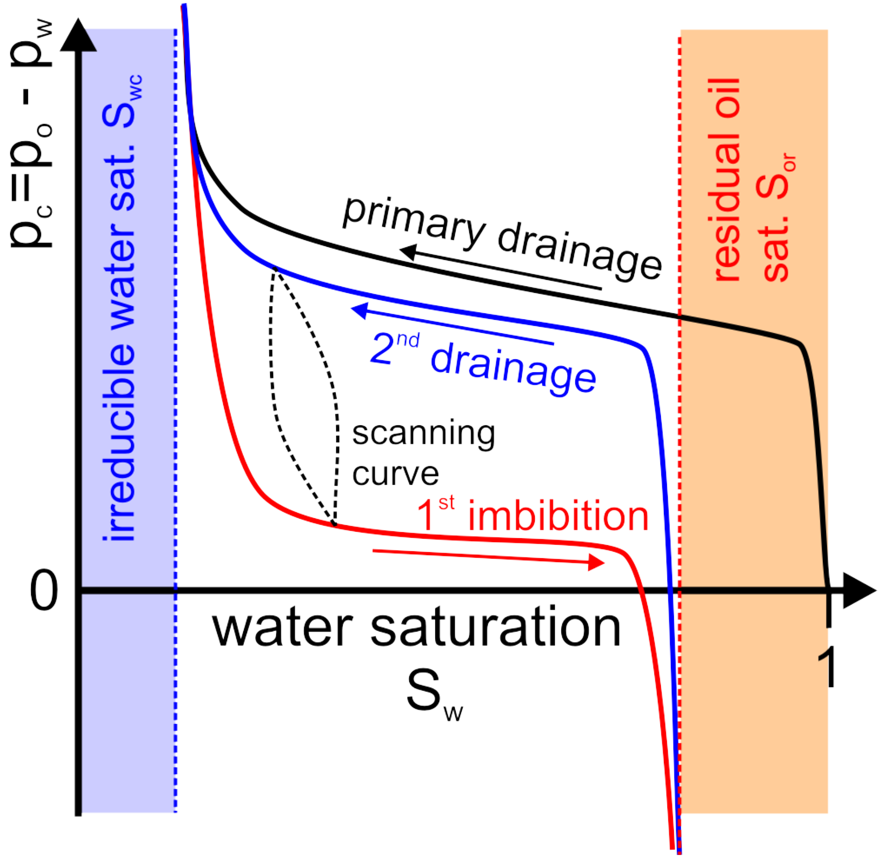

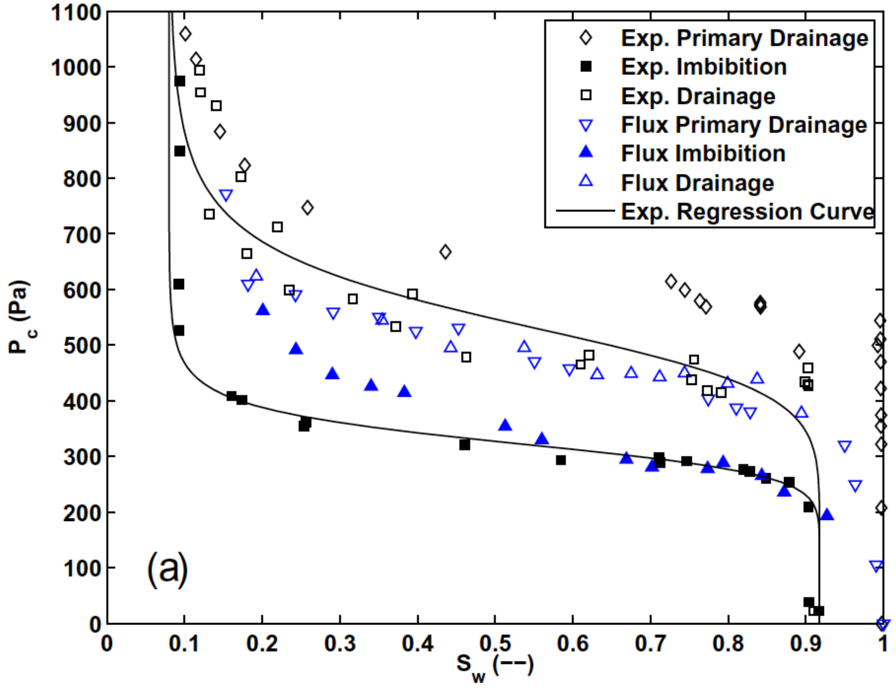

[Porter et al. 2009]

Hysteresis challenges the validity of 2-phase Darcy. But is it really hysteresis ?

What constitutive relationships properly represent multiphase flow?

Consequence of Insufficient Number of State Variables

Example: ideal gas, equation of state

$$p \cdot V = nRT$$

Imagine we did not know about Temperature …

and only do P – V experiments,

without measuring or controlling T …

Carnot cycle

- Isothermal expansion / compression
- Adiabatic expansion / compression

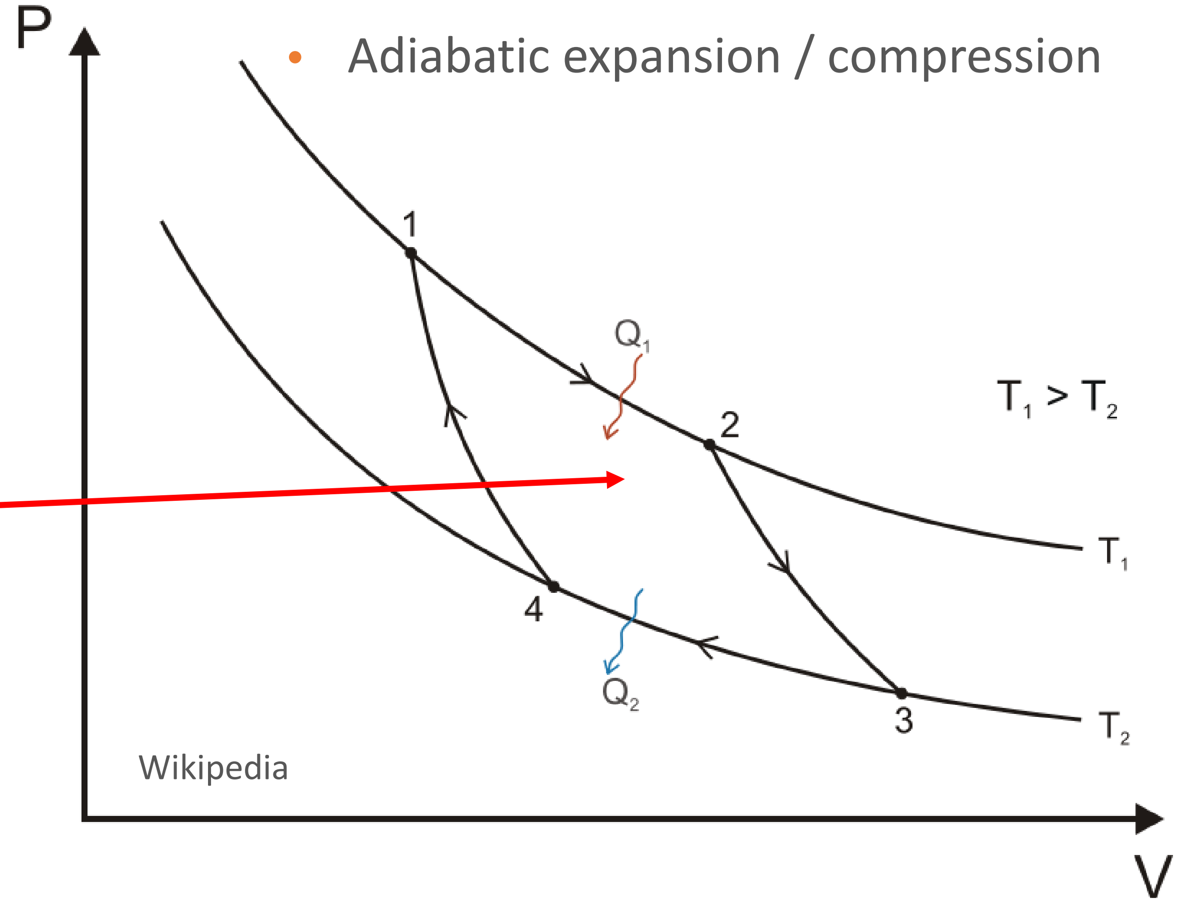

Wikipedia

Apparent

hysteresis

But with correct number of state variables, *p, V,* ***T***,

there is no hysteresis (for an ideal gas).

Saturation S_w and Interfacial Area A_{nw} are State Variables of P_c

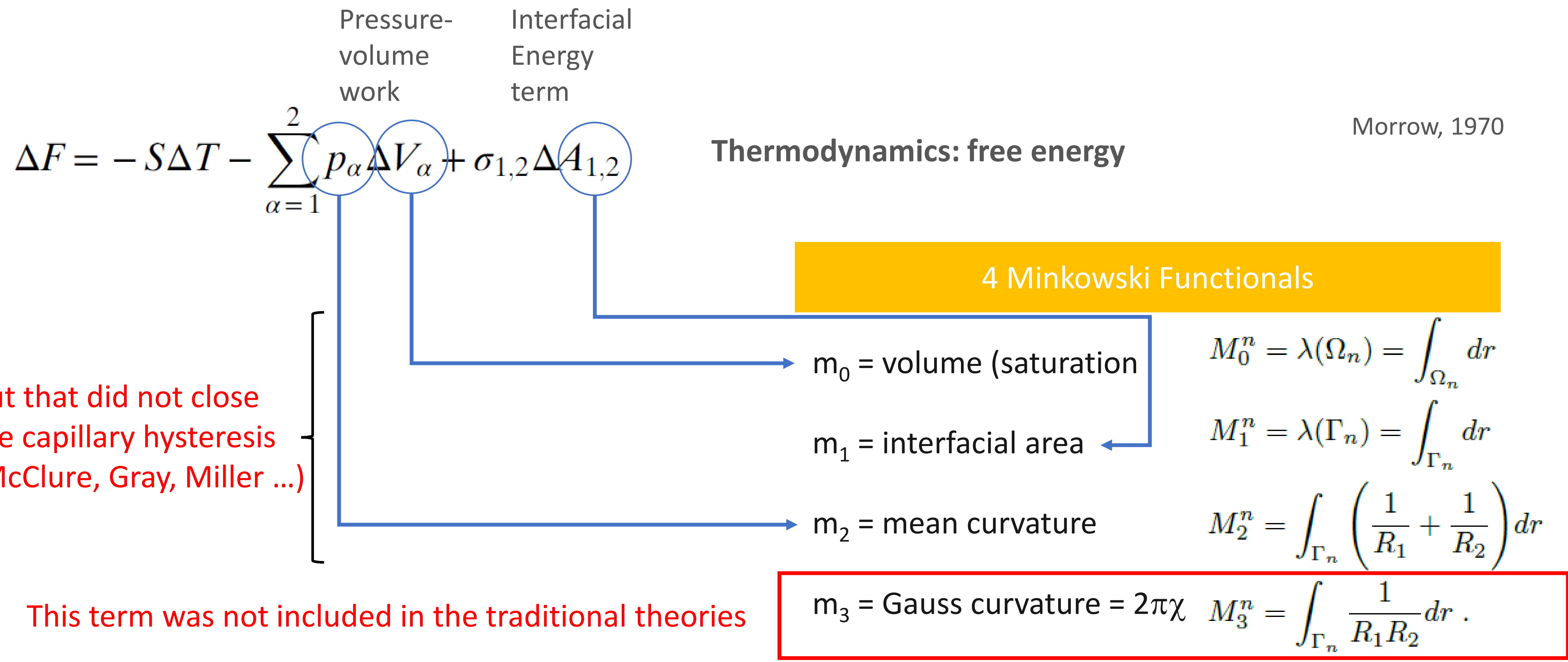

Pressure-volume work

Interfacial Energy term

$$\Delta F = -S\Delta T - \sum_{\alpha=1}^{2} p_\alpha \Delta V_\alpha + \sigma_{1,2}\Delta A_{1,2}$$

Thermodynamics: free energy

Morrow, 1970

4 Minkowski Functionals

m_0 = volume (saturation $$M_0^n = \lambda(\Omega_n) = \int_{\Omega_n} dr$$

m_1 = interfacial area $$M_1^n = \lambda(\Gamma_n) = \int_{\Gamma_n} dr$$

m_2 = mean curvature $$M_2^n = \int_{\Gamma_n} \left(\frac{1}{R_1} + \frac{1}{R_2}\right) dr$$

m_3 = Gauss curvature = $2\pi\chi$ $$M_3^n = \int_{\Gamma_n} \frac{1}{R_1 R_2} dr \, .$$

But that did not close the capillary hysteresis (McClure, Gray, Miller …)

This term was not included in the traditional theories

The Source of Capillary Pressure Hysteresis

Darcy Scale

Pore Scale

Macroscopic Darcy-scale "saturation functions"

=

f(pore scale fluid distribution)

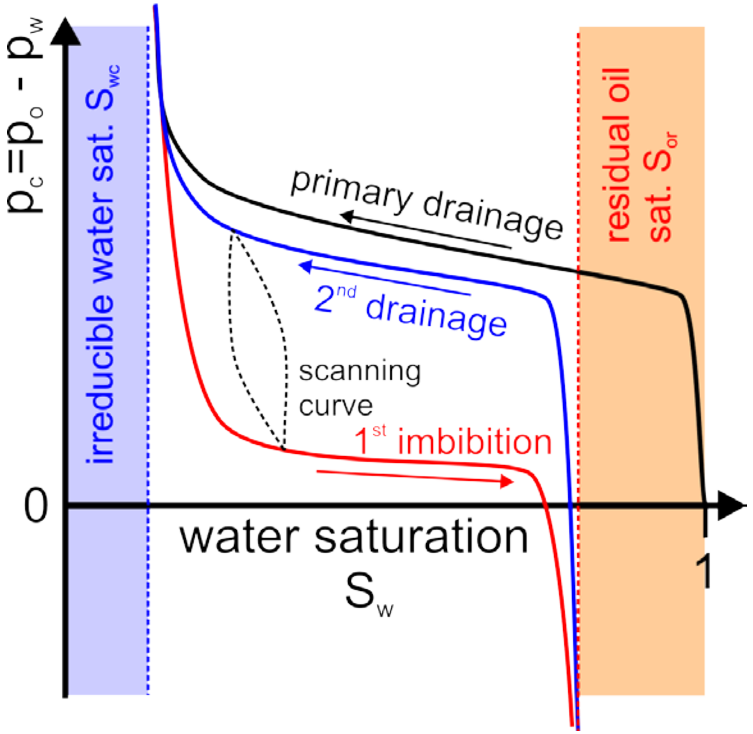

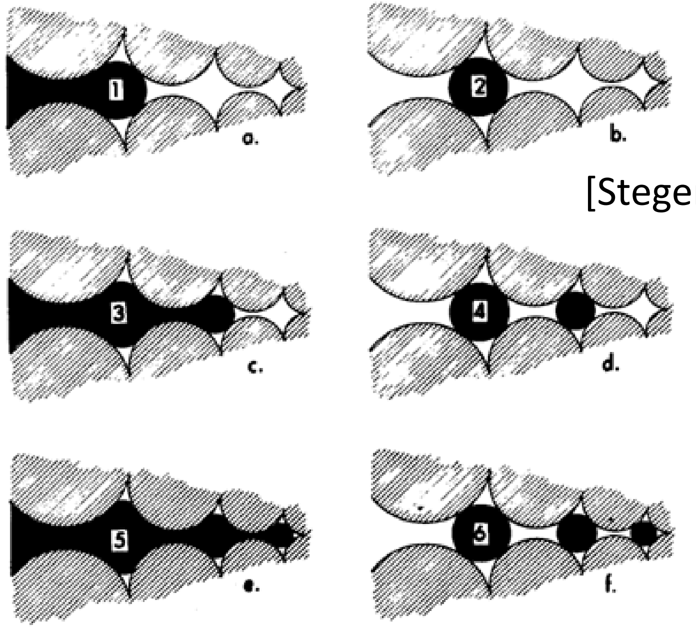

[Stegemeier 1977]

= geometrical shape in 3D

The Source of Capillary Pressure Hysteresis

Darcy Scale

Pore Scale

Macroscopic Darcy-scale “saturation functions” **=** **f(pore scale fluid distribution)**

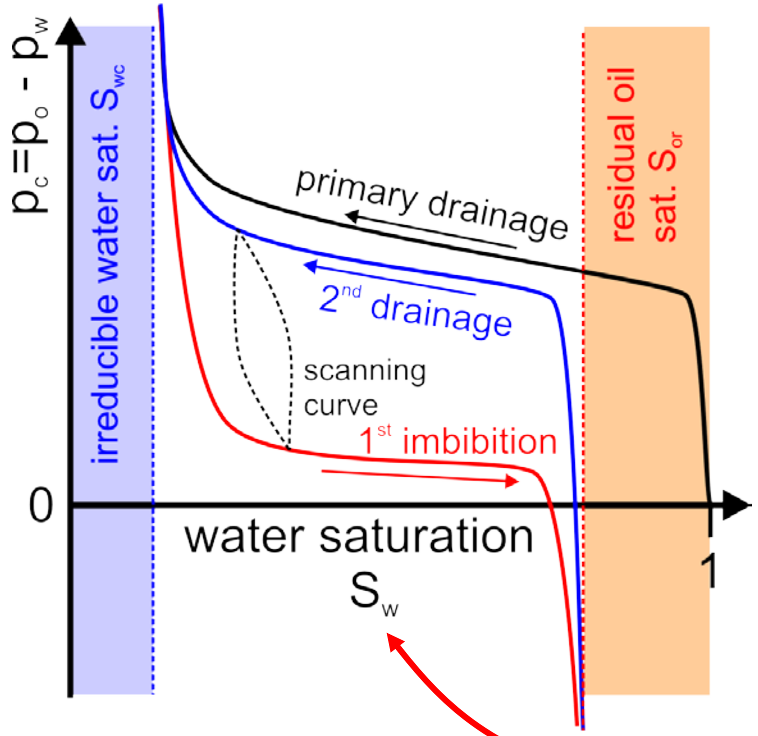

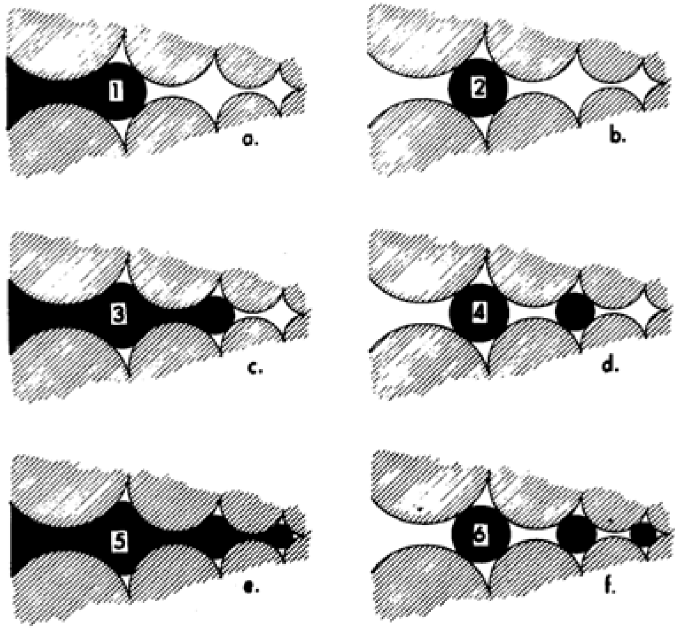

= geometrical shape in 3D

Hadwiger’s Theorem:
Uniquely parameterized by 4 Minkowski Functionals

state
variables

The Minkowski Functionals

Named after **Hermann Minkowski**, Mathematician (1864-1909)

→ Apply to Multiphase Flow

Herring et al. Advances in Water Resources 62, 47-58, 2013.

McClure et al. Phys. Rev. Fluids, 2018

Integral Geometry

Hadwiger's theorem: unique characterization of 3D objects by 4 Minkowski functionals

m_0 = volume (saturation

$$M_0^n = \lambda(\Omega_n) = \int_{\Omega_n} dr$$

m_1 = interfacial area

$$M_1^n = \lambda(\Gamma_n) = \int_{\Gamma_n} dr$$

m_2 = mean curvature (cap. pressure)

$$M_2^n = \int_{\Gamma_n} \left(\frac{1}{R_1} + \frac{1}{R_2} \right) dr$$

m_3 = integral curvature = $2\pi\chi$

$$M_3^n = \int_{\Gamma_n} \frac{1}{R_1 R_2} dr \; .$$

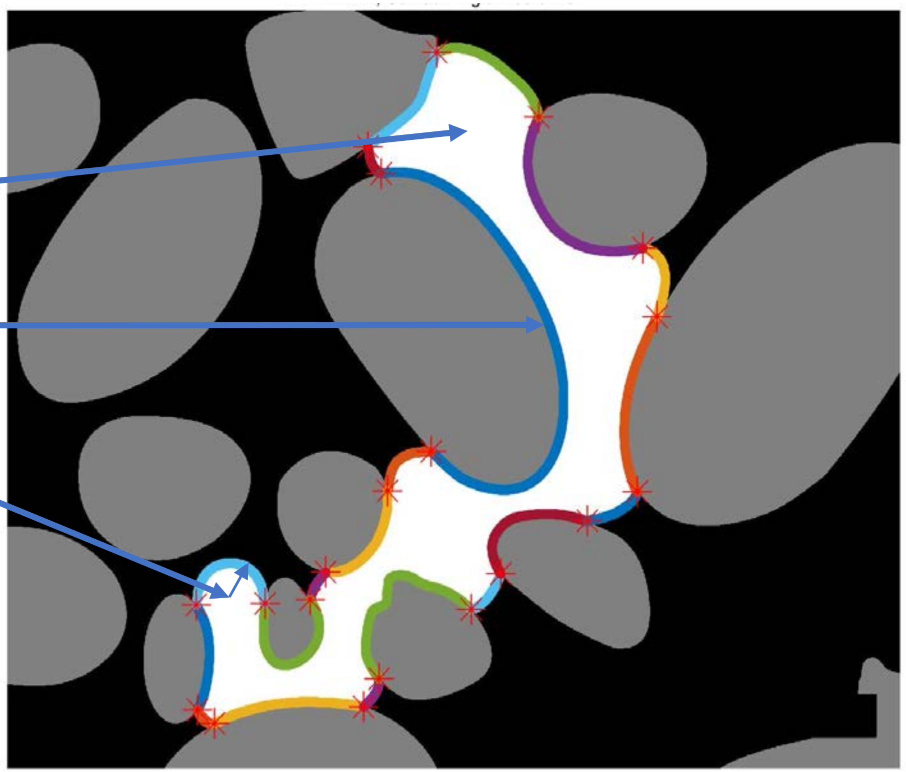

Klaus R. Mecke, Dietrich Stoyan, Statistical Physics and Spatial Statistics. The Art of Analyzing and Modeling Spatial Structures and Pattern Formation, Lecture Notes in Physics, Springer, 2000.

C. H. Arns, M. A. Knackstedt, K. Mecke, 3D Structural Analysis: Sensitivity of Minkowski Functionals. Journal of Microscopy 240, 181-196, 2010.

H.J. Vogel, U. Weller, S. Schlüter, Quantification of Soil Structure Based on Minkowski Functions, Computers & Geosciences 36, 126-1251, 2010.

The Euler Characteristic

Named after **Leonhard Euler**, German Mathematician (1707-1783)

$\frac{1}{r_1}+\frac{1}{r_2}$ mean curvature

$\frac{1}{r_1}\cdot\frac{1}{r_2}$ Gaussian curvature

$$M_3(X) = \int_{\delta X} \underbrace{[1/(r_1 r_2)]}_{\text{Gaussian curvature}} ds = 2\pi\chi(\delta X) = 4\pi\chi(X)$$

- Euler Characteristic measures the **bulk connectivity** of an object

X = Objects – Loops + Voids

[Herring et al. 2012]

Or a collection of objects:

OIL

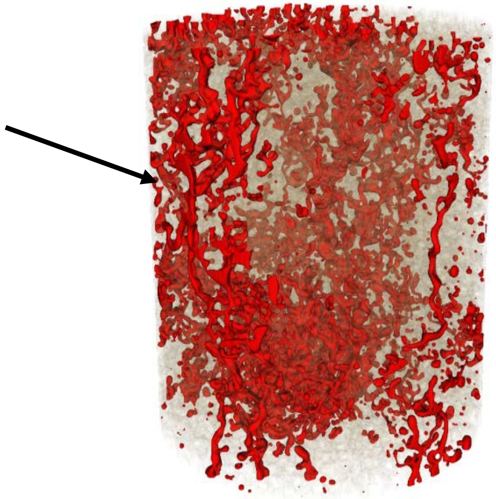

X (OIL) = - 40

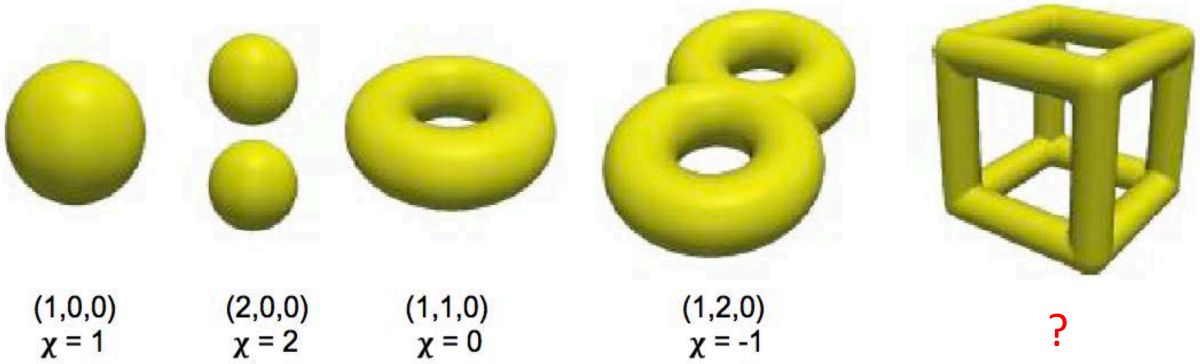

?

… a cube has 6 faces

Leonhard Euler and the Seven Bridges of Königsberg

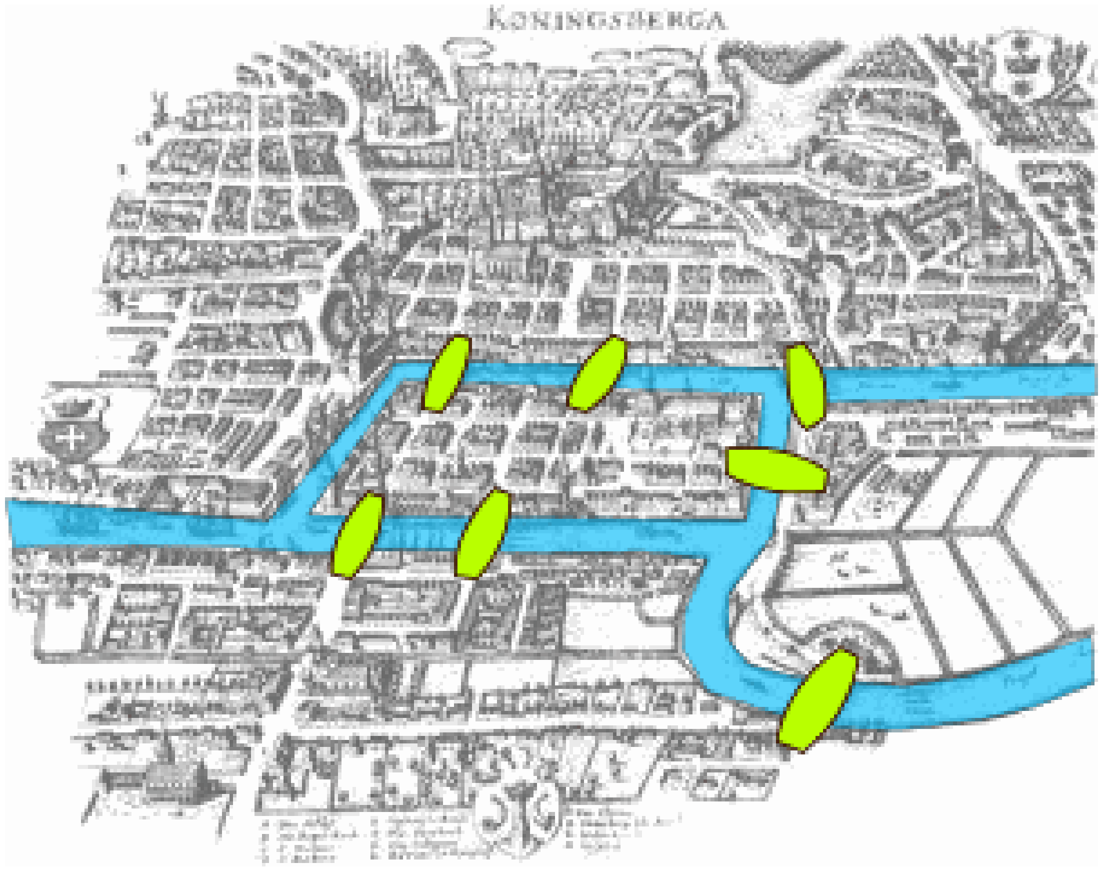

2 islands
separated by a river
7 bridges

Walk to cross each bridge only once ?

L. Euler: not possible + proof

The city of Königsberg in Prussia (now Kaliningrad, Russia) was set on both sides of the Pregel River, and included two large islands - Kneiphof and Lomse - which were connected to each other, or to the two mainland portions of the city, by seven bridges. The problem was to devise a walk through the city that would cross each of those bridges once and only once (Source: Wikipedia)
https://en.wikipedia.org/wiki/Seven_Bridges_of_K%C3%B6nigsberg

The Euler Characteristic

$$M_3(X) = \int_{\delta X} [1/(r_1 r_2)] ds = 2\pi\chi(\delta X) = 4\pi\chi(X)$$

- Euler Characteristic measures the **bulk connectivity** of an object

χ *= Objects – Loops + Voids*

[Herring et al. 2012]

Or a collection of objects:

OIL

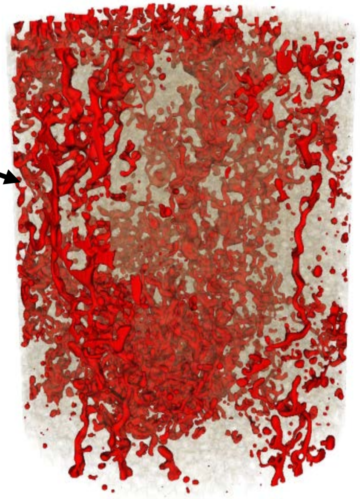

X (OIL) = - 40

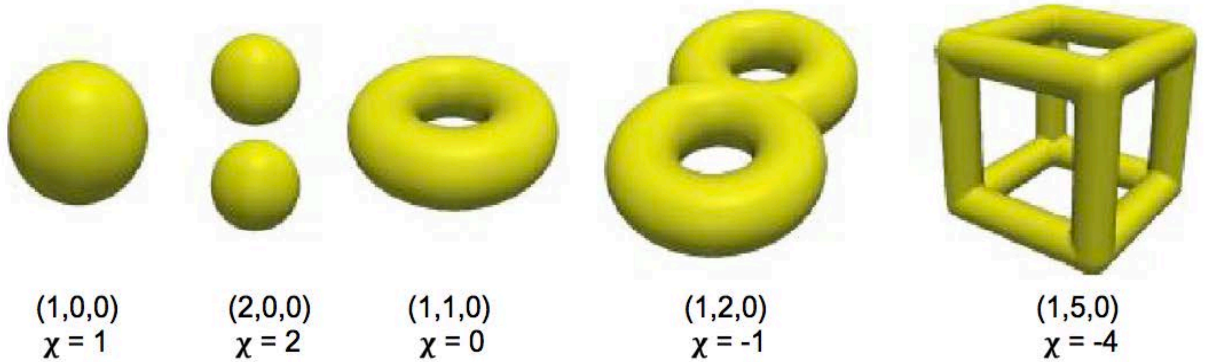

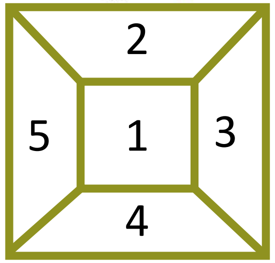

(1) Hadwiger's Theorem

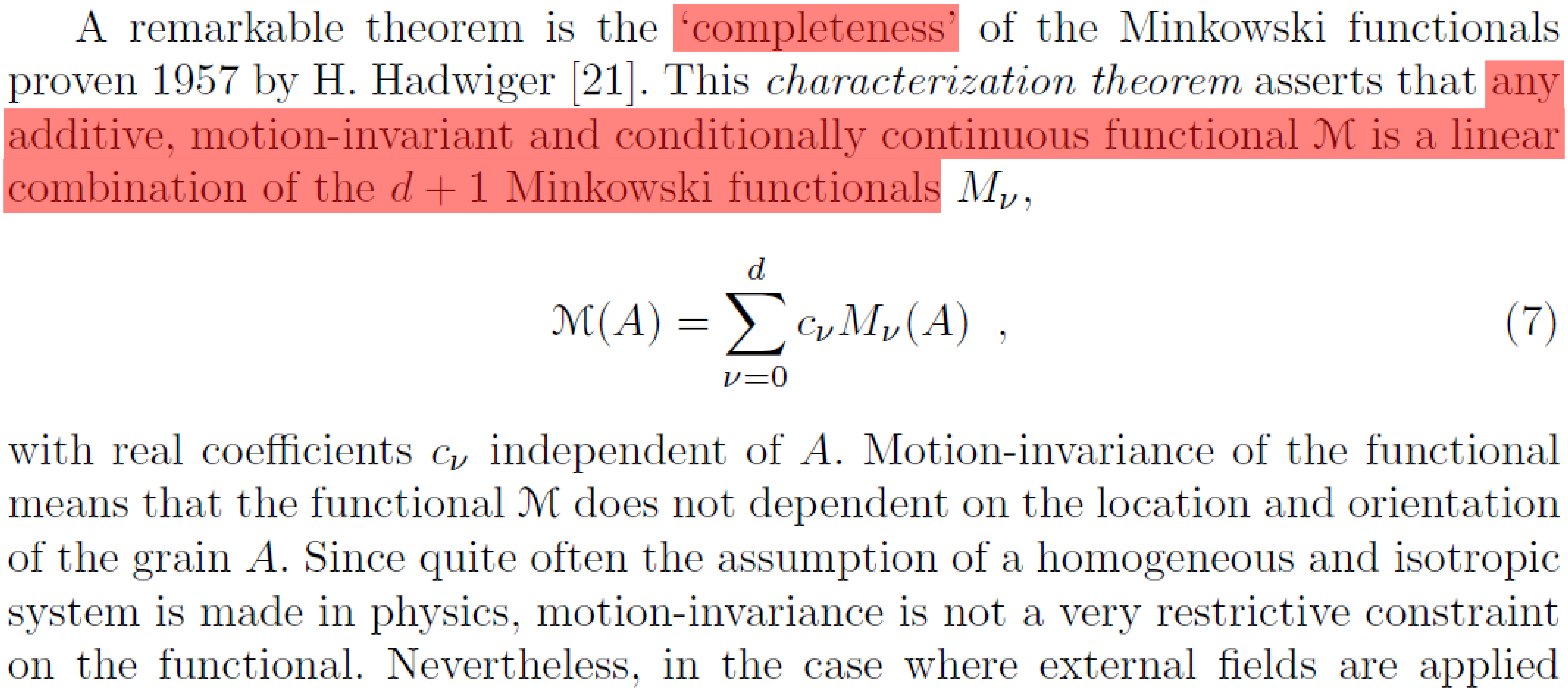

A remarkable theorem is the 'completeness' of the Minkowski functionals proven 1957 by H. Hadwiger [21]. This *characterization theorem* asserts that any additive, motion-invariant and conditionally continuous functional $\mathcal{M}$ is a linear combination of the $d+1$ Minkowski functionals M_ν,

$$\mathcal{M}(A) = \sum_{\nu=0}^{d} c_\nu M_\nu(A) \ , \tag{7}$$

with real coefficients c_ν independent of A. Motion-invariance of the functional means that the functional $\mathcal{M}$ does not dependent on the location and orientation of the grain A. Since quite often the assumption of a homogeneous and isotropic system is made in physics, motion-invariance is not a very restrictive constraint on the functional. Nevertheless, in the case where external fields are applied

K. Mecke, Additivity, Convexity, and Beyond: Applications of Minkowski Functionals in Statistical Physics
Statistical Physics and Spatial Statistics (Springer), pp 111-184, 2000.

(2) Gauss-Bonnet Theorem

Explains the relationship between Gaussian curvature and topology.

Gaussian curvature

$$k_f = \left(\frac{1}{r_1} \cdot \frac{1}{r_2}\right)$$

$$\int_S [1/(r_1 r_2)]ds + \int_B k_g dl = 2\pi\chi(S)$$

$$p_c(S_w) = \gamma \cdot \underbrace{\left(\frac{1}{r_1} + \frac{1}{r_2}\right)}_{\text{Mean curvature}}$$

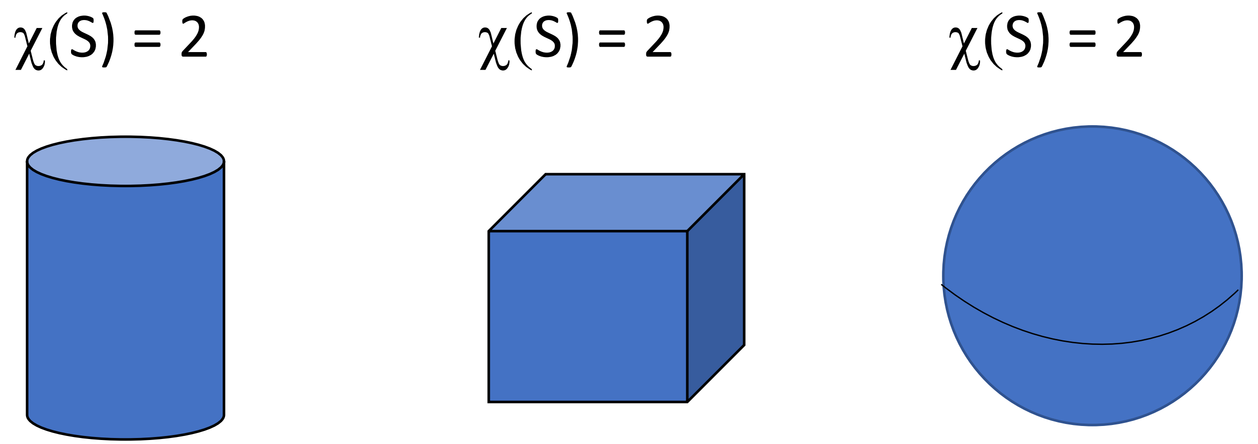

The curvature is either on the surface (Gaussian Curvature) or at the **edges** (**Geodesic Curvature**)

(3) Steiner's Formula

Provides a means to identify relationships between the Minkowski functionals

Volume

↓

$$\lambda(X \oplus \partial r) - \lambda(X) = \sum_{i=1}^{3} a_i M_i r^i$$

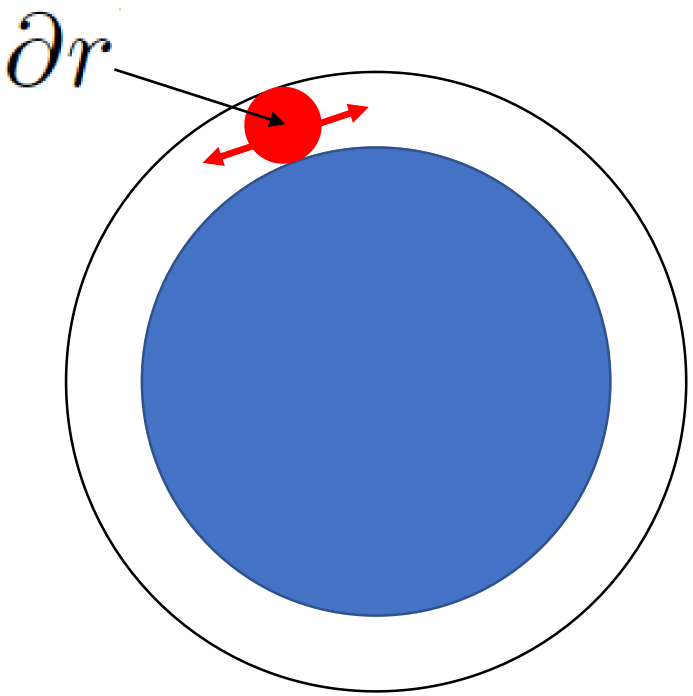

Explains how the volume (dependent) of an object changes depending on the objects morphology (independent)

Example: sphere …

$$V(\Omega_i \oplus \delta\zeta) - V(\Omega_i) = \frac{4}{3}\pi(r + \delta r)^2 - \frac{4}{3}\pi(r)^2 = A_i \delta r + H_i(\delta r)^2 + \frac{4}{3}\pi\chi_i(\delta r)^3$$

↑

Mean width $H_i = \int_{\Gamma_i} \frac{\kappa_1 + \kappa_2}{2} dS$

$$\begin{aligned} A_i &= 4\pi r^2 \\ H_i &= 4\pi r \\ \chi_i &= 1 \end{aligned}$$

Background: Cluster Dynamics in SCAL Experiments

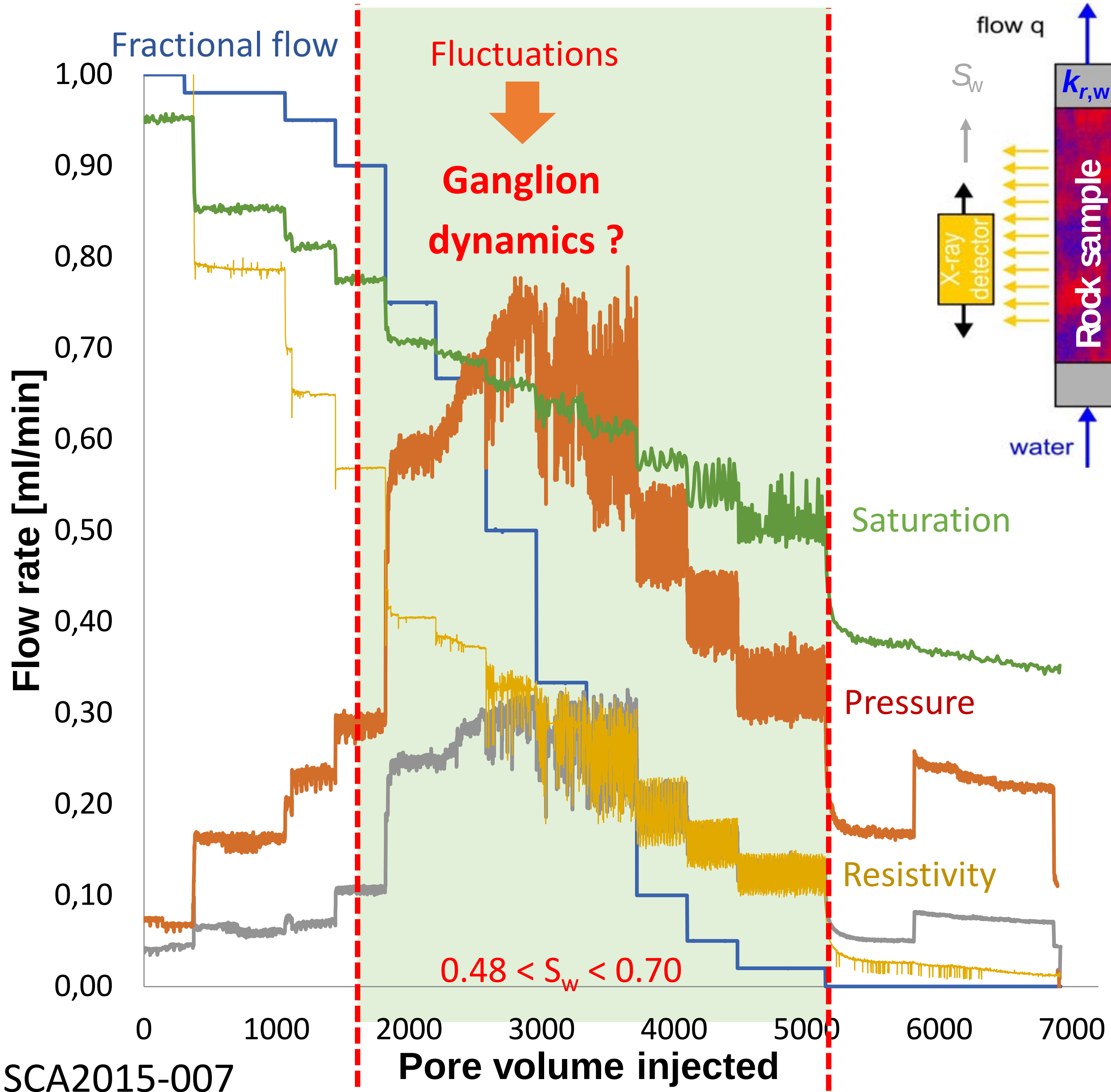

SCA2015-007

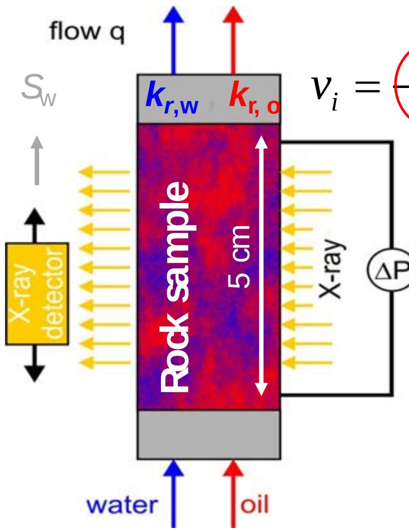

$$v_i = -k_{r,i} \frac{K}{\mu_i} \frac{dp_i}{dx}$$

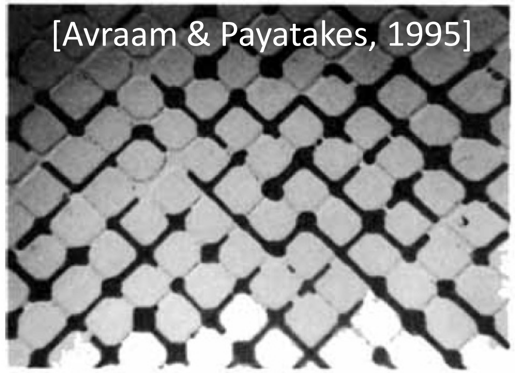

[Avraam & Payatakes, 1995]

ganglion dynamics

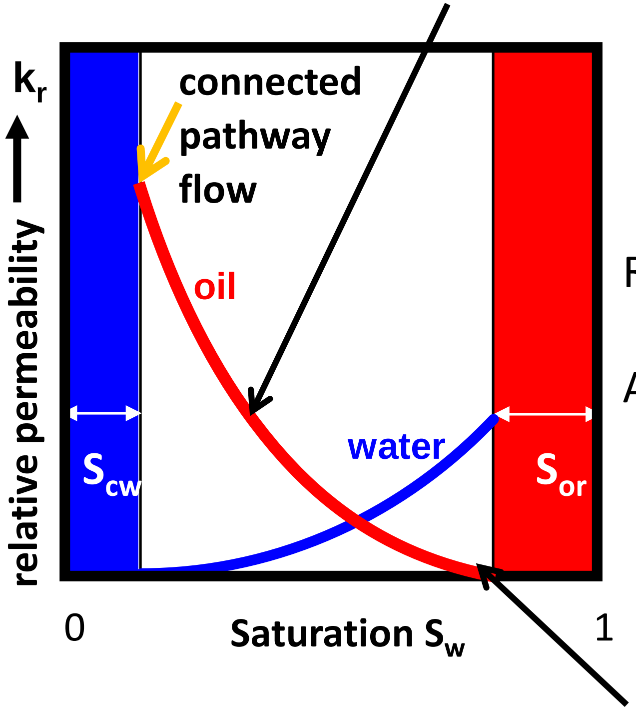

Imaged by fast μCT

Rücker et al. GRL, 2015

GRL, 2019

Armstrong et al. WRR 2018

Cluster Dynamics Introduces Topological Changes

Strongly water-wet

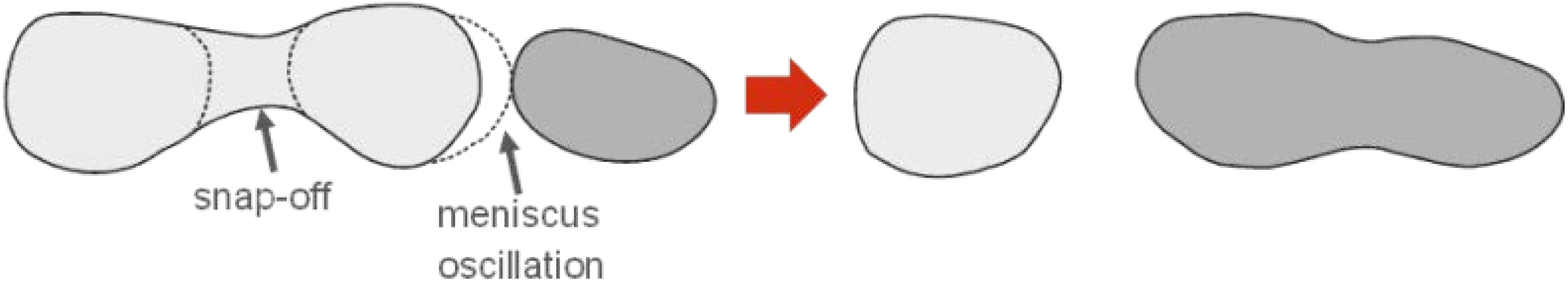

Introduces Topological Changes

Rücker et al. GRL 2015

Cluster Dynamics Introduces Topological Changes

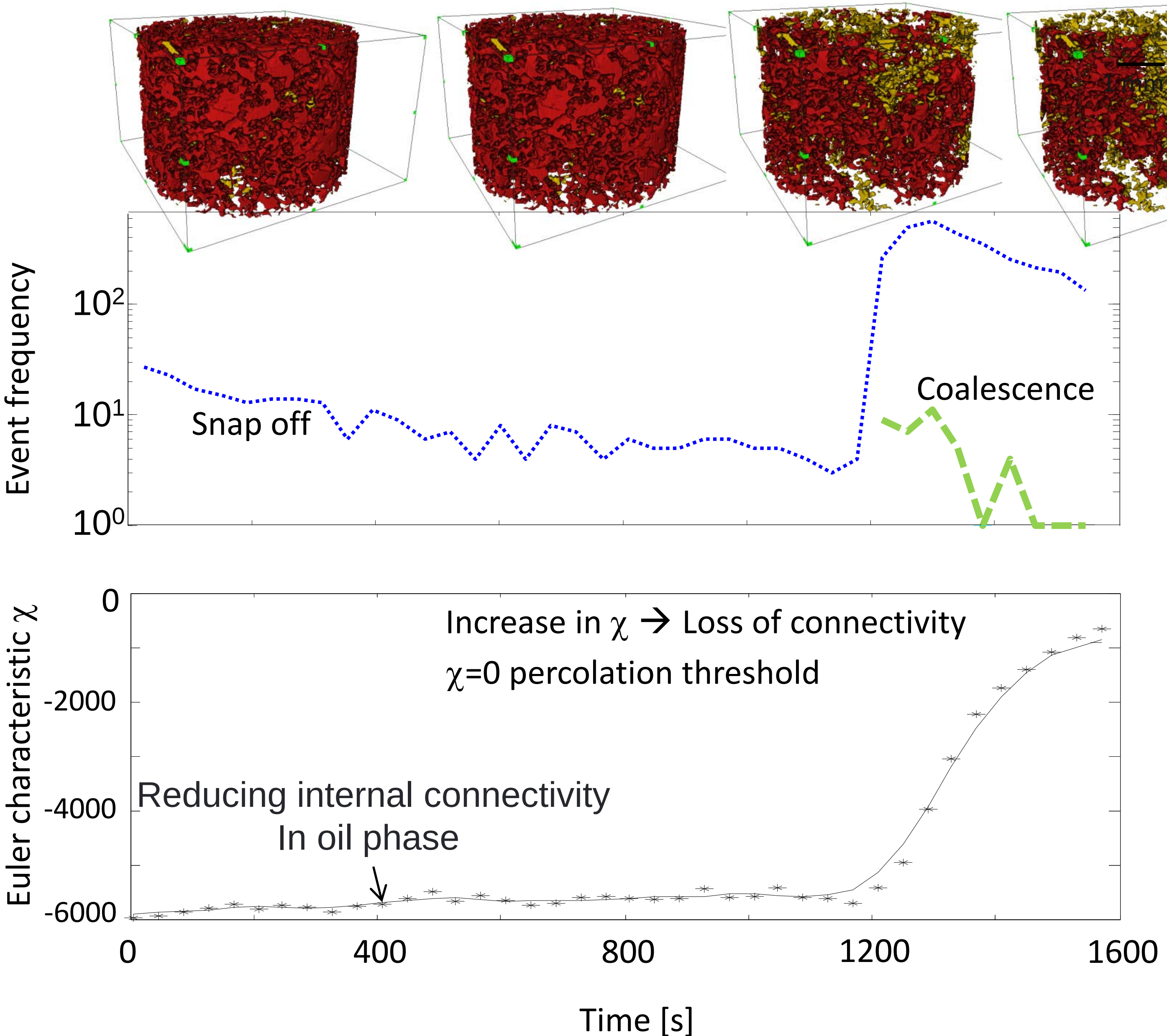

Rücker et al. GRL, 2015

$$\chi = Objects - Loops + Voids$$

Snap-off
→ disconnection
→ #objects increases
→ χ increases

Coalescence
→ connection
→ #objects decreases
→ χ decreases

Here: #snap-off > #coalescence
→ net χ increase

Schlüter et al. WRR, 2016

The Discovery of the 4th State Variable

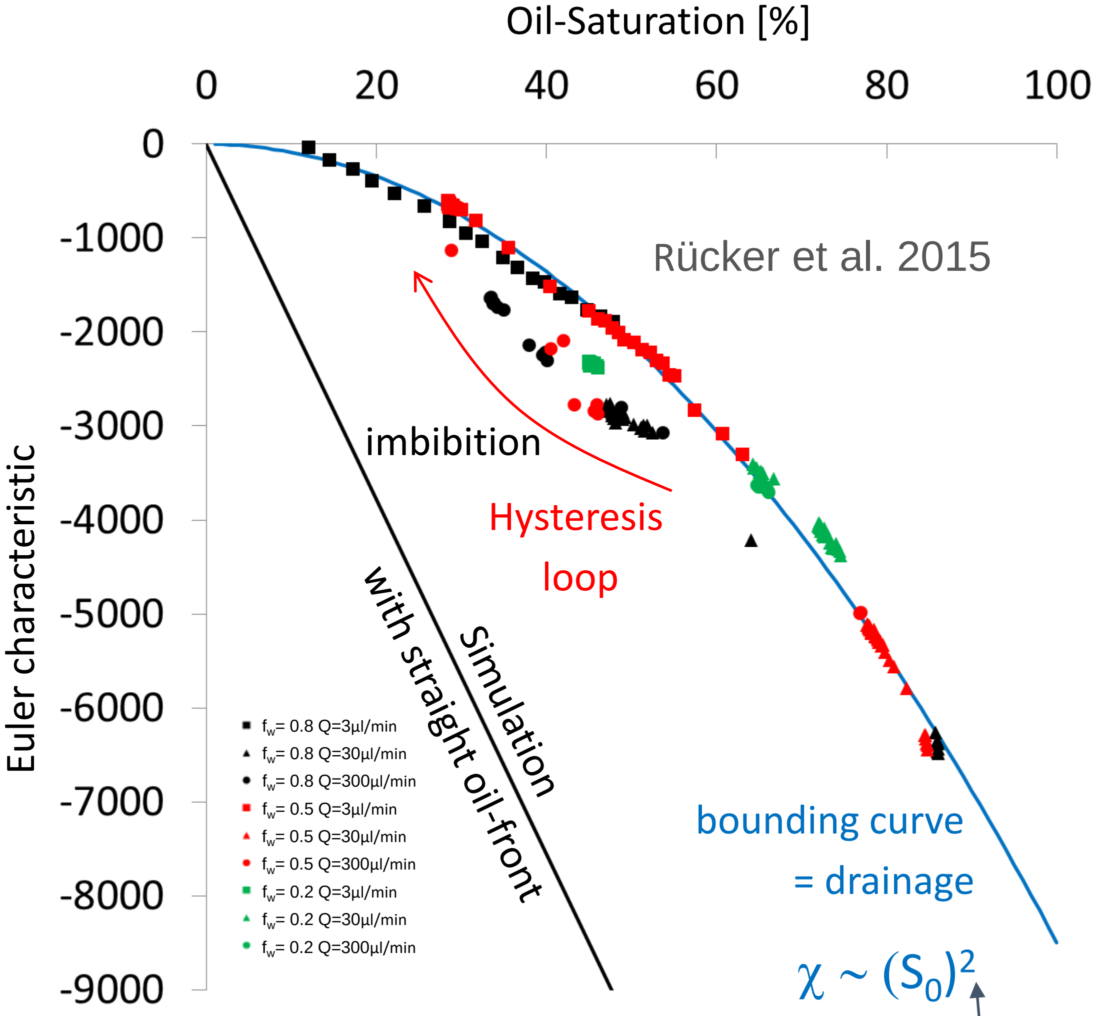

$\chi \sim (S_0)^2$

Exponent depends on rock type

Drainage =
maintaining connectivity
(avoid forming loops)

Imbibition =
Snap-off → formation of
clusters and loops

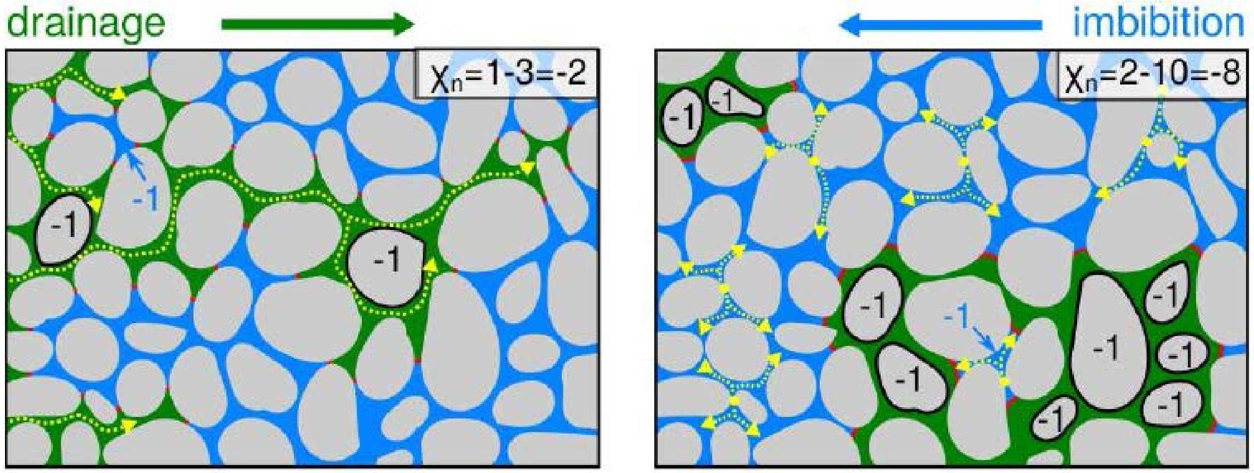

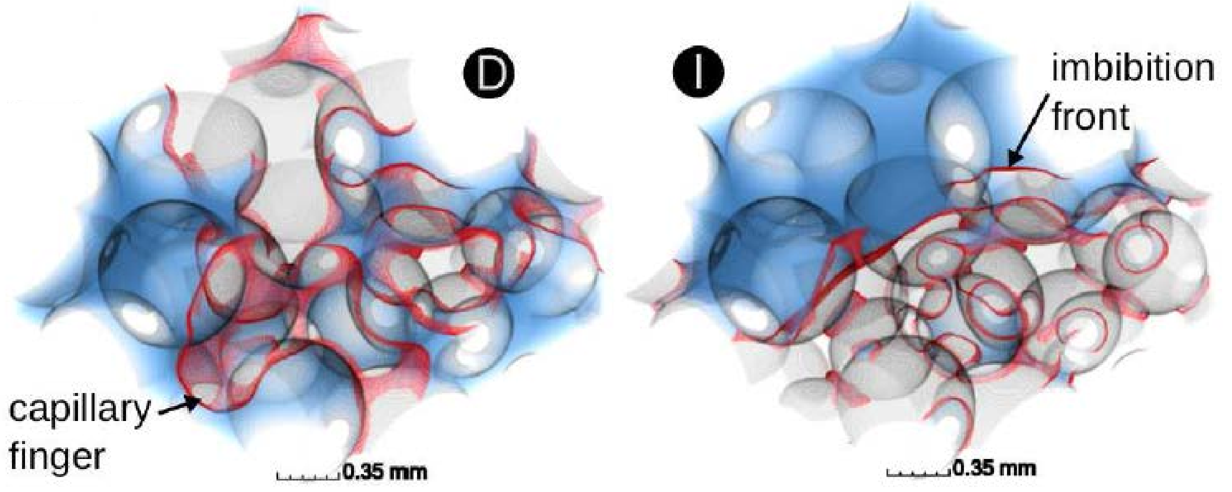

Proof by Direct Numerical Simulation

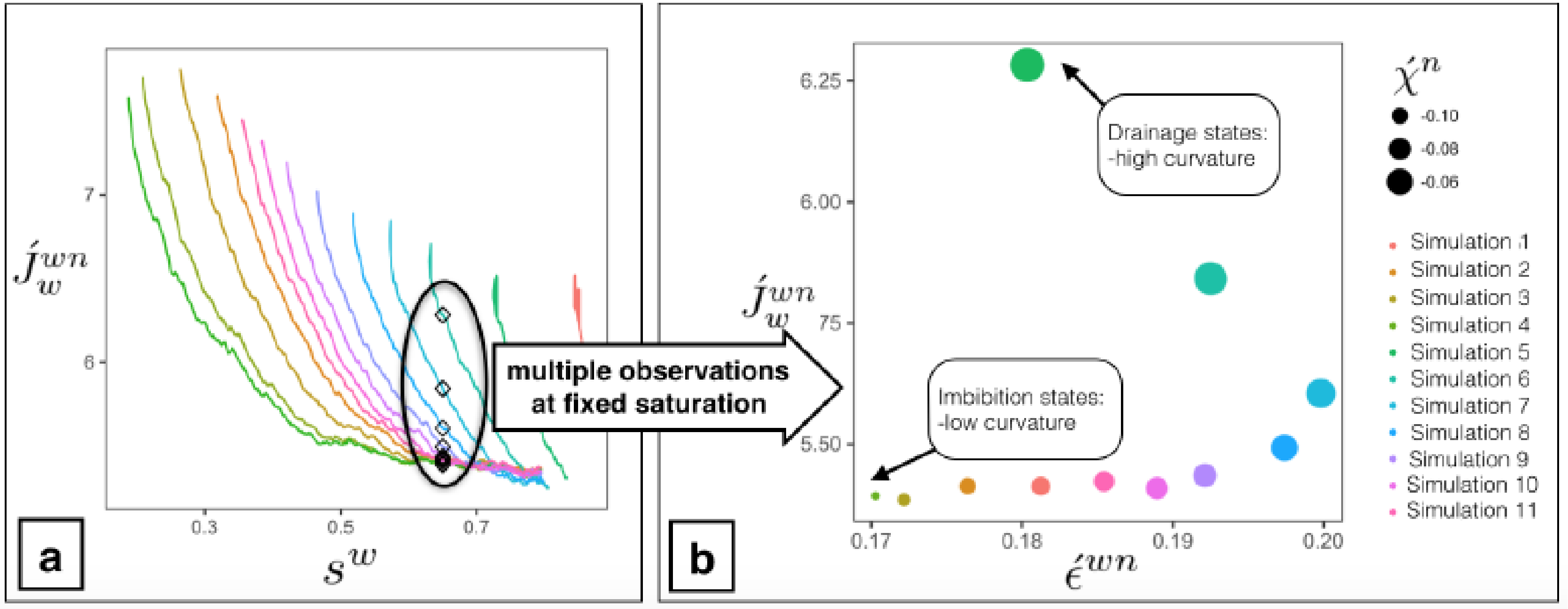

FIG. 6. Traditional models assume that the macroscale capillary pressure is a function only of the saturation of the wetting fluid. Two-fluid displacement simulations within a sand pack show that: (a) At fixed saturation, s^w, the relative mean curvature $\acute{J}_w^{wn}$ can attain many possible values depending on the system history; (b) $\acute{J}_w^{wn}(s^w, \acute{\epsilon}^{wn})$ is non-unique for $s^w = 0.65$.

McClure et al. Phys. Rev. Fluids, 2018

Media	ϵ	D(mm)	Size (voxels)	Sim.	Config.
Castlegate	0.205	0.111	512 × 512 × 512	A,D	23,123
Estaillades	0.111	0.124	834 × 834 × 556	A,B,D	23,599
Gildehauser	0.188	0.133	852 × 852 × 569	A,B,D	38,788
Robuglass	0.345	0.173	988 × 988 × 598	A,B,D	49,515
Sand pack	0.376	0.368	512 × 512 × 512	A,C,D	64,650
Sphere pack	0.369	1.00	900 × 900 × 900	A,C,D	59,341

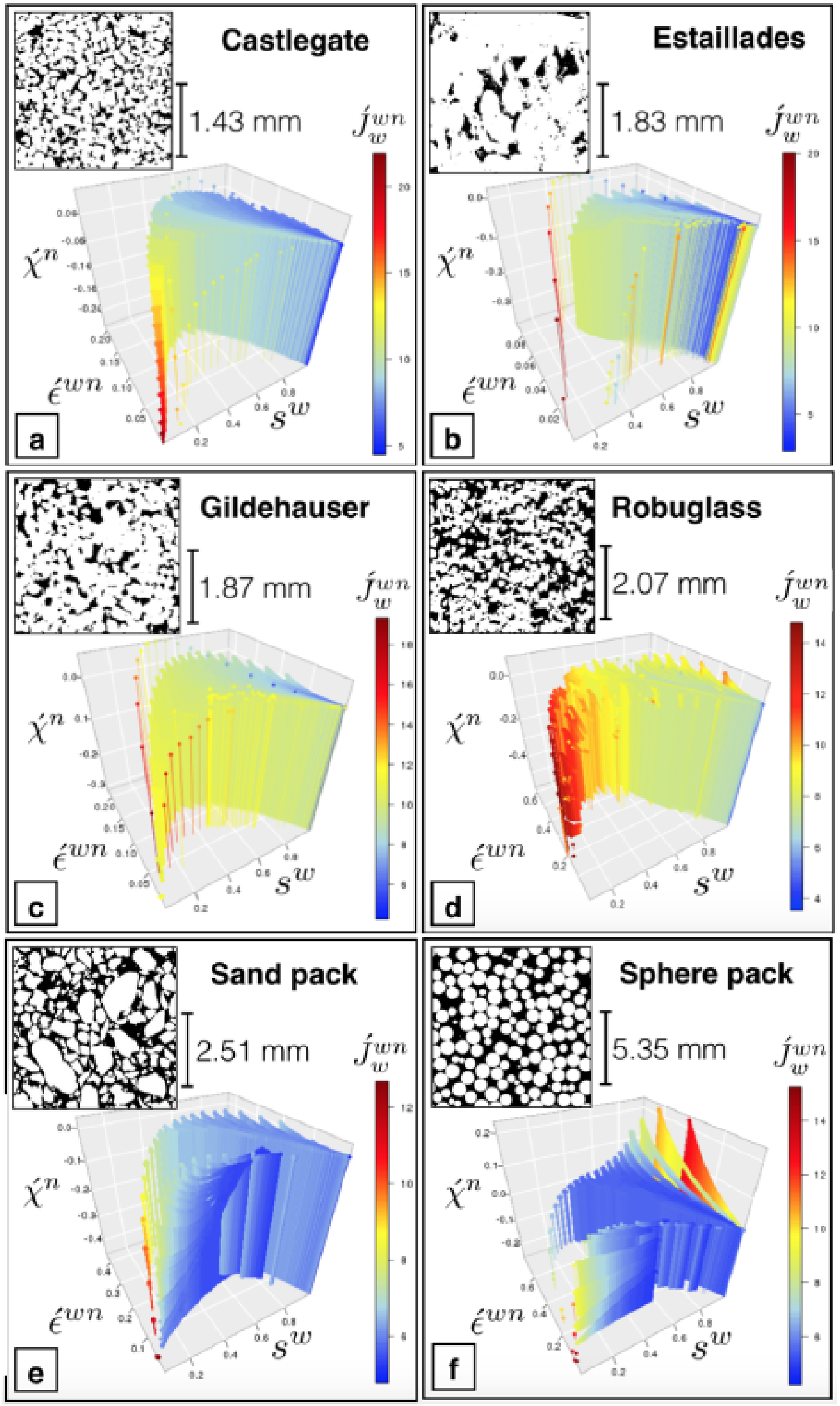

Proof by Direct Numerical Simulation

McClure et al. Phys. Rev. Fluids, 2018

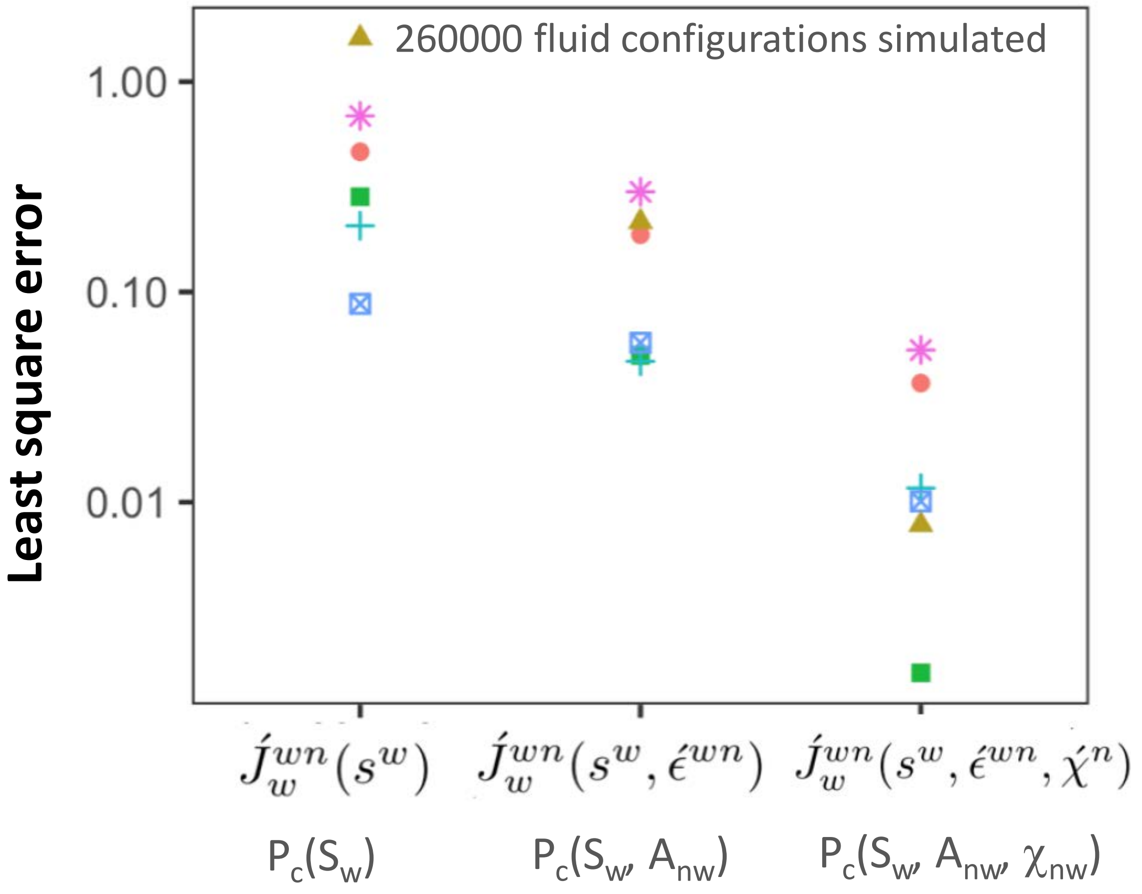

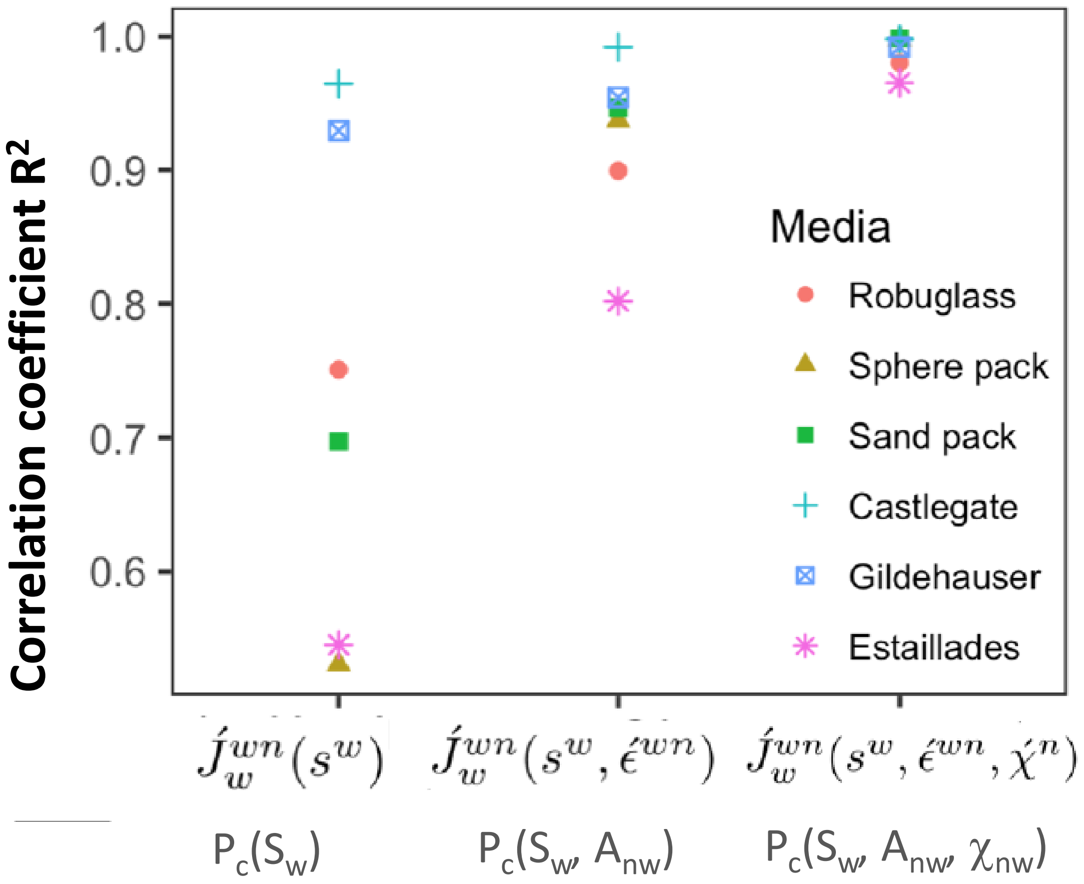

Saturation and Saturation + Interfacial Area are not sufficient to fully parameterize hysteresis (error > 10%)
→ Saturation + Interfacial Area + Euler Characteristic: error < 10% → full set of state variables

Upscaling from Pore to the Darcy Scale

“Pore scale”

Single pores
continuum oil & water phases
Single interfaces

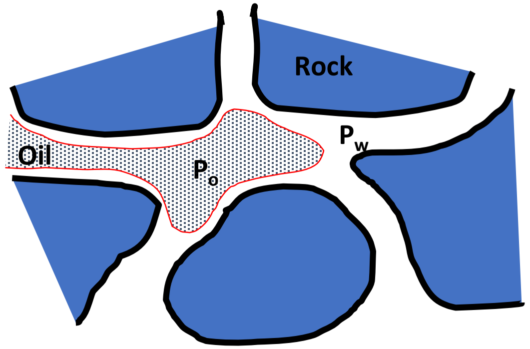

“Cluster scale”

Non-wetting phase clusters,
Cooperative dynamics

Coalescence & breakup
→ **Changing topology**

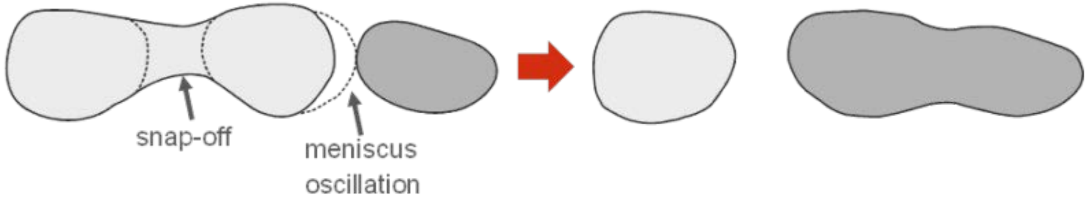

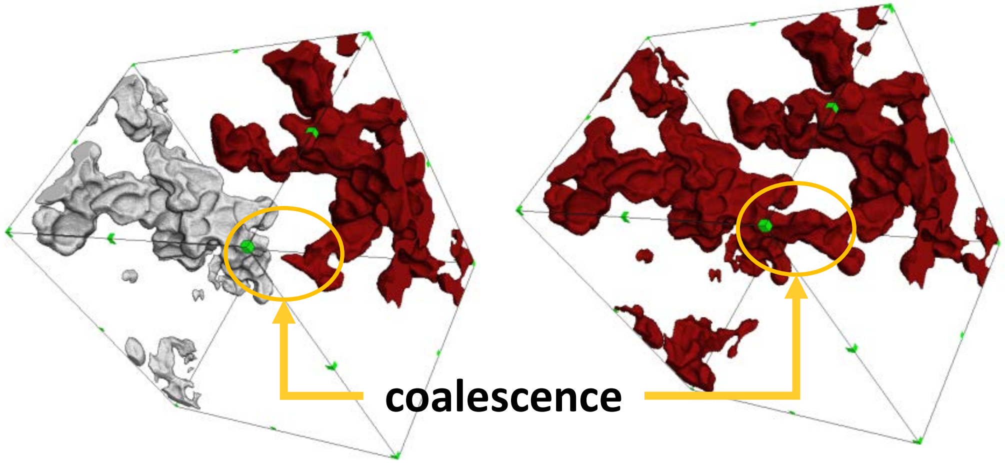

coalescence

Multiphase REV ?

“Darcy scale”

Continuum mechanics:
porosity, permeability, saturation
phenomenological description

$$v_i = -k_{r,i} \frac{K}{\mu_i} \frac{dp_i}{dx}$$

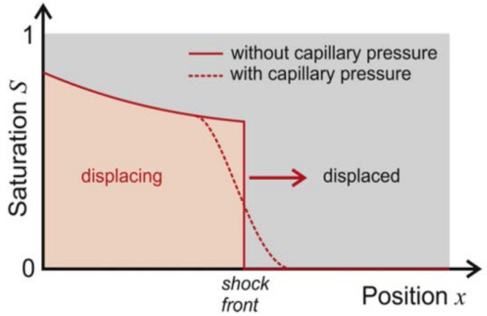

Capillary

Viscous

State variables:
Minkowski functionals

µm
mm
cm
m

How to Compute - Software Packages

0. Image processing
1. Avizo
2. ImageJ and FIJI: BoneJ plugin
3. Python – scikit-image (currently only 2D)
4. Matlab
5. Quantim (https://www.ufz.de/export/data/2/94413_quantim4_ref_manual.pdf)
6. Boundary and connectivity issues
7. Dragonfly/DeepRocks – compute χ on network

Image Processing

μCT image

segmentation

Segmented

select phase

Oil Phase

object analysis

Oil clusters

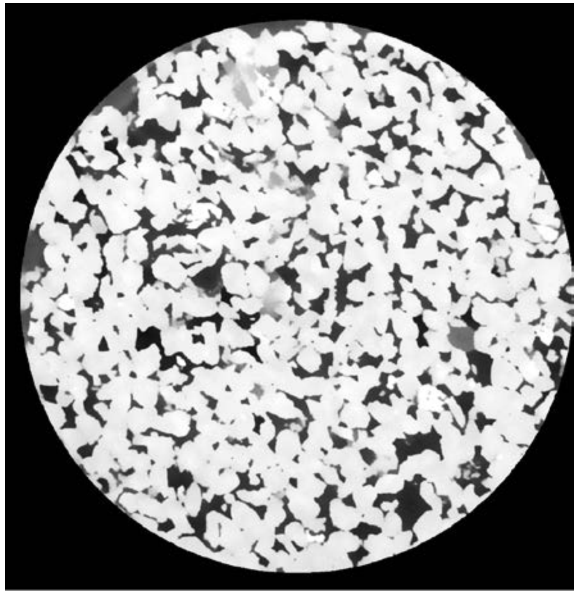

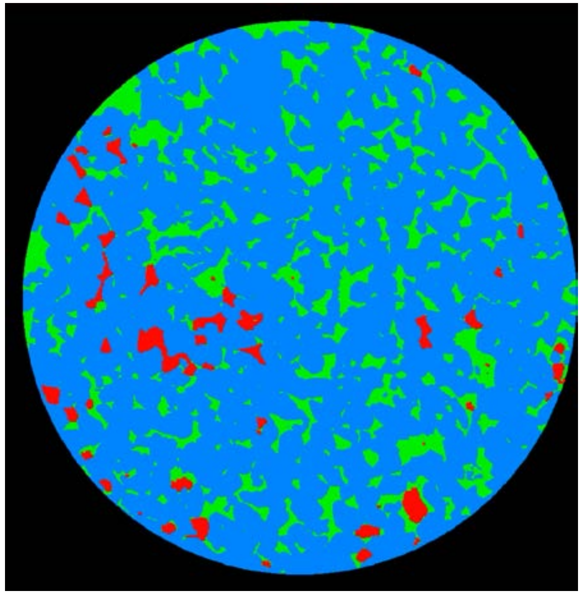

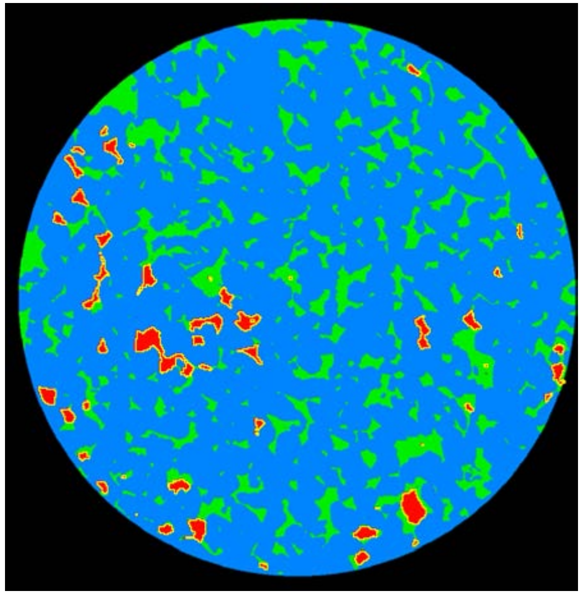

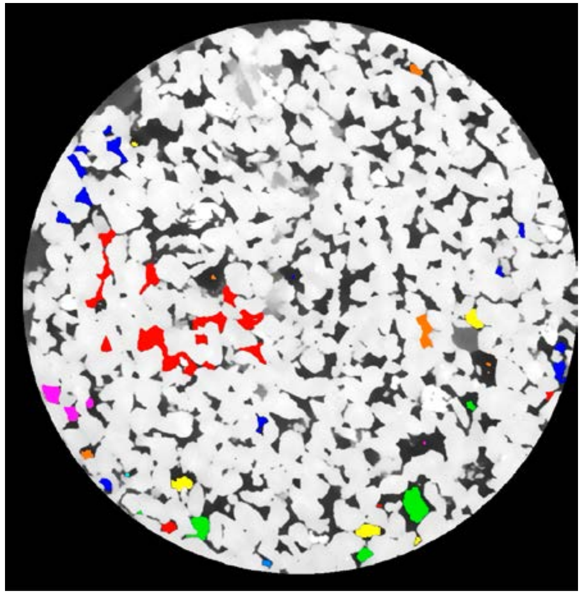

16 bit grey level
(potentially filter)

Segmented image
Blue = rock
Red = oil
Green = gas

For each **phase** compute

For each **cluster** compute

- Volume
- Interfacial area
- Mean curvature
- Euler characteristic

Avizo: Mean Curvature

segmentation

Label analysis

- Volume
- Area
- Euler char.

Generate surface
(spline interpolation)

- Mean curvature
- Gaussian curvature

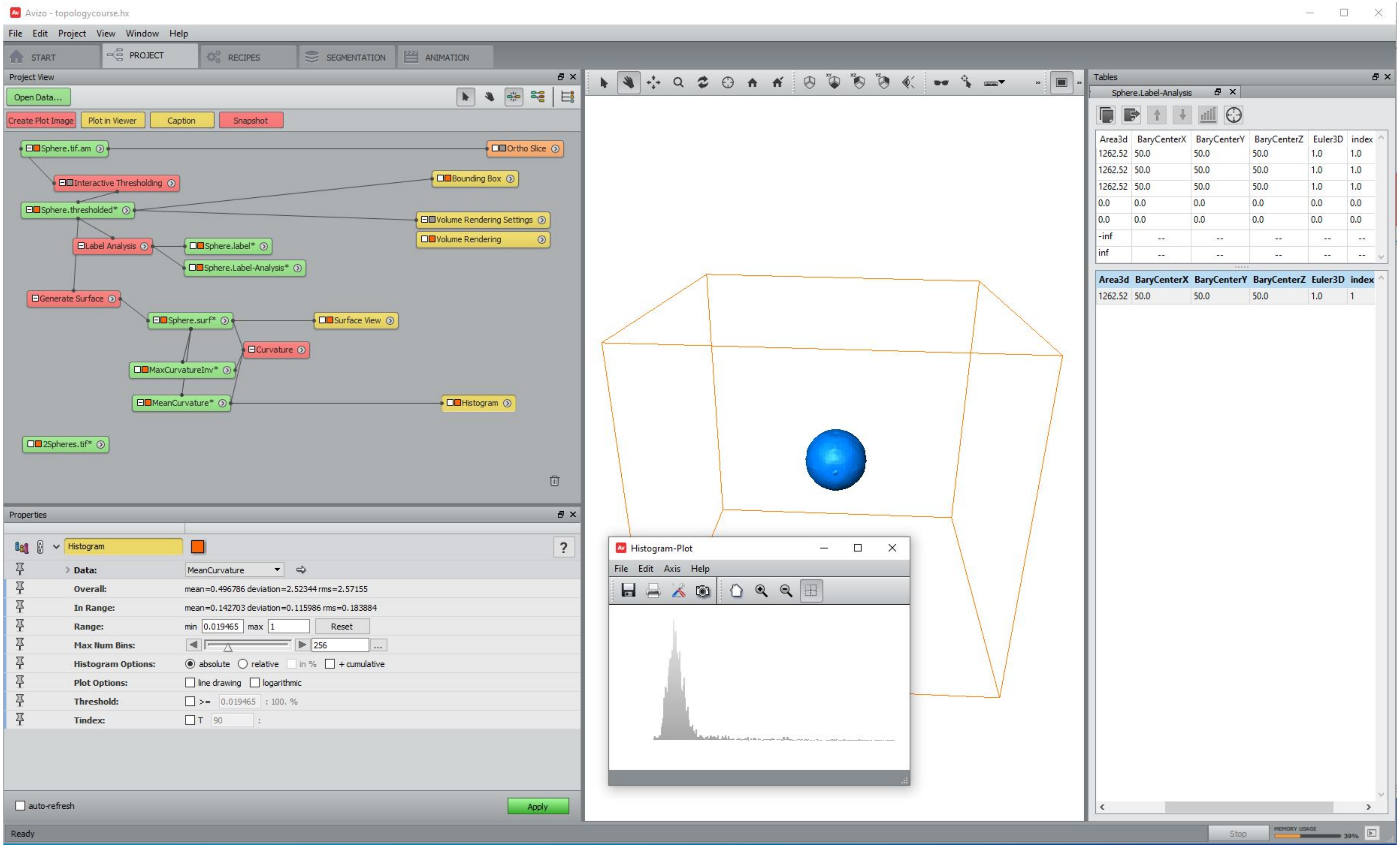

Data: MeanCurvature

Overall: mean=0.496786 deviation=2.52344 rms=2.57155

In Range: mean=0.142703 deviation=0.115986 rms=0.183884

Range: min 0.019465 max 1 Reset

Max Num Bins: 256

Histogram Options: ● absolute ○ relative ☐ in % ☐ + cumulative

Plot Options: ☐ line drawing ☐ logarithmic

Threshold: ☐ >= 0.019465 : 100. %

Tindex: ☐ T 90 :

Area3d	BaryCenterX	BaryCenterY	BaryCenterZ	Euler3D	index
1262.52	50.0	50.0	50.0	1.0	1.0
1262.52	50.0	50.0	50.0	1.0	1.0
1262.52	50.0	50.0	50.0	1.0	1.0
0.0	0.0	0.0	0.0	0.0	0.0
0.0	0.0	0.0	0.0	0.0	0.0
-inf	--	--	--	--	--
inf	--	--	--	--	--

Area3d	BaryCenterX	BaryCenterY	BaryCenterZ	Euler3D	index
1262.52	50.0	50.0	50.0	1.0	1

Avizo : Surface meshes

- Surface property calculation
  - **Curvature**
  - Distance
  - Roughness
  - Thickness

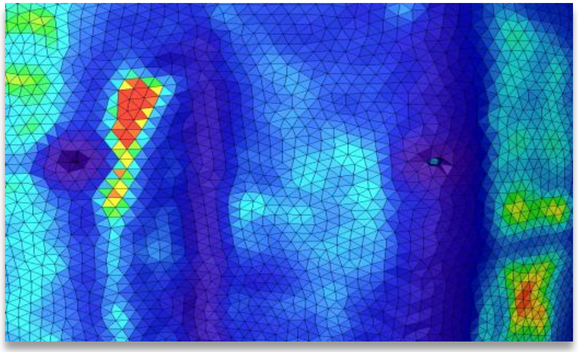

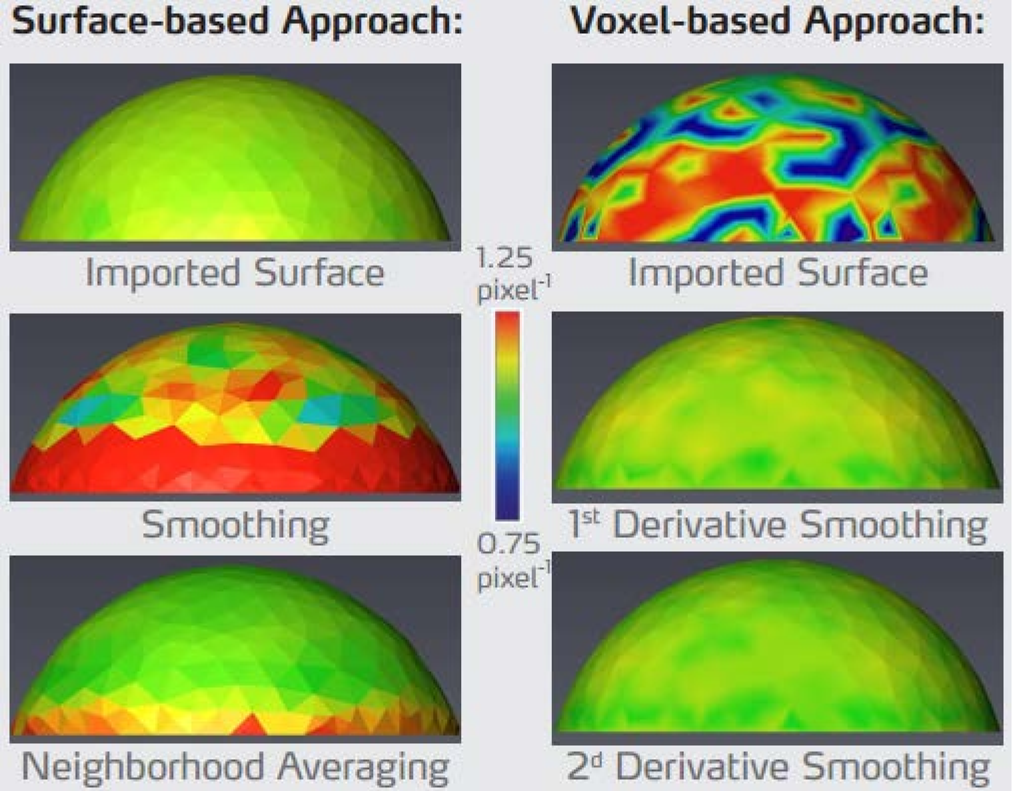

SCA2012-55

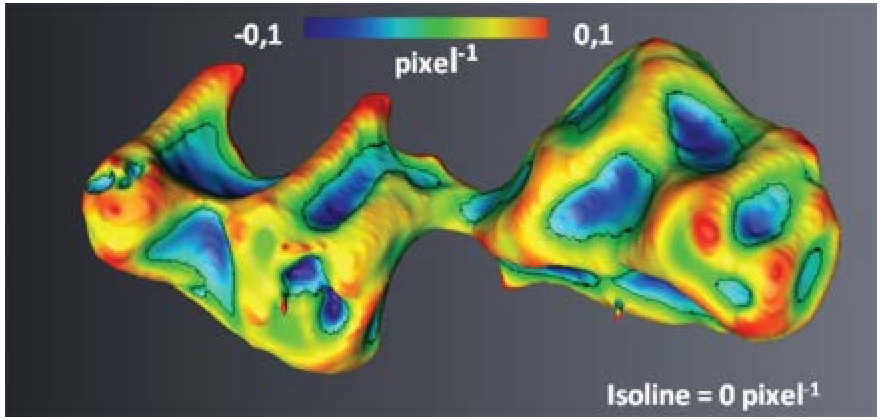

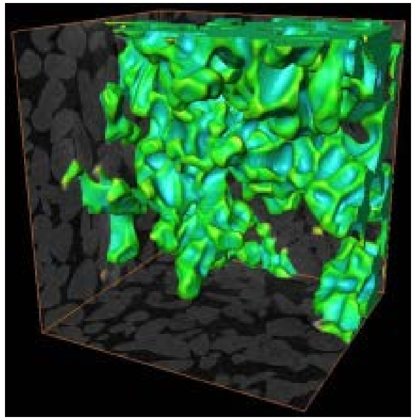

[courtesy of ThermoFisher]

Avizo : Object Analysis

- Analysis
  - Shape factor
  - Equivalent diameter
  - **Volume, area**
  - **Euler**
  - Orientation
  - Roundness
  - Sphericity
  - Rugosity
  - Crofton
- Classification

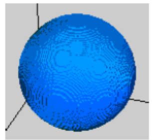	Solid sphere Empty sphere	Euler3D = 1 Euler3D = 2
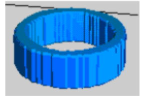	Rectangular section Torus	Euler3D = 0

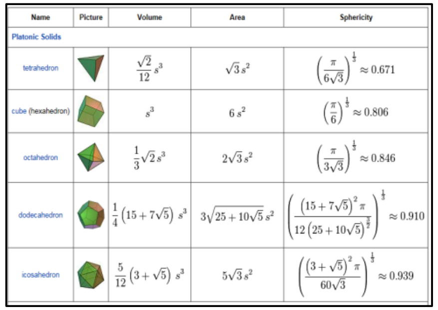

Name	Picture	Volume	Area	Sphericity
Platonic Solids				
tetrahedron		$\frac{\sqrt{2}}{12}s^3$	$\sqrt{3}\,s^2$	$\left(\frac{\pi}{6\sqrt{3}}\right)^{\frac{1}{3}} \approx 0.671$
cube (hexahedron)		s^3	$6\,s^2$	$\left(\frac{\pi}{6}\right)^{\frac{1}{3}} \approx 0.806$
octahedron		$\frac{1}{3}\sqrt{2}\,s^3$	$2\sqrt{3}\,s^2$	$\left(\frac{\pi}{3\sqrt{3}}\right)^{\frac{1}{3}} \approx 0.846$
dodecahedron		$\frac{1}{4}\left(15+7\sqrt{5}\right)\,s^3$	$3\sqrt{25+10\sqrt{5}}\,s^2$	$\left(\frac{\left(15+7\sqrt{5}\right)^2\pi}{12\left(25+10\sqrt{5}\right)^{\frac{3}{2}}}\right)^{\frac{1}{3}} \approx 0.910$
icosahedron		$\frac{5}{12}\left(3+\sqrt{5}\right)\,s^3$	$5\sqrt{3}\,s^2$	$\left(\frac{\left(3+\sqrt{5}\right)^2\pi}{60\sqrt{3}}\right)^{\frac{1}{3}} \approx 0.939$

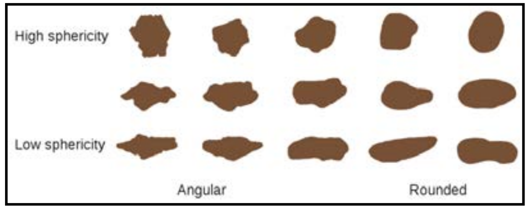

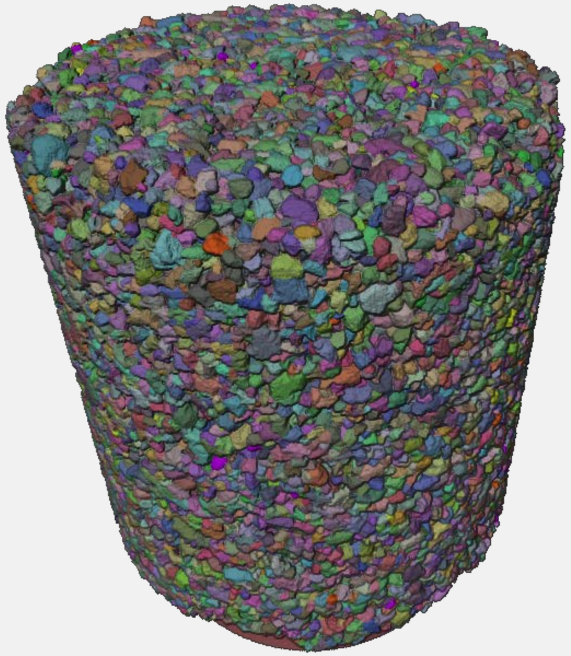

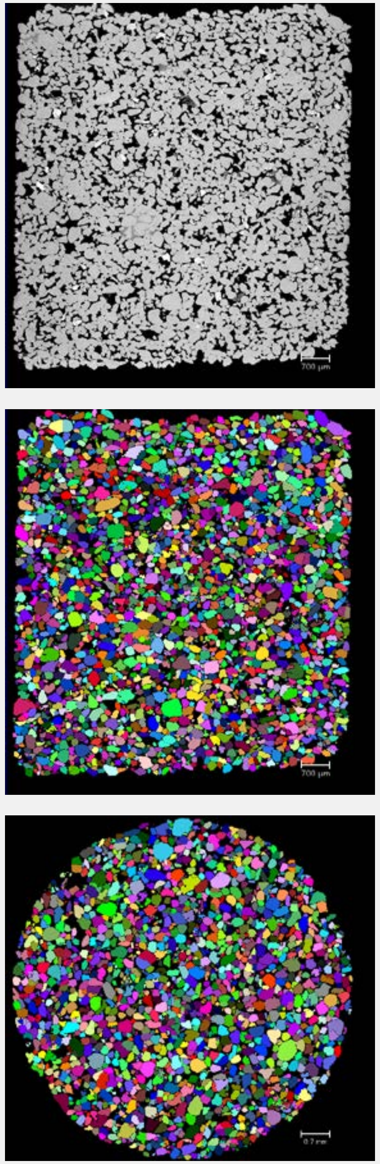

Grain separation on a 40GB Sandstone 5µm

[courtesy of ThermoFisher]

Avizo: Euler Characteristic

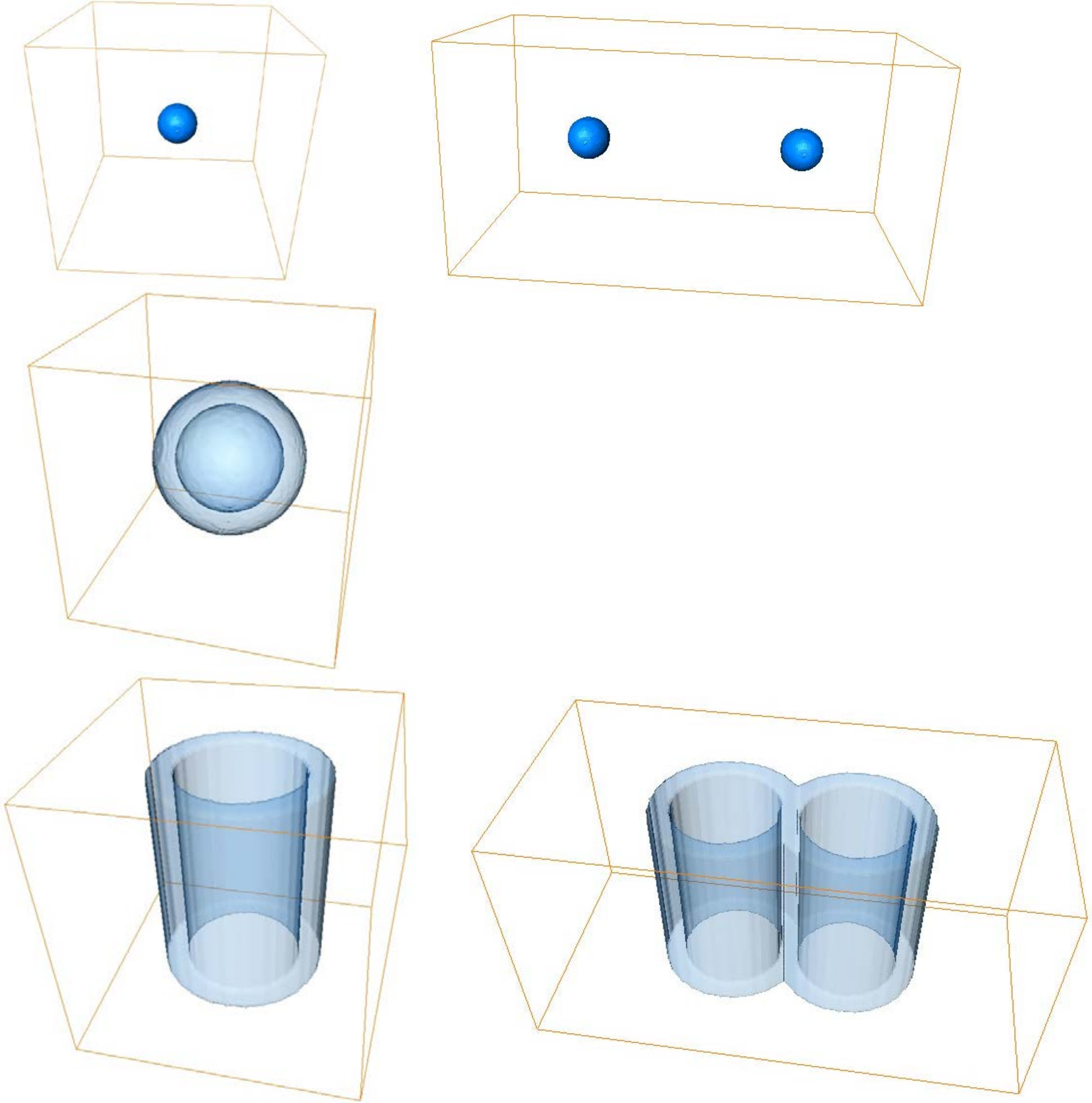

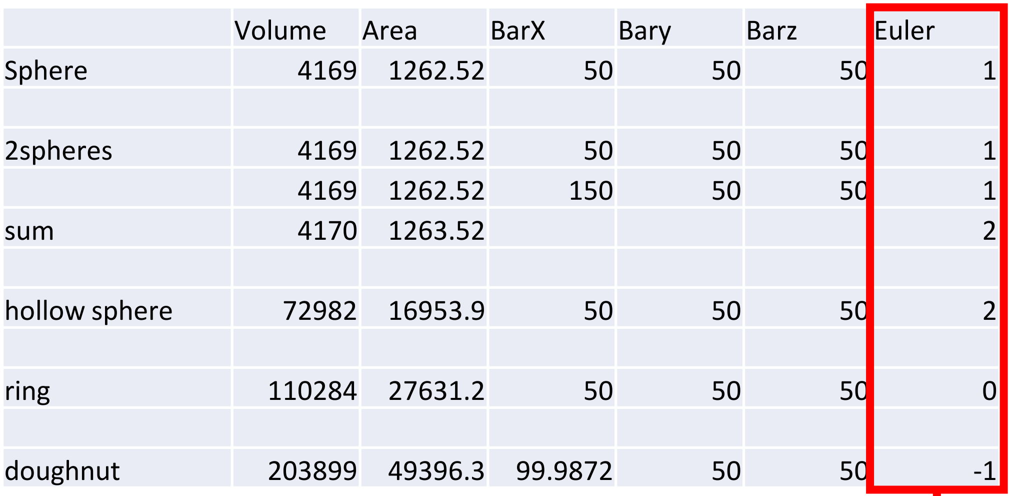

	Volume	Area	BarX	Bary	Barz	Euler
Sphere	4169	1262.52	50	50	50	1
2spheres	4169	1262.52	50	50	50	1
	4169	1262.52	150	50	50	1
sum	4170	1263.52				2
hollow sphere	72982	16953.9	50	50	50	2
ring	110284	27631.2	50	50	50	0
doughnut	203899	49396.3	99.9872	50	50	-1

Euler Characteristic χ =
Objects – Loops (+ Inclusions)

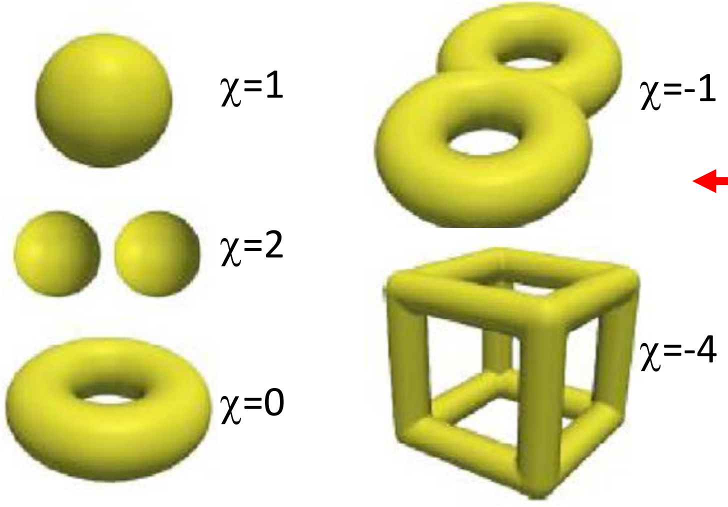

Herring, AWR 2013

ImageJ and FIJI: BoneJ plugin (OpenSource)

ImageJ - https://imagej.nih.gov/ij/
FIJI - https://fiji.sc/
BoneJ - http://bonej.org/

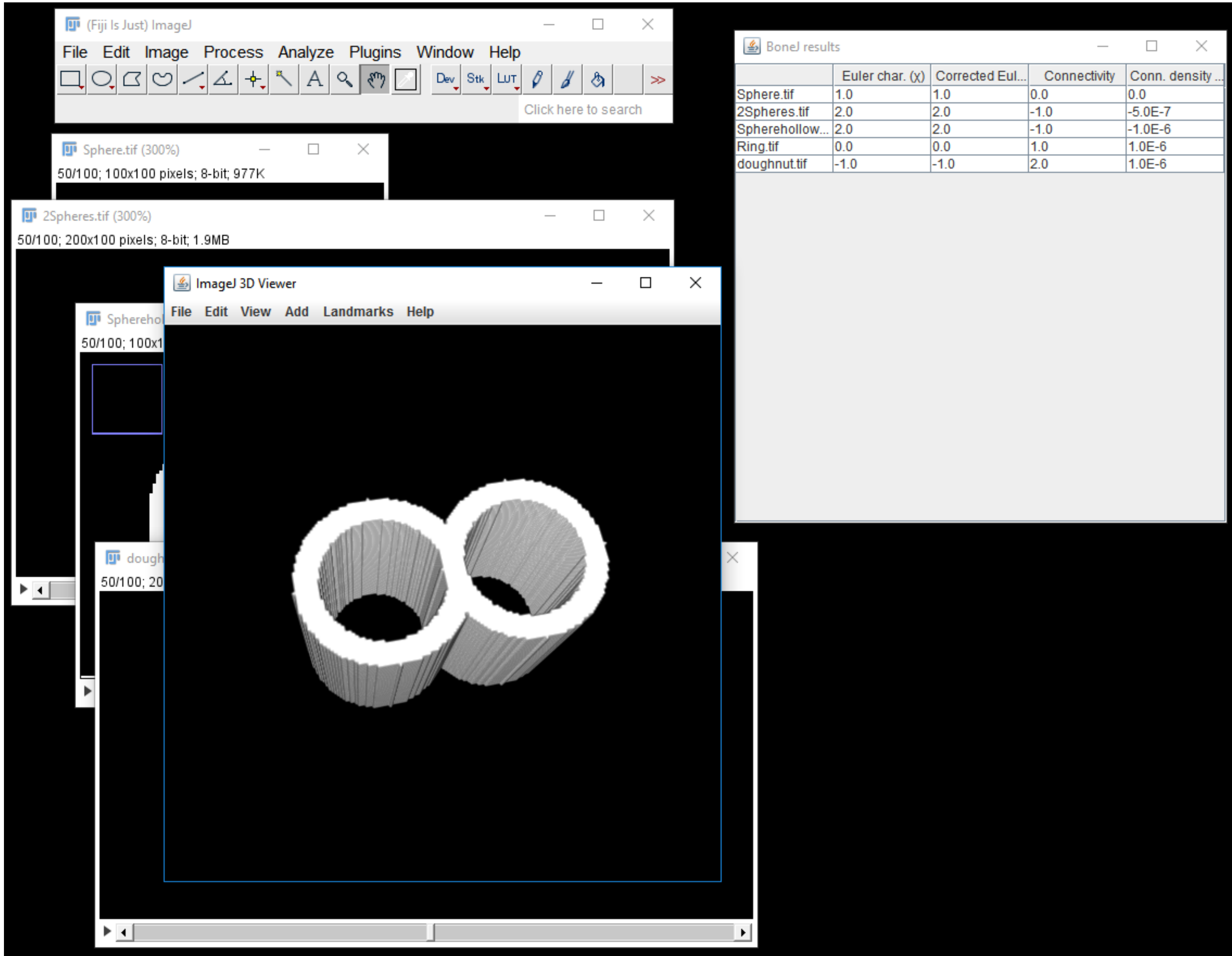

	Euler char. (χ)	Corrected Eul...	Connectivity	Conn. density ...
Sphere.tif	1.0	1.0	0.0	0.0
2Spheres.tif	2.0	2.0	-1.0	-5.0E-7
Spherehollow...	2.0	2.0	-1.0	-1.0E-6
Ring.tif	0.0	0.0	1.0	1.0E-6
doughnut.tif	-1.0	-1.0	2.0	1.0E-6

ImageJ and FIJI: BoneJ plugin (OpenSource)

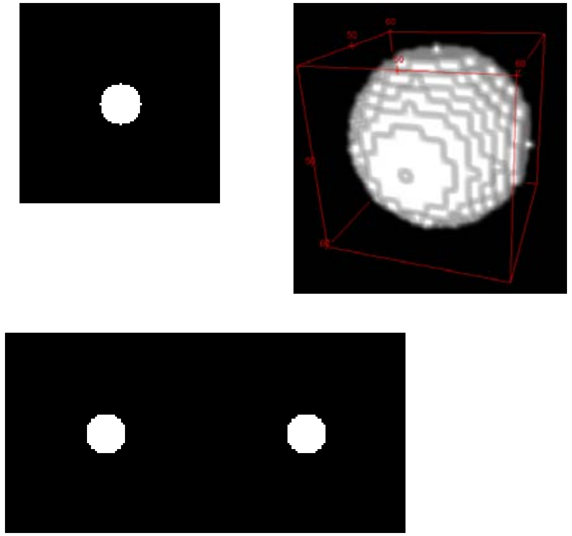

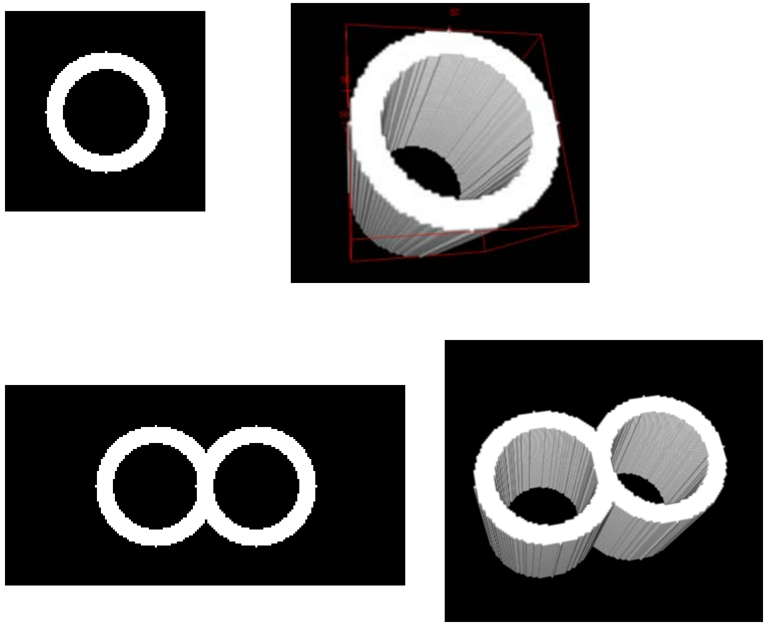

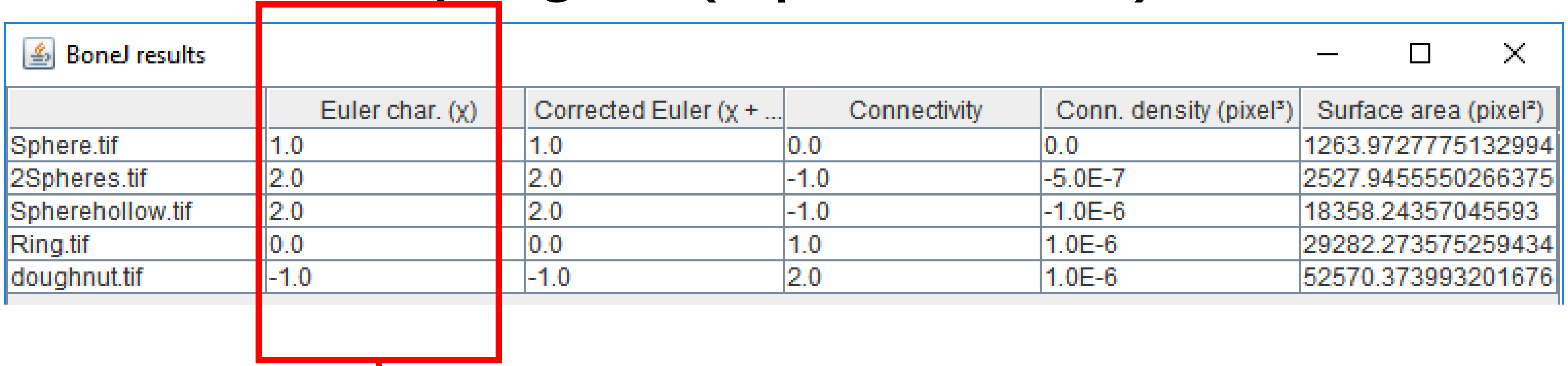

BoneJ results

	Euler char. (χ)	Corrected Euler (χ + ...	Connectivity	Conn. density (pixel^3)	Surface area (pixel^2)
Sphere.tif	1.0	1.0	0.0	0.0	1263.9727775132994
2Spheres.tif	2.0	2.0	-1.0	-5.0E-7	2527.9455550266375
Spherehollow.tif	2.0	2.0	-1.0	-1.0E-6	18358.24357045593
Ring.tif	0.0	0.0	1.0	1.0E-6	29282.273575259434
doughnut.tif	-1.0	-1.0	2.0	1.0E-6	52570.373993201676

Euler Characteristic χ =
Objects – Loops (+ Inclusions)

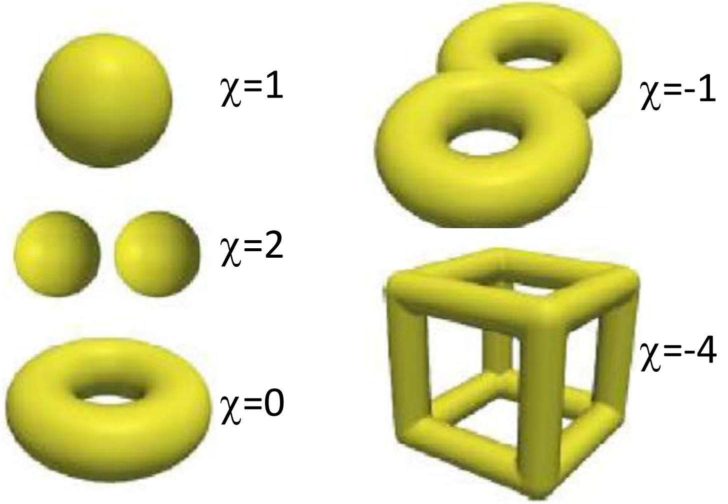

Herring, AWR 2013

Python

scikit-image
image processing in python

https://scikit-image.org/docs/dev/api/skimage.measure.html

Many functions unfortunately currently only in 2D !

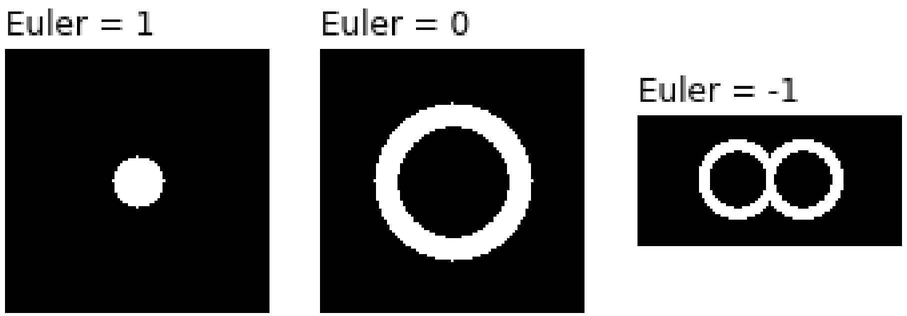

Euler Characteristic χ =
Objects – Loops (+ Inclusions)

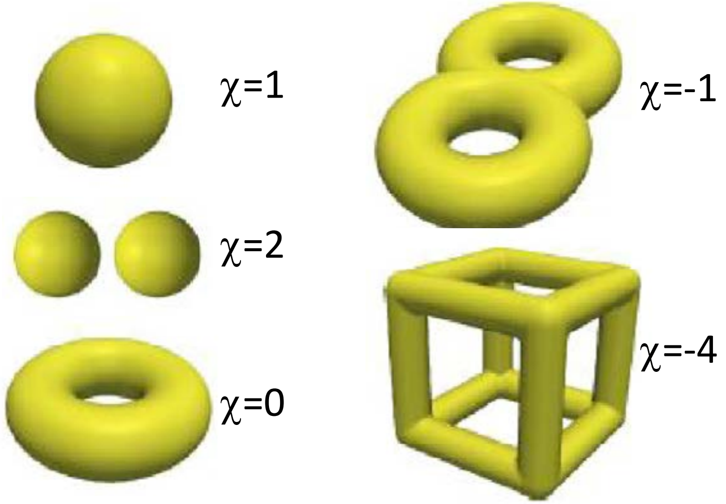

Herring, AWR 2013

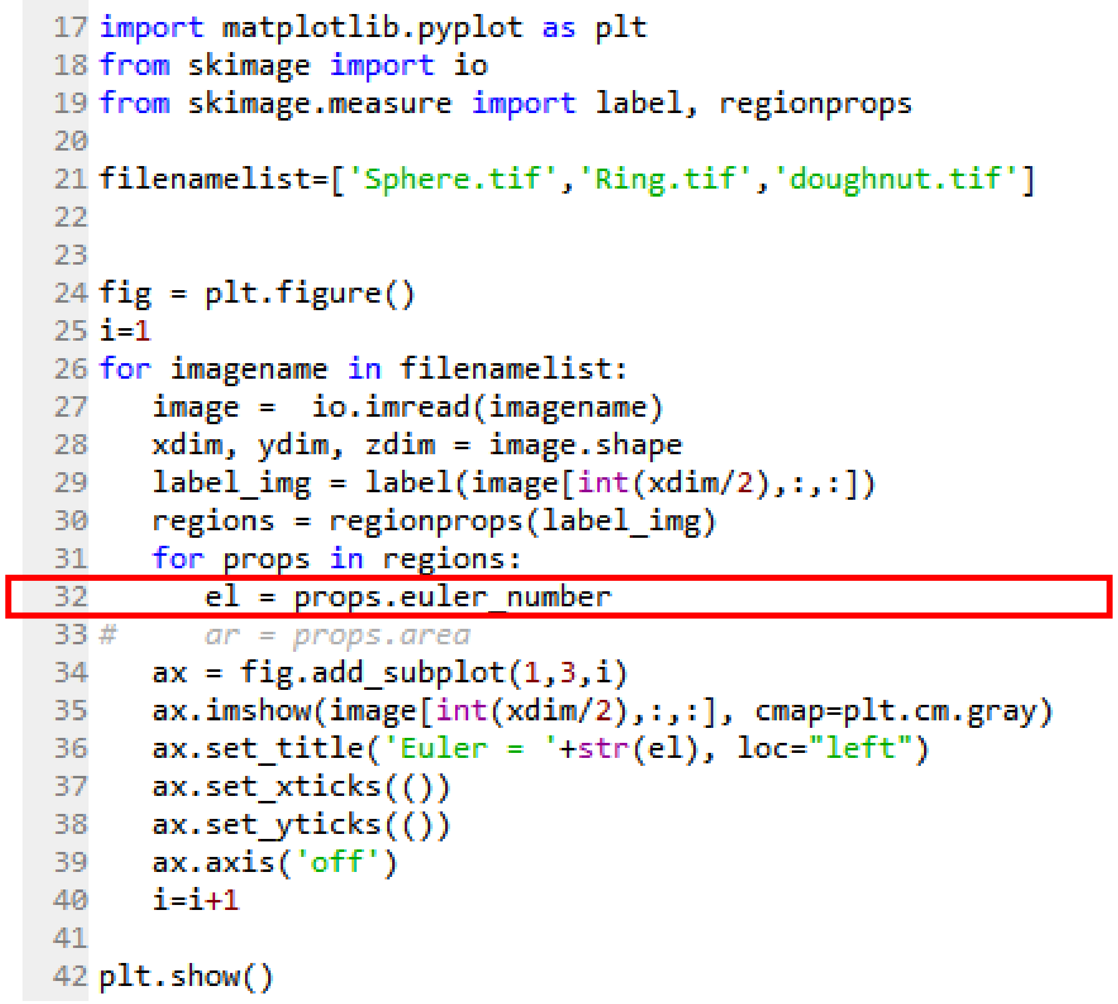

```
import matplotlib.pyplot as plt
from skimage import io
from skimage.measure import label, regionprops

filenamelist=['Sphere.tif','Ring.tif','doughnut.tif']


fig = plt.figure()
i=1
for imagename in filenamelist:
    image =  io.imread(imagename)
    xdim, ydim, zdim = image.shape
    label_img = label(image[int(xdim/2),:,:])
    regions = regionprops(label_img)
    for props in regions:
        el = props.euler_number
#       ar = props.area
    ax = fig.add_subplot(1,3,i)
    ax.imshow(image[int(xdim/2),:,:], cmap=plt.cm.gray)
    ax.set_title('Euler = '+str(el), loc="left")
    ax.set_xticks(())
    ax.set_yticks(())
    ax.axis('off')
    i=i+1

plt.show()
```

MATLAB

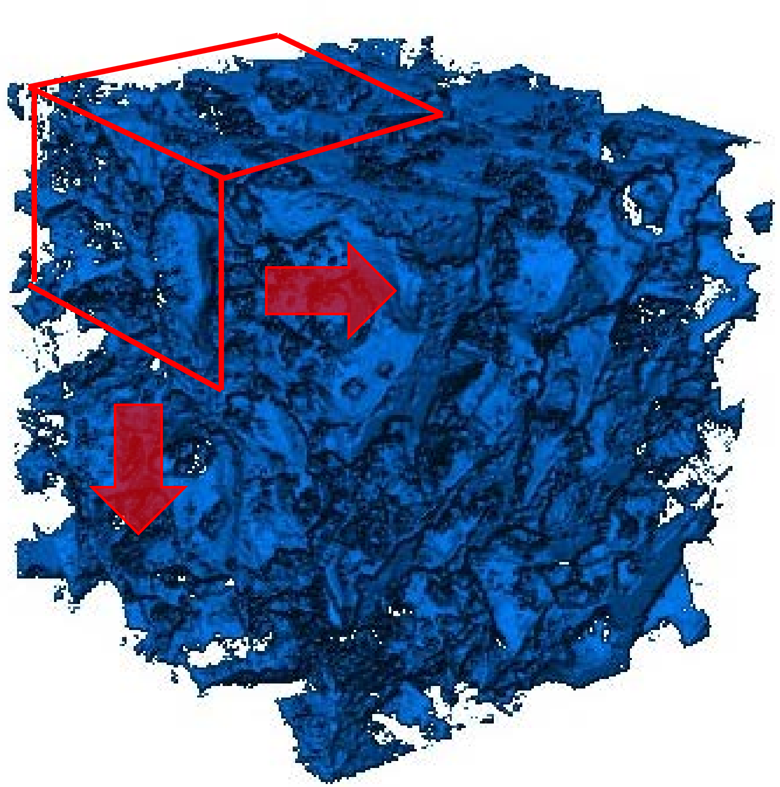

https://github.com/mattools/matImage

Legland, D.; Kiêu, K. & Devaux, M.-F. Computation of Minkowski measures on 2D and 3D binary images. Image Anal. Stereol., 2007, 26, 83-92

```
for w_idx = [900]      % ROI size
    w_surface = [];
    w_labels = [];
    i_loc = ((mask_x - w_idx)/2)+1;
    j_loc = ((mask_y - w_idx)/2)+1;
    k_loc = ((mask_z - w_idx)/2)+1;
    roi   =   FinalImage(i_loc:i_loc+w_idx-1,   j_loc:j_loc+w_idx-1,
k_loc:k_loc+w_idx-1);
    [Euler_roi, Euler_labels]= imEuler3d(roi);
% Implements Euler number codes
    w_Euler = vertcat(w_Euler, Euler_roi);
    w_labels = vertcat(w_labels, Euler_labels);
    file_name = [num2str(w_idx), ‘Filename_900.mat'];
    save(file_name, ‘w_Euler', 'w_labels')
end
```

Boundary and Connectivity Issues

ROI size	Euler3D calculated by Avizo	Euler3D calculated with MATLAB codes
200	-5.07E+02	-5.62E+02
300	-2.70E+03	-2.69E+03
400	-6.76E+03	-6.80E+03

Pixel Connectivity

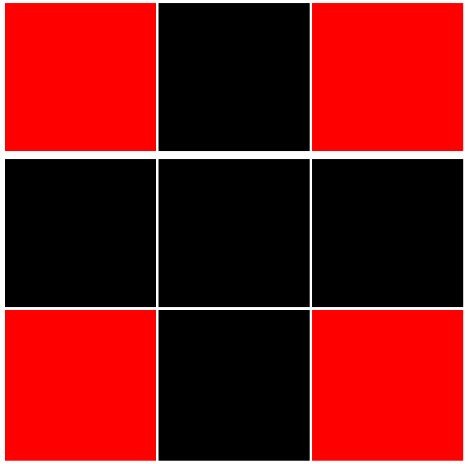

Do these two objects connect?

YES → Euler = 1
No → Euler = 2

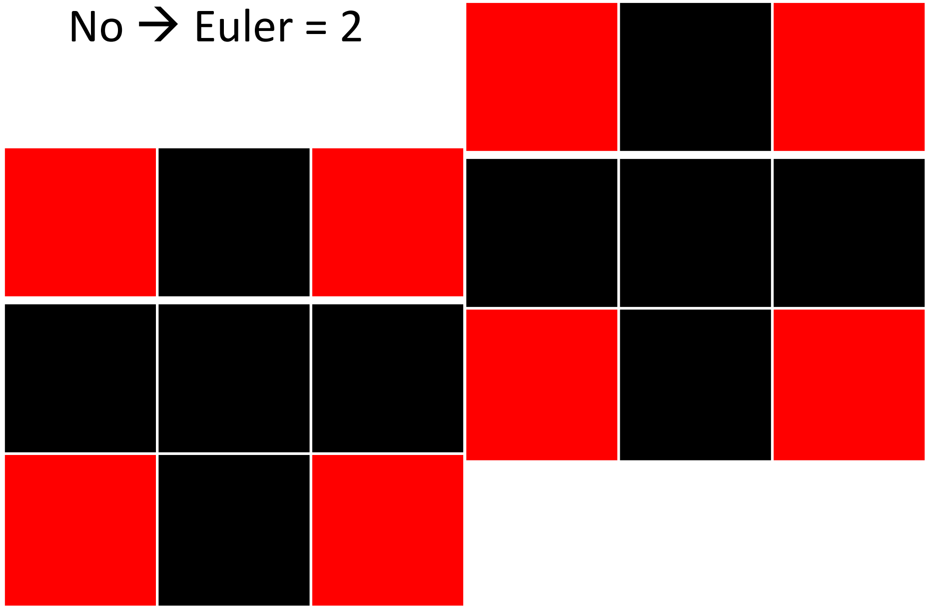

Boundary Issues

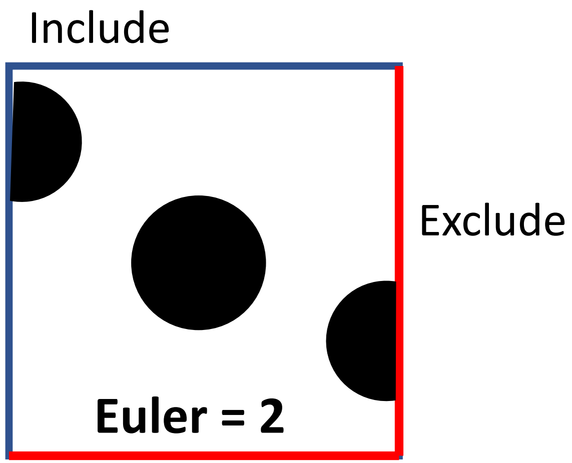

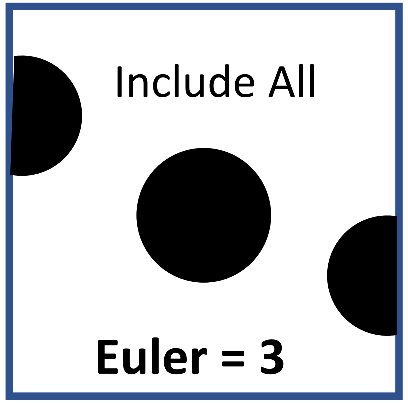

DEEP ROCKS

Measurements on Segmented Voxels

Digital Rock Imaging Platform
Powered by Deep Learning

Whole Core
Medical CT, Core photography

Plugs and Cuttings
Micro-CT, Nano-CT, FIB-SEM

Thin Section
LM, SEM, TEM, CL, Mineralogy

Color and Sort by measurement

- Volume
- Surface area
- Aspect Ratio
- Phi
- Theta
- Position (x,y,z)
- Intensity (mean, min, max, stdev)

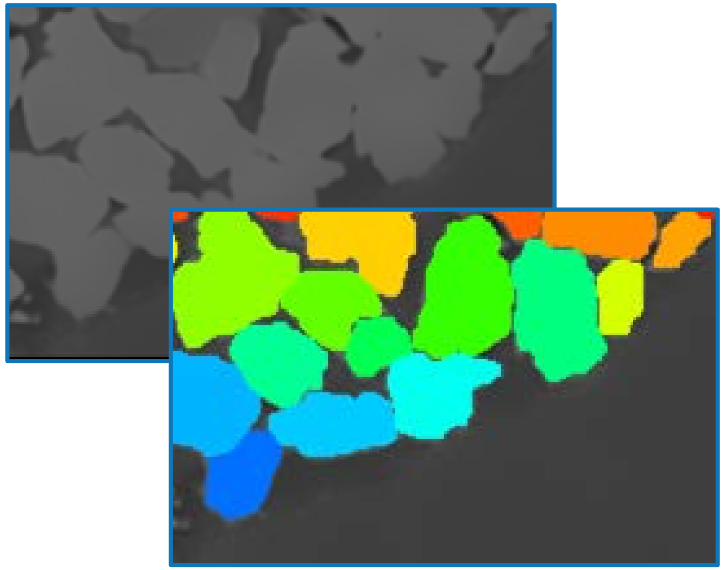

Grain separation and labeling by Deep Watershed

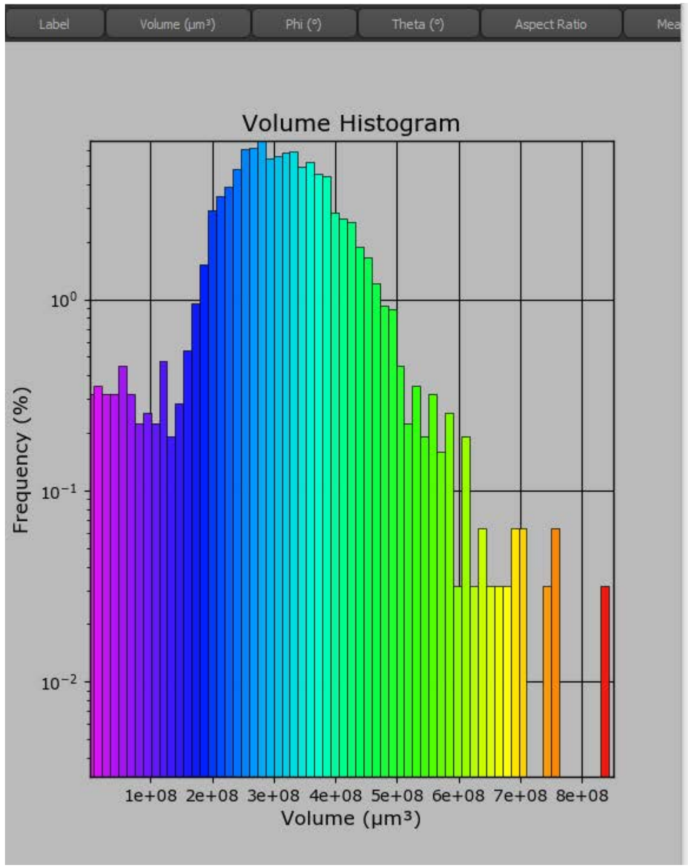

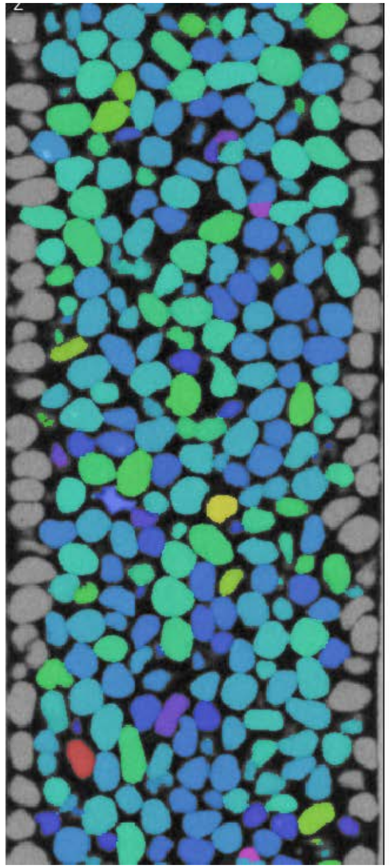

Courtesy of TheObjects

Measurements Directly on Surface Meshes and Graphs

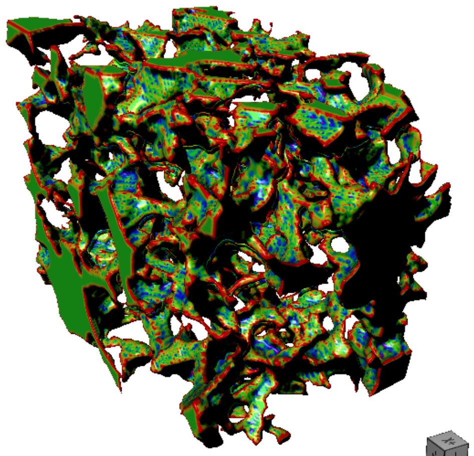

Curvature Mesh

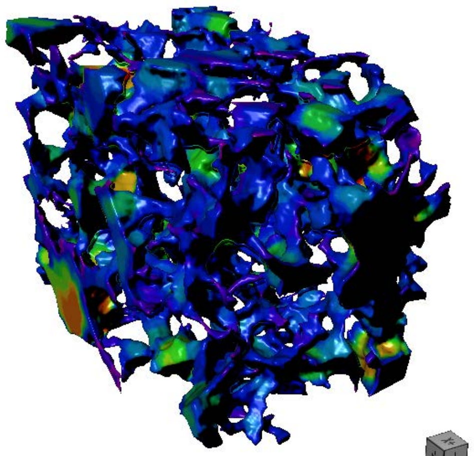

Thickness Mesh

Mesh operations

- Smoothing
- Decimation
- Thickness
- **Mean Curvature**
- **Gaussian Curvature**

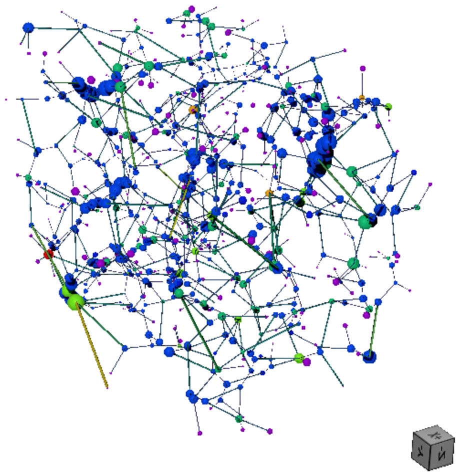

Pore network

- Nodes scaled by pore body radius
- Nodes colored by connectivity index
- Edges colored by edge length
- **χ= -212 (Euler characteristic)**

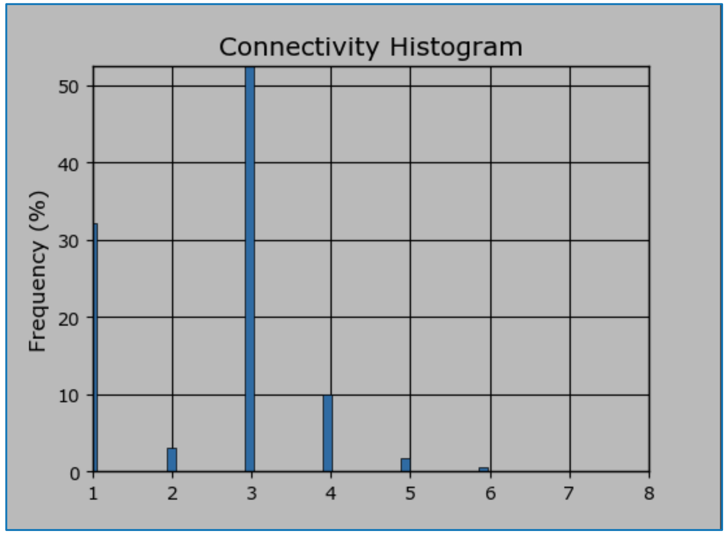

Courtesy of TheObjects

Applications

1. Digital Rock: Validation of pore scale simulators: relative permeability
2. new route to relative permeability
3. Phase connectivity inferred from resistivity measurements
4. Phase connectivity in critical gas saturation
5. Hysteresis models for Darcy-scale flow
6. Wettability: Description of contact angle as deficit curvature
7. Wettability: bi-continuous interfaces in intermediate/mixed-wet rock
8. Petrology mineral analysis for interpreting relative permeability
9. Permeability in fracture networks

Application: Validation of Pore Scale Simulation

LBM fractional flow simulation: match with exp. data

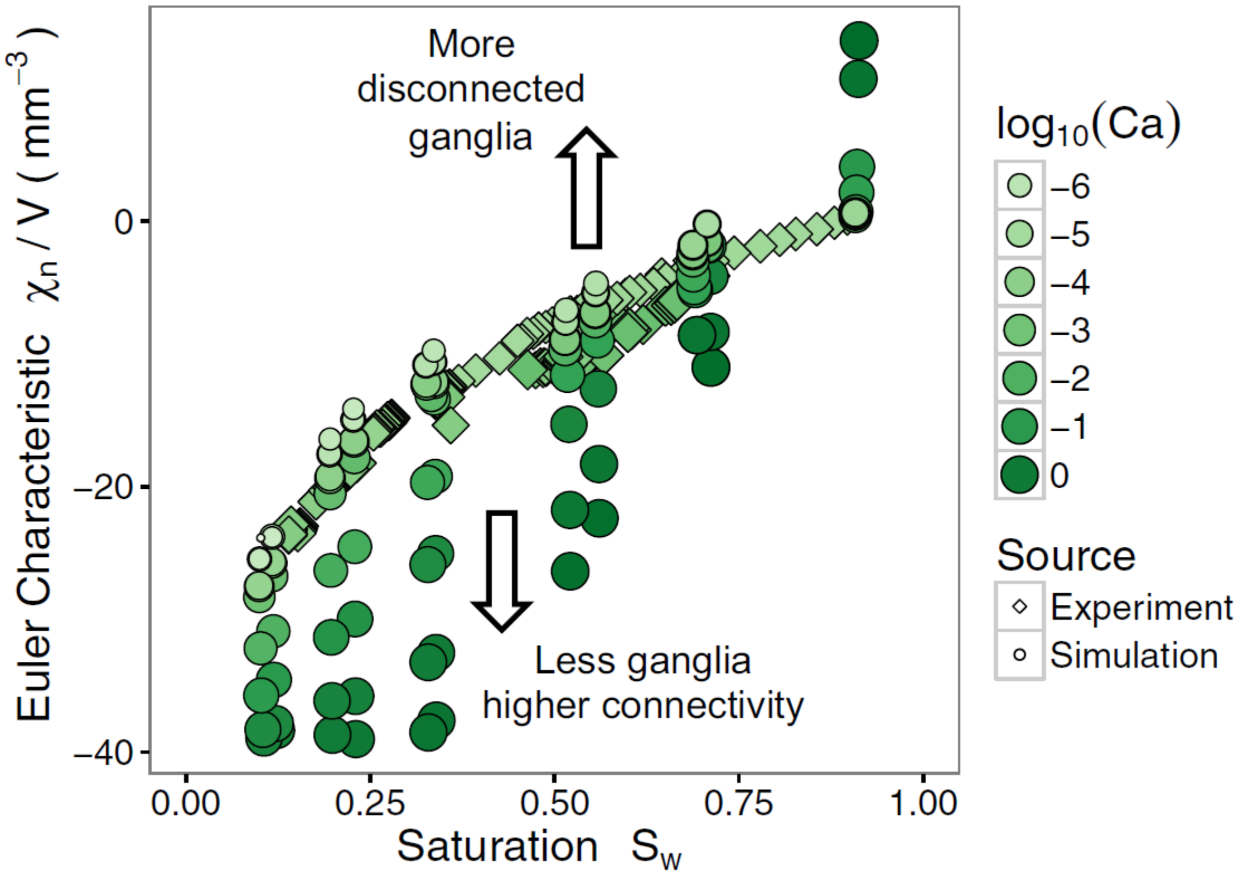

McClure et al, PRE, 2016

Free-Energy LBM correctly predicts connectivity !

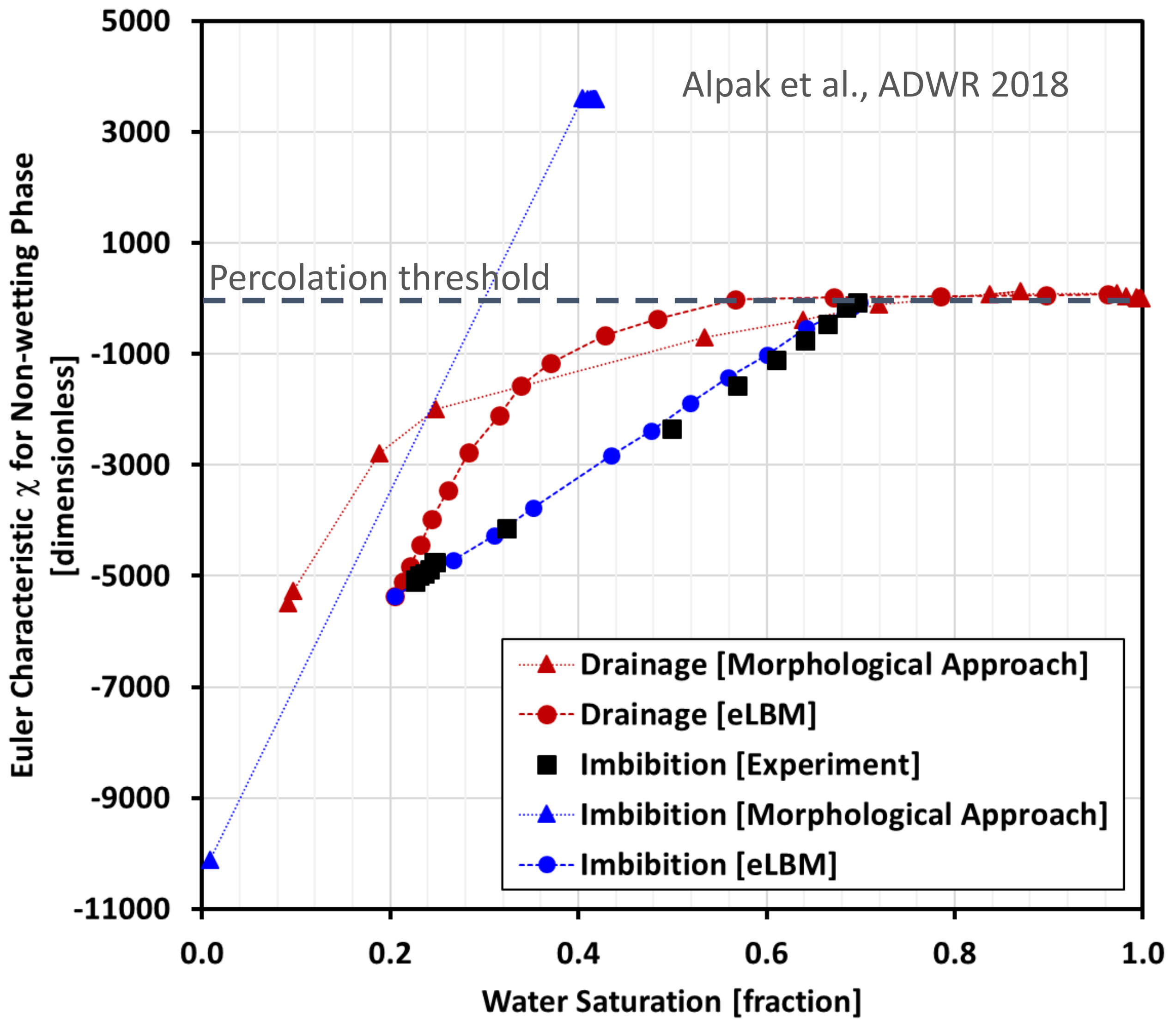

Application: Validation of Pore Scale Simulation

Model: quasi-static Pore Network Model (Ruspini et al. 2018)
Rock: Gildehauser sandstone (similar to Bentheimer)
Imbibition

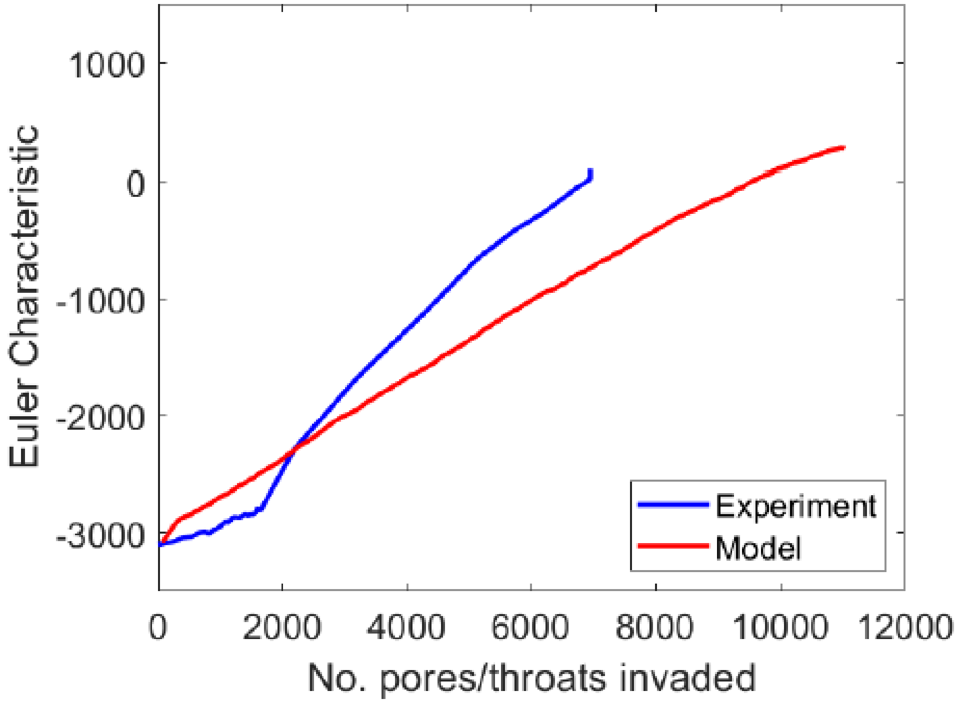

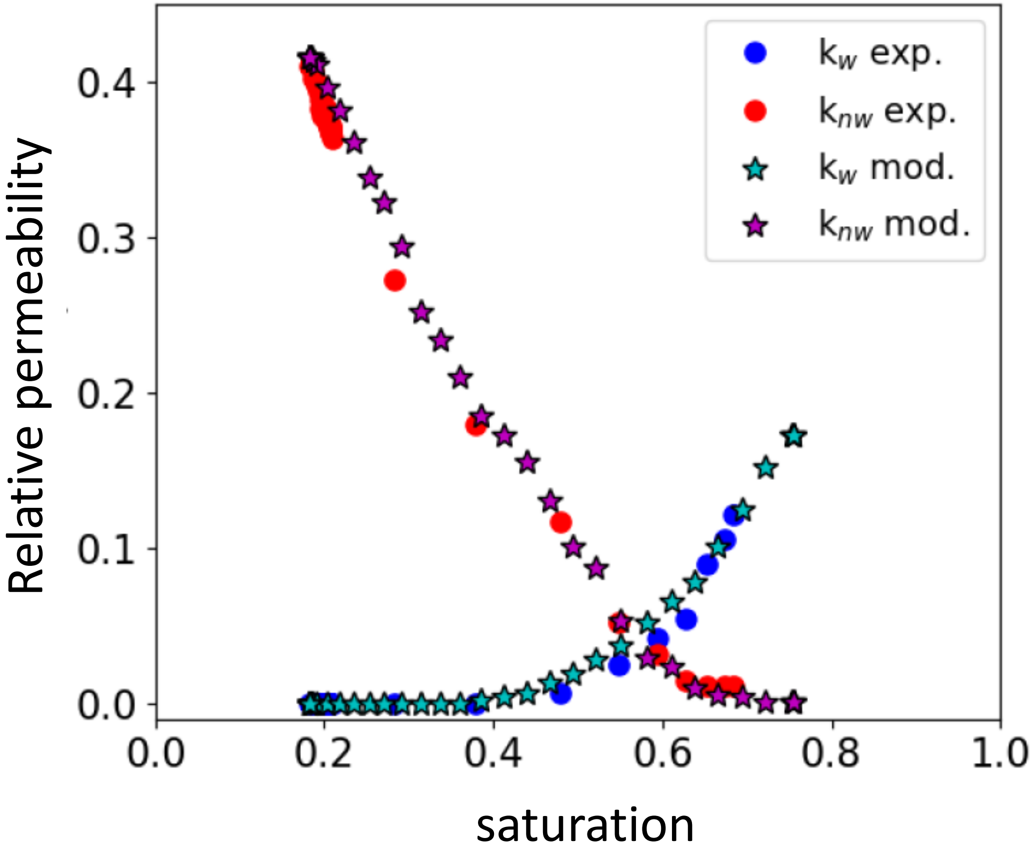

Bultreys et al. under review

Application: new route to relative permeability

Non-wetting phase relative permeability has high sensitivity with Euler characteristic

Non-wetting phase relative permeability is simple

Power law function of Euler characteristic

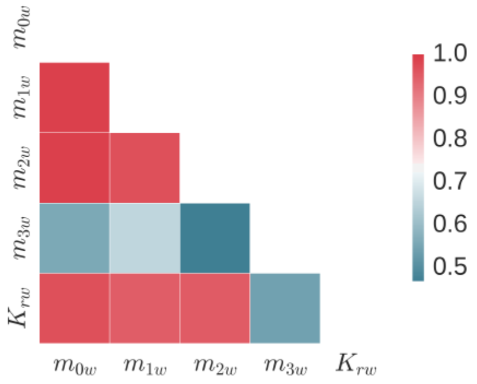

(a) WP of CT in FFD

Sensitivity

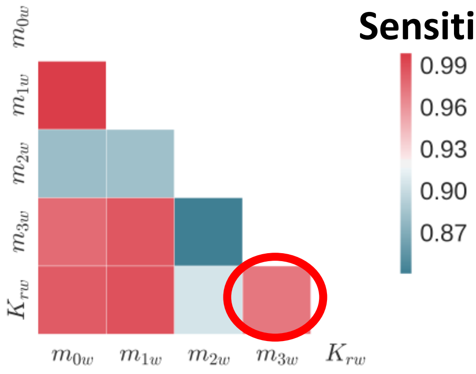

(b) NWP of CT in FFD

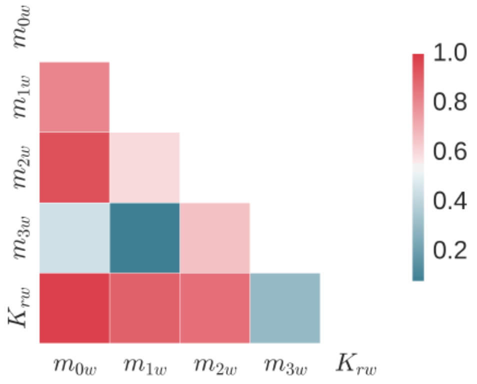

(c) WP of CT in QPD

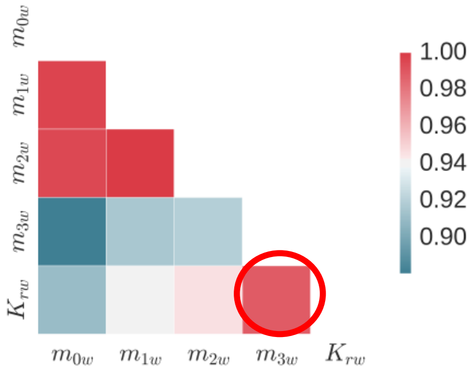

(d) NWP of CT in QPD

Armstrong et al.
TIPM 2017

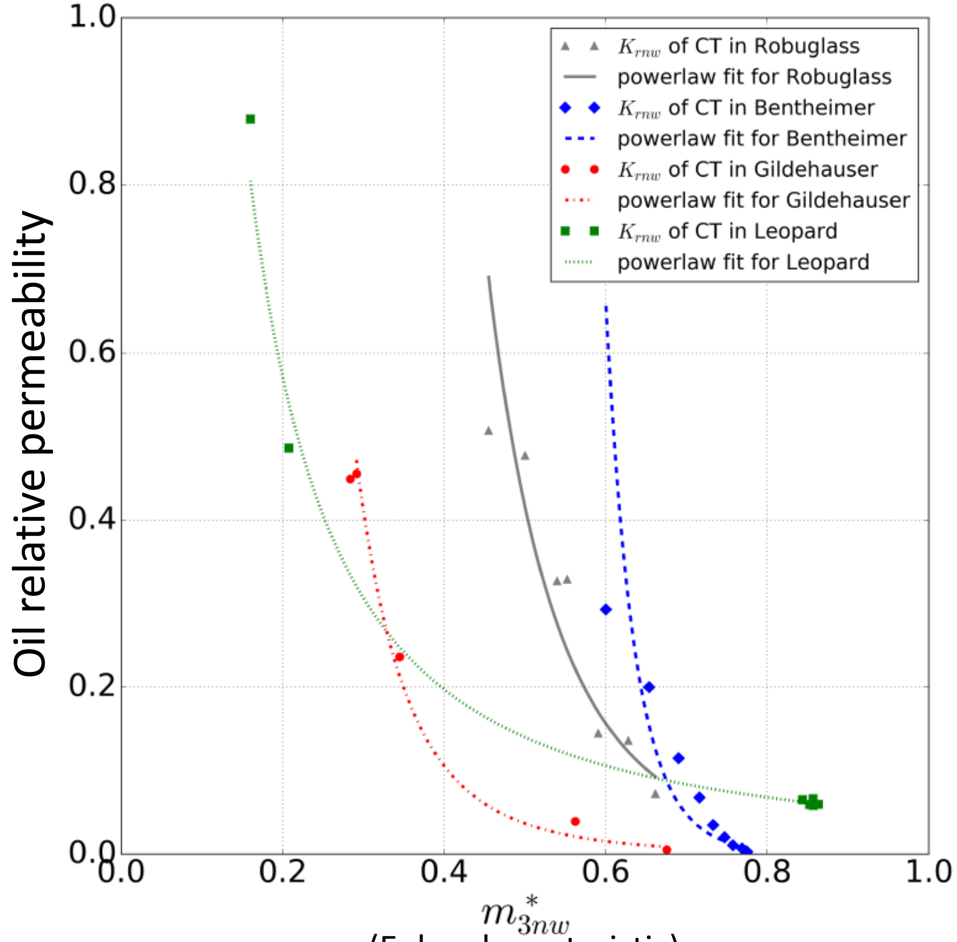

(Euler characteristic)

Scholz et al. Permeability of Porous Materials Determined from the Euler Characteristic, Physical Review Letters 109, 264504, 2012.

Bi-Continuous Interfaces

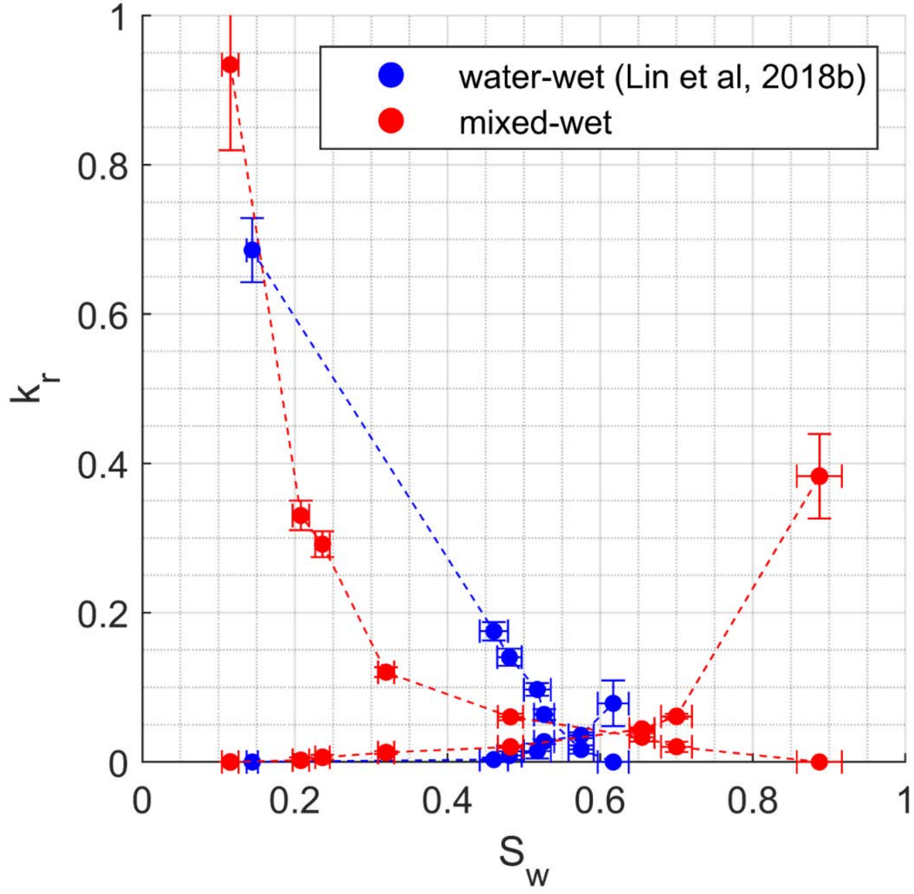

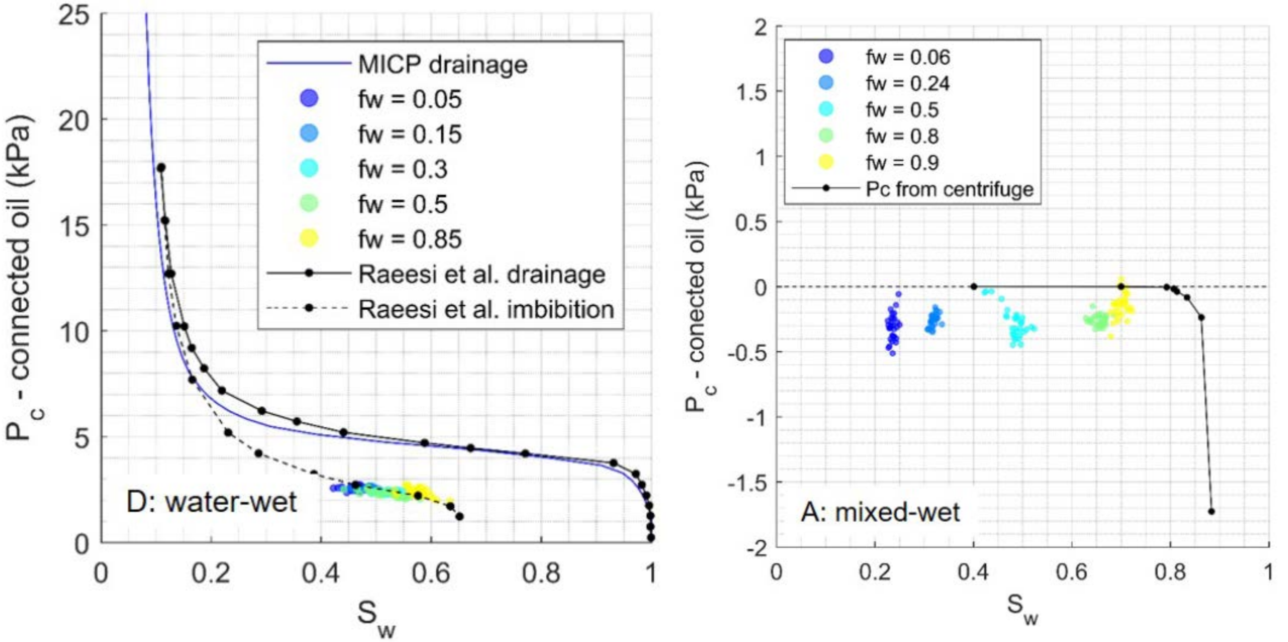

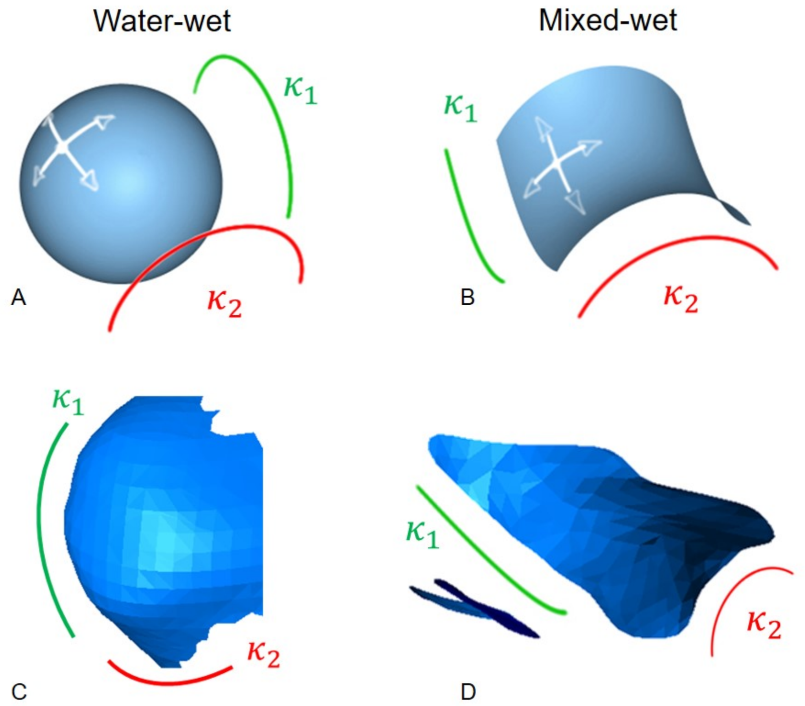

$K = \kappa_1 \kappa_2 > 0$

$K = \kappa_1 \kappa_2 \leq 0$

- Mean curvature ~ 0
- Gaussian curvature < 0

  → bi-continuous interfaces with high connectivity

Lin et al. *Phys. Rev. E, 2019*

Resistivity Index and Topology

[Liu et al. 2018]

Percolation Theory:

$$\xi \sim (p - p_c)^{\beta}$$

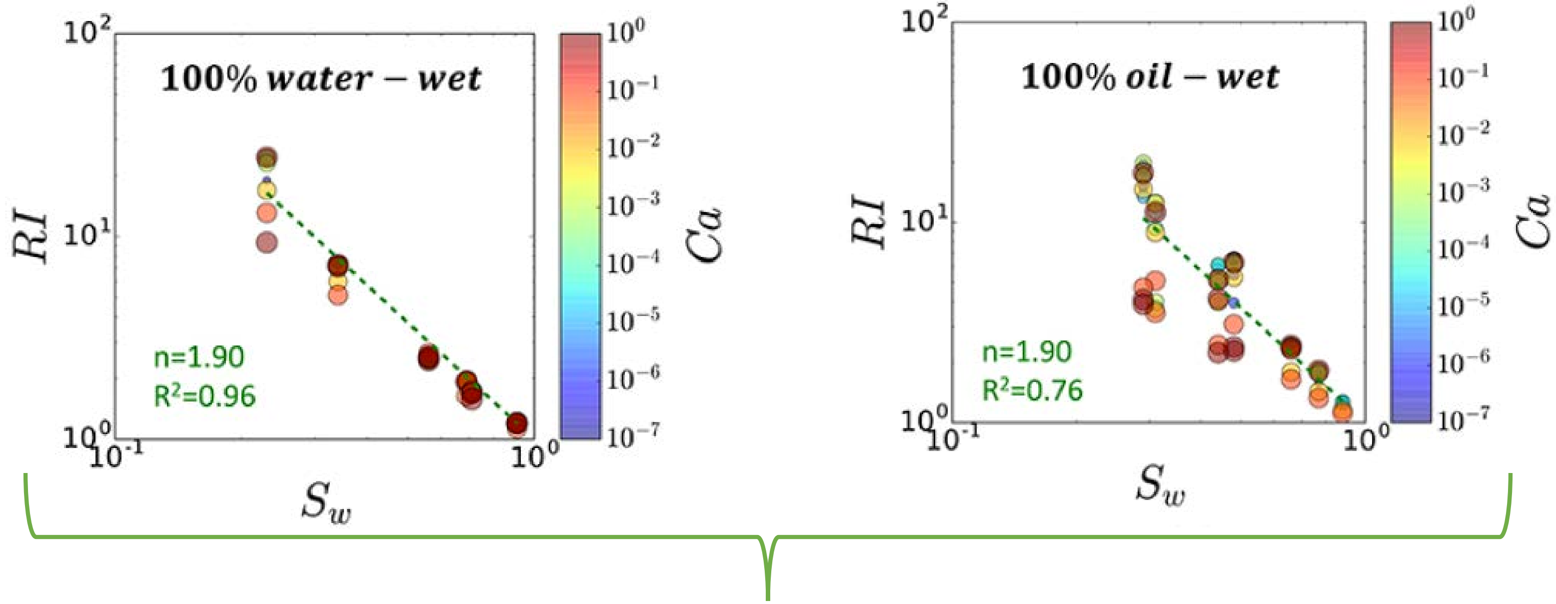

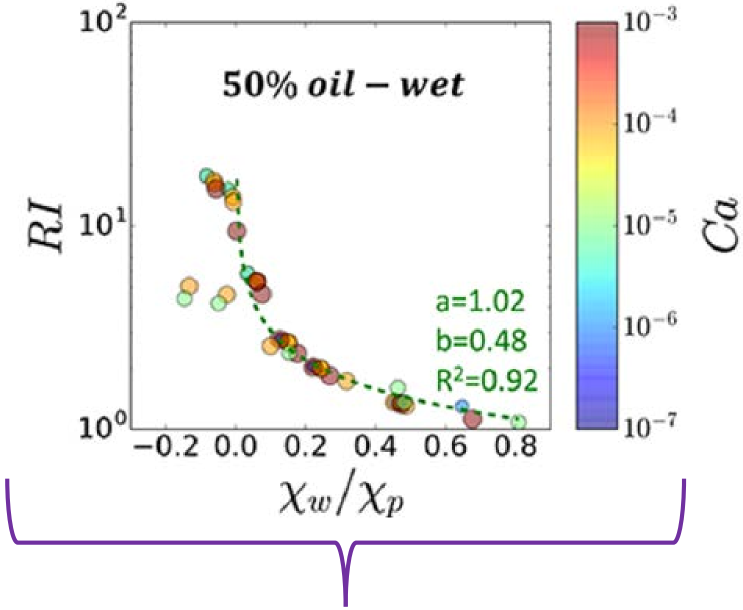

Percolation parameter = Saturation

Percolation parameter = Topology

Models comparing percolation parameters for various wetting conditions.

Wettability	$lg(RI) \sim lg(S_w)$	$lg(RI) \sim lg(\chi_w/\chi_p)$
100% water-wet	0.98	0.22
50% water-wet	0.97	0.97
50% oil-wet	0.88	0.96
100% oil-wet	0.82	0.90

Euler characteristic inferred from RI

Phase Connectivity in Critical Gas Saturation

[Berg et al. SCA 2019]

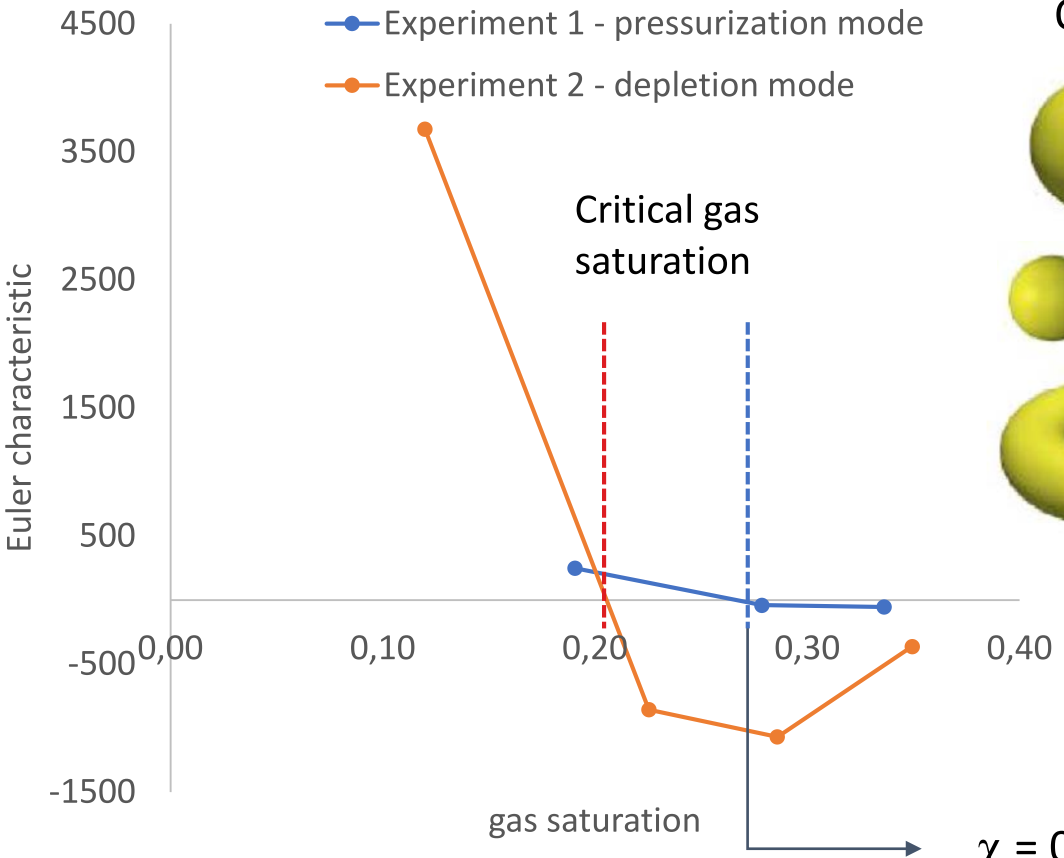

χ = 0 → percolation threshold

Euler Characteristic χ =
Objects – Loops (+ Inclusions)

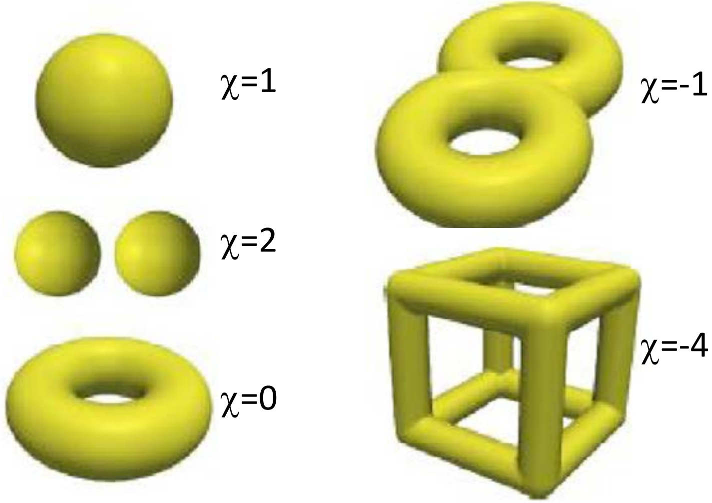

→ See SCA021 on Wednesday, 11:30

Application: Relative Permeability Hysteresis Modelling

Advantage of state-variable description: path-independence

1. **Can express any parameter, e.g. k_r as total differential of state variables**

$$\mathrm{d}k_r = \underbrace{\frac{\partial k_r}{\partial S}\mathrm{d}S + \frac{\partial k_r}{\partial \hat{\chi}}\mathrm{d}\hat{\chi}}_{\text{Phase distribution}} + \overbrace{\frac{\partial k_r}{\partial I}\mathrm{d}I}^{\text{Wettability}} + \underbrace{\frac{\partial k_r}{\partial N_{CA}}\mathrm{d}N_{CA}}_{\text{Capillary number}} + \overbrace{\frac{\partial k_r}{\partial \lambda}\mathrm{d}\lambda}^{\text{Rock structure}}$$

SPE-182655 (Penn State group)

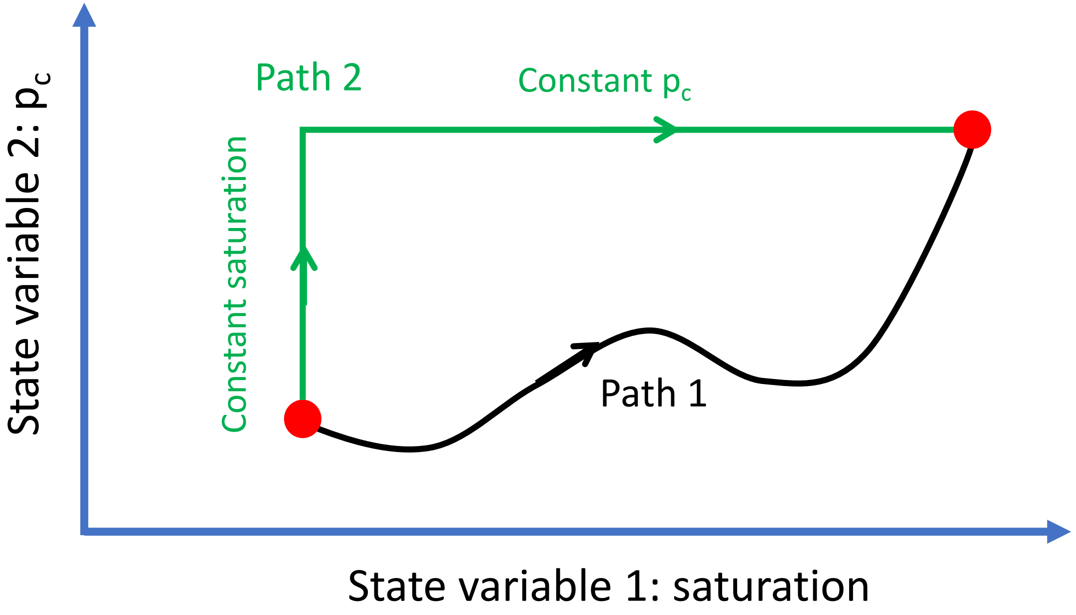

2. **Can choose different paths to measure k_r**
   - e.g. branch 1: constant saturation (steady-state, constant fractional flow Fw)

     branch 2: constant p_c (porous plate)

Application: Relative Permeability Hysteresis Modelling

Relative permeability as an

Equation of State (EOS)

SPE-182655 (R. T. Johns)

$$\mathrm{d}k_r = \underbrace{\frac{\partial k_r}{\partial S}\mathrm{d}S + \frac{\partial k_r}{\partial \hat{\chi}}\mathrm{d}\hat{\chi}}_{\text{Phase distribution}} + \overbrace{\frac{\partial k_r}{\partial I}\mathrm{d}I}^{\text{Wettability}} + \underbrace{\frac{\partial k_r}{\partial N_{CA}}\mathrm{d}N_{CA}}_{\text{Capillary number}} + \overbrace{\frac{\partial k_r}{\partial \lambda}\mathrm{d}\lambda}^{\text{Rock structure}}$$

	$\frac{\partial S}{\partial t} > 0$	$\frac{\partial S}{\partial t} < 0$
$\frac{\partial \hat{\chi}}{\partial S}$	$\alpha_\chi \left(\frac{\hat{\chi}-1}{S-1}\right)$	$\frac{1}{C_\chi (\hat{\chi} S)^{n_\chi}}$

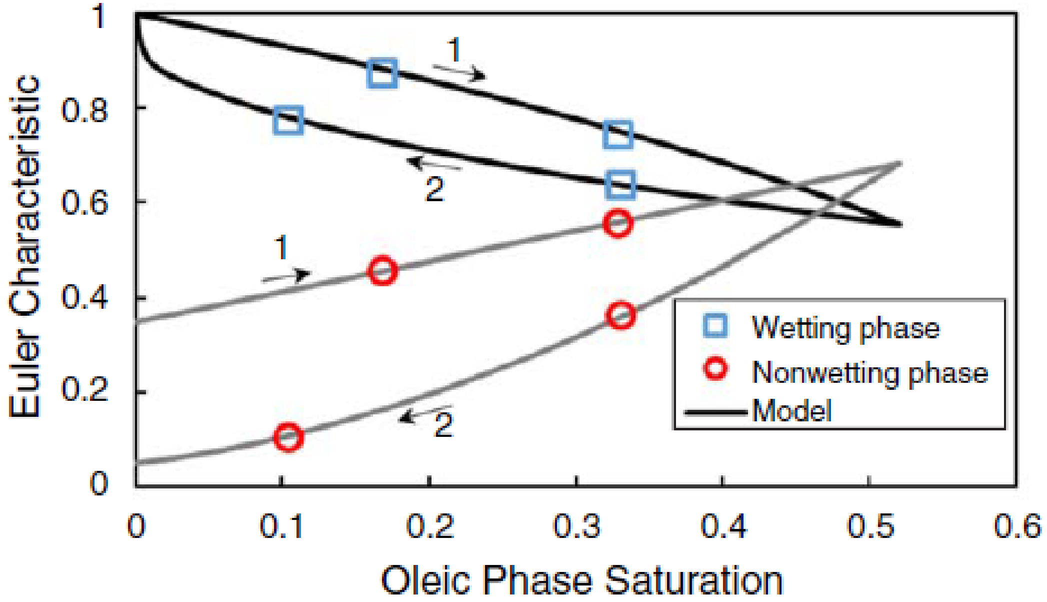

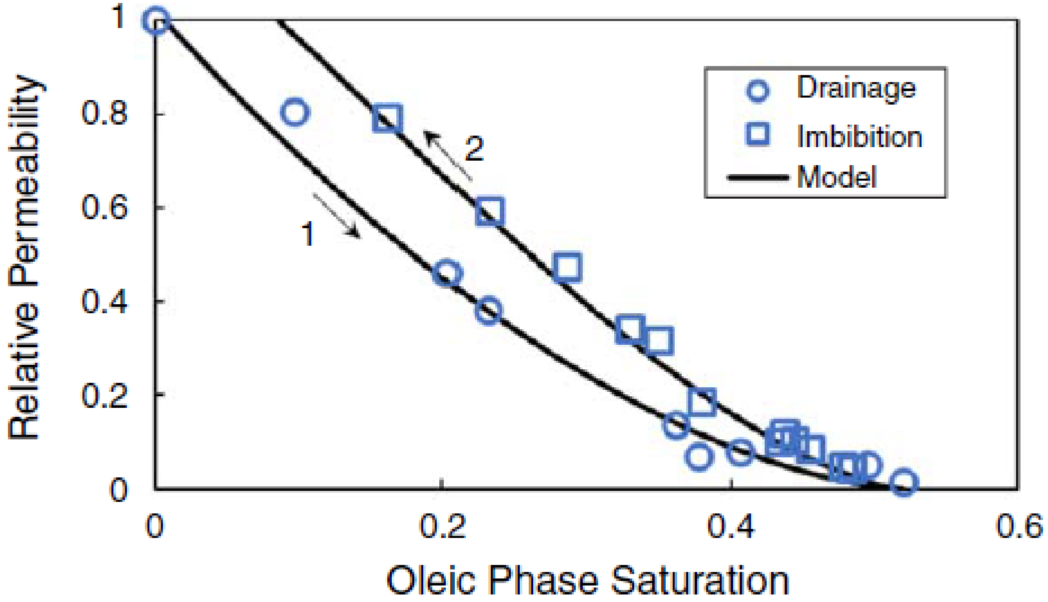

Application: Wettability

Pore scale

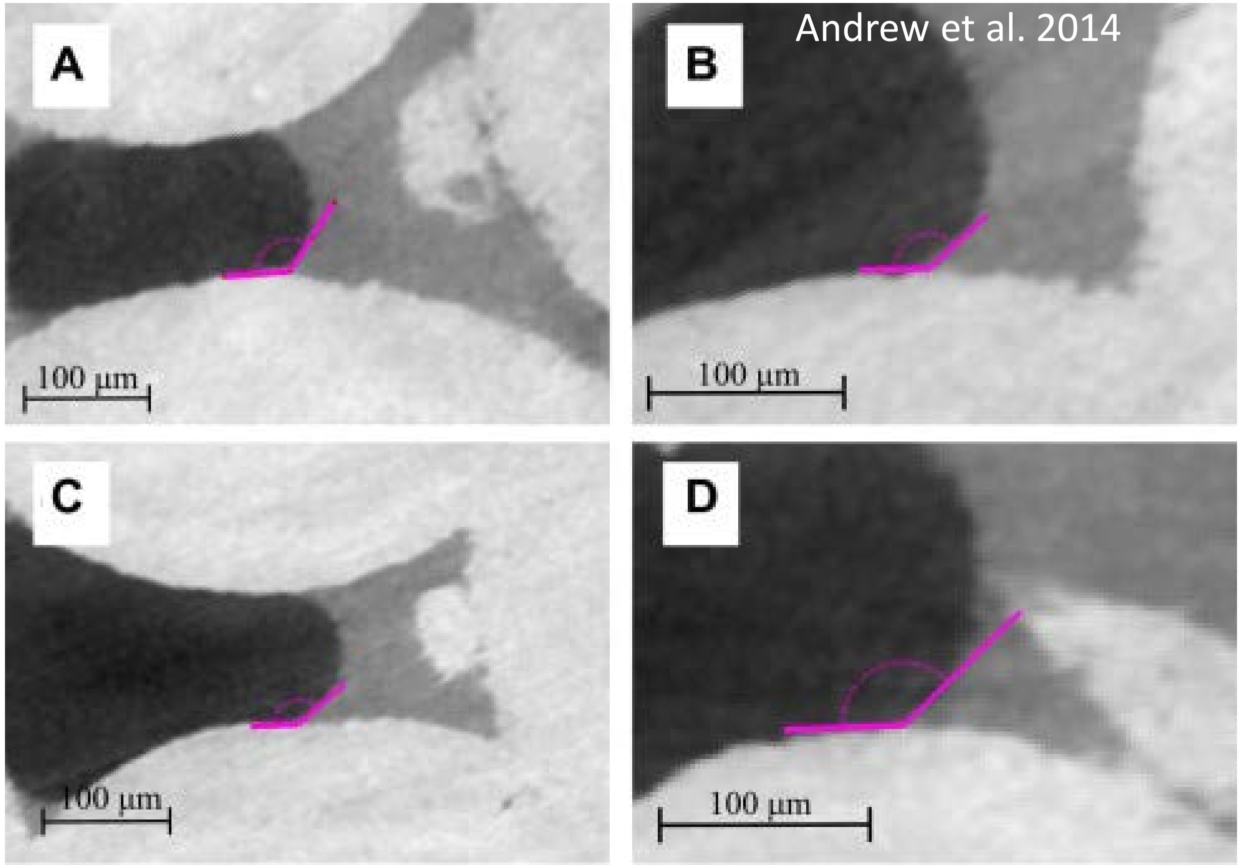

Andrew et al. 2014

Effective contact angle ≠ intrinsic contact angle

(Intrinsic contact angle ~ surface energy)

Darcy-SCAL scale

via capillary pressure curve

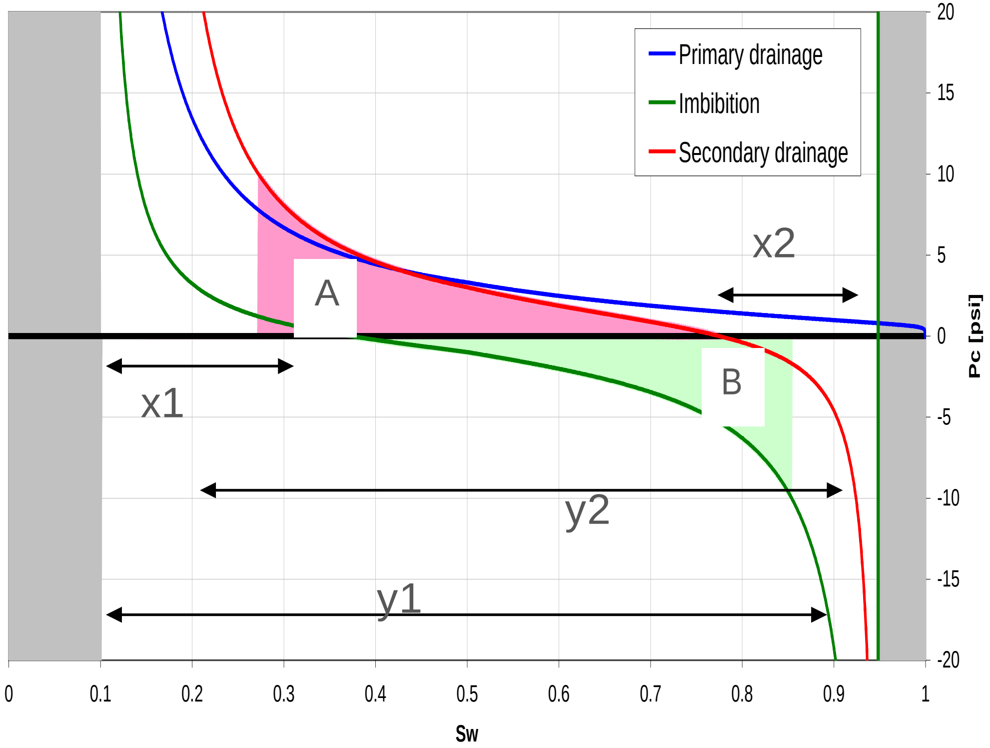

Prodanovic, M., Lindquist, W.B., Seright, S.R.: Residual fluid blobs and contact angle measurements from X-ray images of fluid displacement. In: XVI International Conference on Computational Methods in Water Resources, Copenhagen, Denmark (2006)

Contact Angle from Deficit Curvature

Gauss-Bonnet Theorem

$$\int_S [1/(r_1 r_2)]ds + \boxed{\int_B k_g dl} = 2\pi\chi(S)$$

Total geodesic curvature along the contact line

Deficit Curvature, k_d

Macroscopic contact angle $$\theta_{macro} = \frac{\kappa_d}{4N_c}$$

Sessile Drop

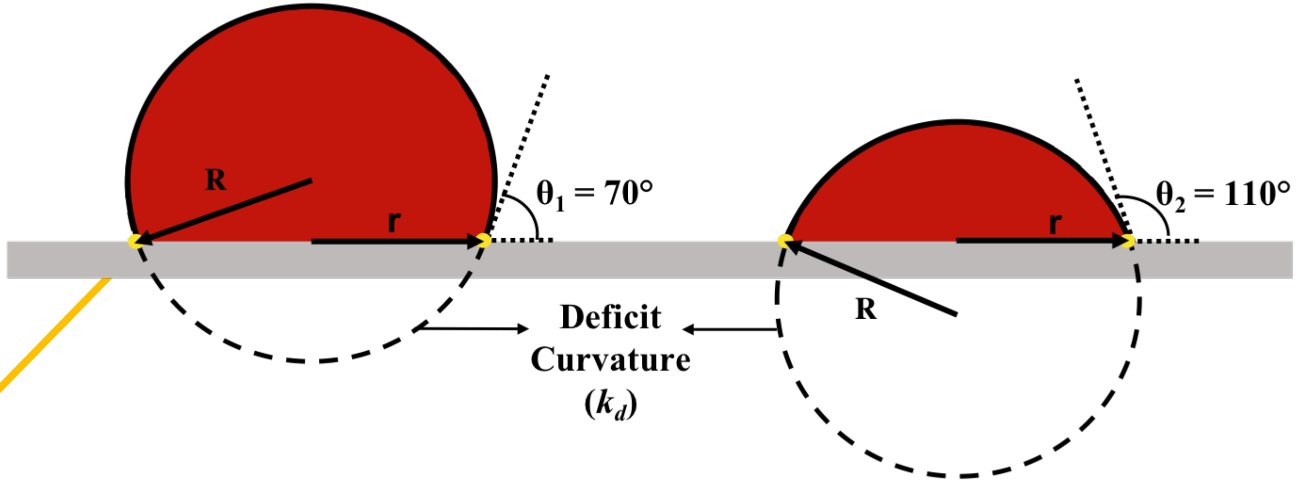

3D Oil Cluster

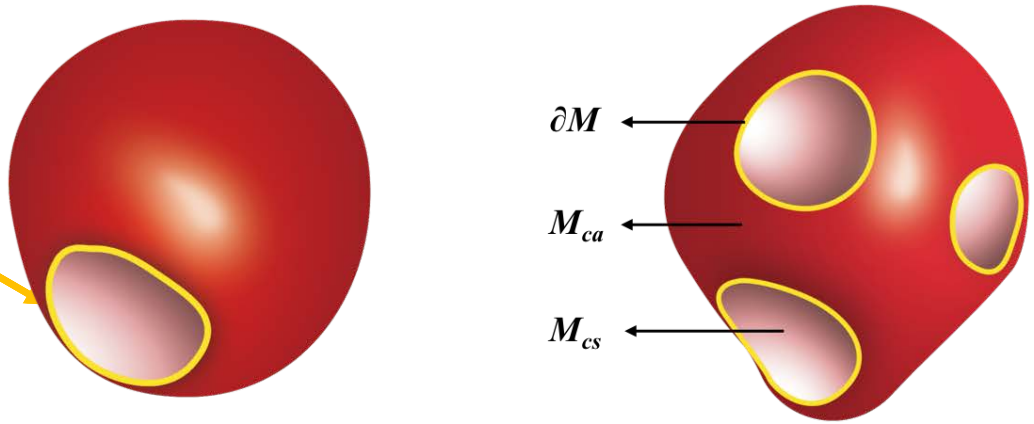

Contact Angle = Deficit Curvature

Armstrong et al. *under review*

Gaussian curvature

Geodesic curvature

Gauss Bonnet Theorem

$$2\pi\chi(M) = \int_M \kappa_T dS + \int_{\partial M} \kappa_g dC$$

For each region:

Fluid-Fluid

$$2\pi\chi(M_{ab}) = \int_{M_{ab}} \kappa_T dS + \int_{\partial M_{ab}} \kappa_g dC,$$

Fluid-solid

$$2\pi\chi(M_{bs}) = \int_{M_{bs}} \kappa_T dS + \int_{\partial M_{bs}} \kappa_g dC.$$

$$\begin{aligned} 4\pi\chi(C) &= 2\pi\chi(M_{ab}) + 2\pi\chi(M_{bs}) \\ &= \int_{M_{ab}} \kappa_T dS + \int_{M_{bs}} \kappa_T dS + \int_{\partial M} (\kappa_{g_{ab}} + \kappa_{g_{bs}}) dC \end{aligned}$$

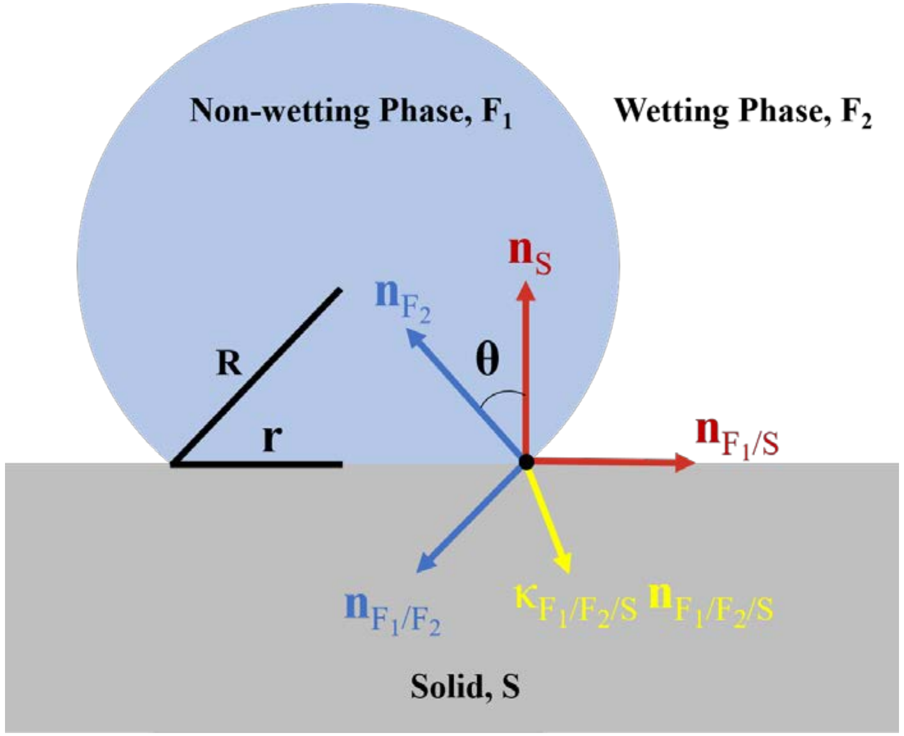

Contact Angle = Deficit Curvature

Armstrong et al. *under review*

$$k_d = 4\pi\chi(C) - \kappa_{ab}A_{ab} - \kappa_{bs}A_{bs}$$

$$\begin{aligned} 4\pi\chi(C) &= 2\pi\chi(M_{ab}) + 2\pi\chi(M_{bs}) \\ &= \int_{M_{ab}} \kappa_T dS + \int_{M_{bs}} \kappa_T dS + \int_{\partial M} (\kappa_{g_{ab}} + \kappa_{g_{bs}}) dC \end{aligned}$$

with

$$\kappa_{ab} = \frac{1}{A_{ab}} \int_{M_{ab}} \kappa_T dS,$$

$$\kappa_{bs} = \frac{1}{A_{bs}} \int_{M_{bs}} \kappa_T dS,$$

$$k_d = \int_{\partial M} (\kappa_{g_{ab}} + \kappa_{g_{bs}}) dC = \int_{\partial M} \kappa_{abs} \mathbf{n}_{abs} \cdot [\mathbf{n}_S \sin\theta + \mathbf{n}_{bs}(1-\cos\theta)] dC$$

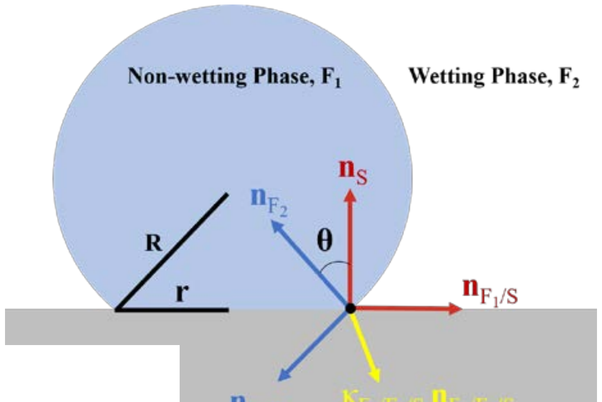

For N_c contacts with solid

$$k_d = \sum_{j=1}^{N_c} \int_{\partial M_j} \kappa_{abs} \mathbf{n}_{abs} \cdot [\mathbf{n}_S \sin\theta + \mathbf{n}_{bs}(1-\cos\theta)] dC$$

Macroscopic contact angle $\theta^{macro} = \frac{k_d}{4N_c}$

Number of contacts N_c

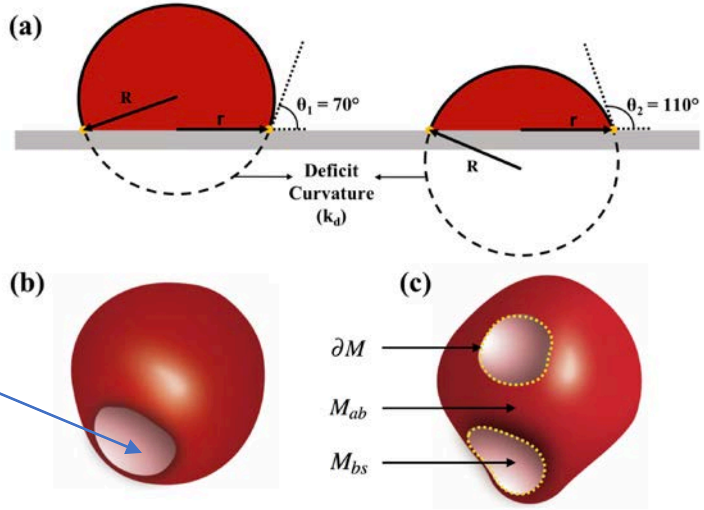

Contact Angle = Deficit Curvature

Armstrong et al. *under review*

Macroscopic contact angle $\theta^{macro} = \dfrac{k_d}{4N_c}$

For 1 sessile droplet:

$$\kappa_{g_{ab}} = -\sqrt{1-(r/R)^2}/r \qquad \kappa_{g_{bs}} = 1/r$$

$$r = R\sin\theta.$$

$$\begin{aligned} k_d &= \int_{\partial M} \frac{1}{r}\left(1-\sqrt{1-(r/R)^2}\right) dC \\ &= 2\pi\left(1-\sqrt{1-(R\sin\theta/R)^2}\right) \\ &= 2\pi(1-\cos\theta). \end{aligned}$$

$$\theta^{macro} = \frac{\pi(1-\cos\theta)}{2}$$

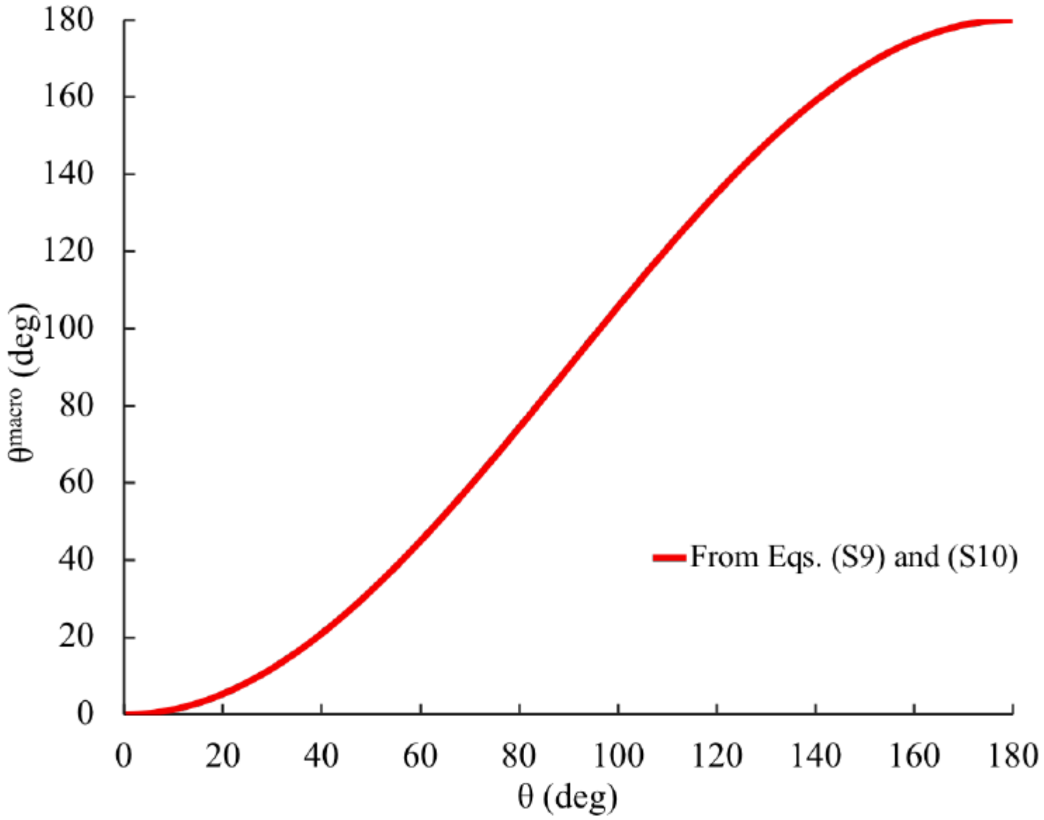

Contact Angle = Deficit Curvature

Armstrong et al. *under review*

Macroscopic contact angle $\theta^{macro} = \frac{k_d}{4N_c}$

For 1 sessile droplet:

$$\kappa_{g_{ab}} = -\sqrt{1-(r/R)^2}/r \qquad \kappa_{g_{bs}} = 1/r$$

$$r = R\sin\theta.$$

$$\begin{aligned} k_d &= \int_{\partial M}\frac{1}{r}\left(1-\sqrt{1-(r/R)^2}\right)dC \\ &= 2\pi\left(1-\sqrt{1-(R\sin\theta/R)^2}\right) \\ &= 2\pi(1-\cos\theta). \end{aligned}$$

$$\theta^{macro} = \frac{\pi(1-\cos\theta)}{2}$$

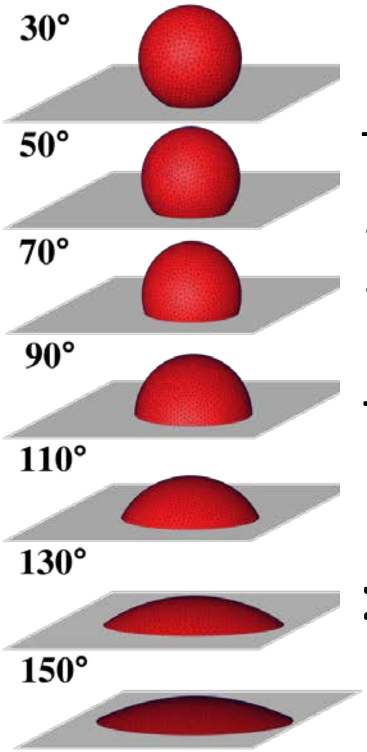

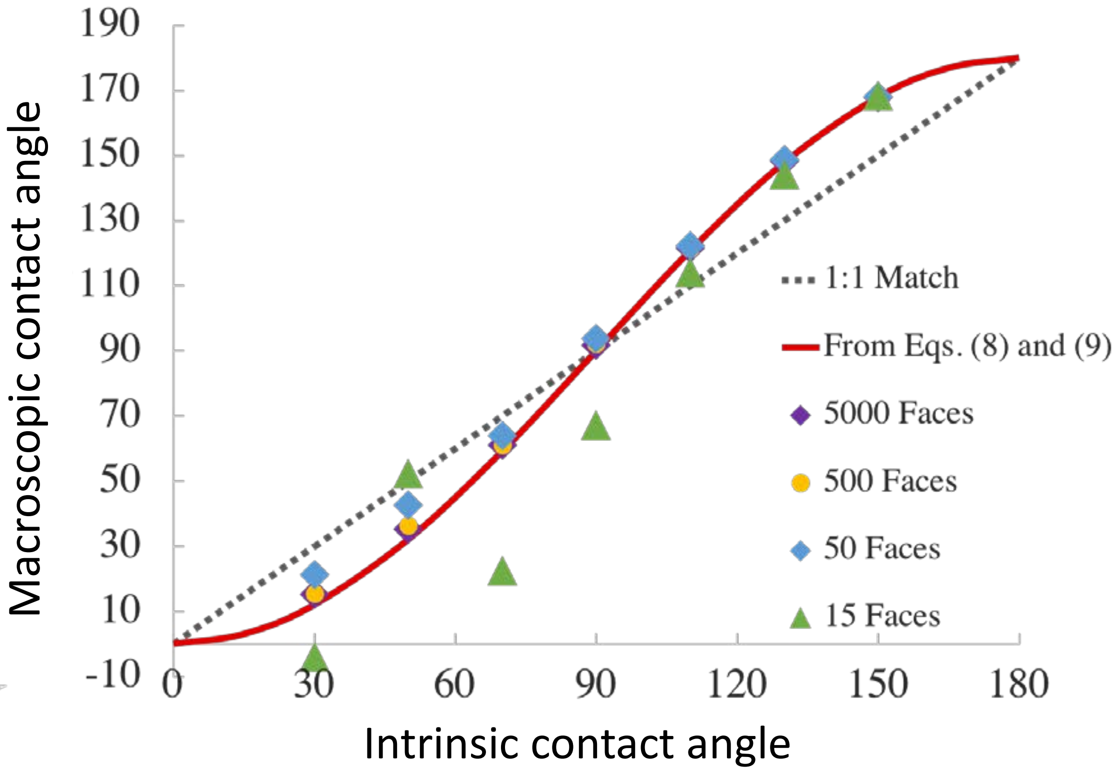

Validation: Advancing and Receding Contact angle

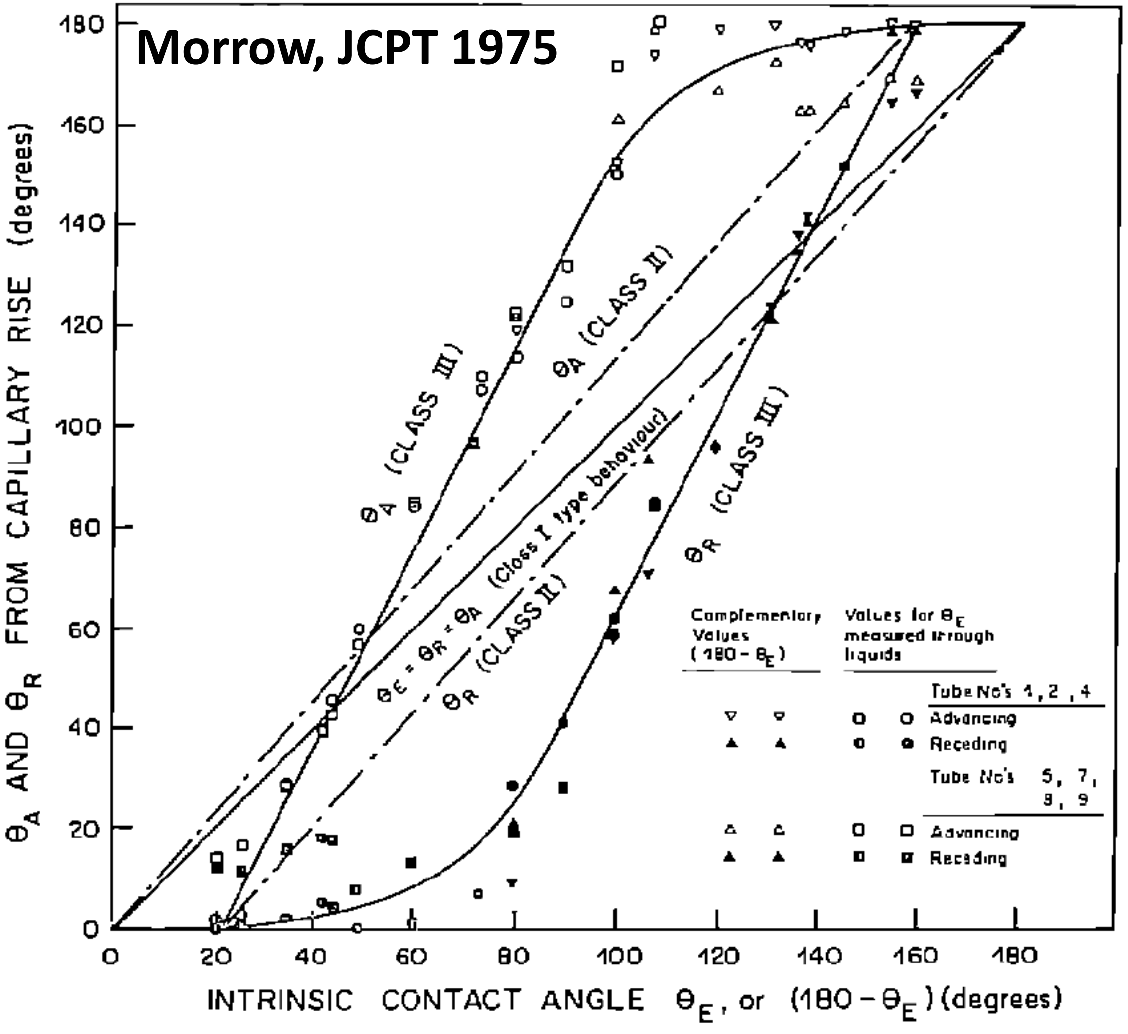

Morrow, JCPT 1975

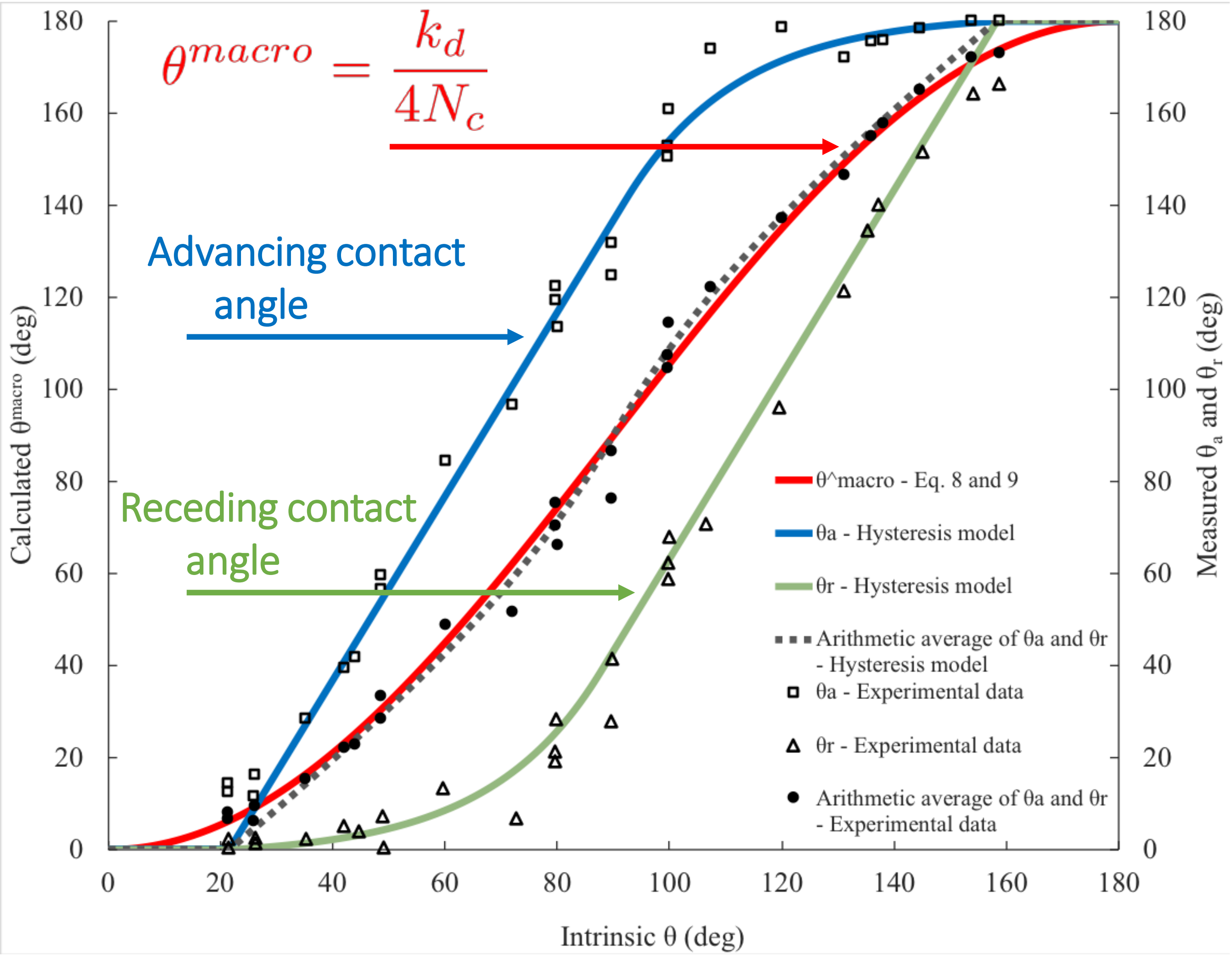

$$\theta^{macro} = \frac{k_d}{4N_c}$$

Advancing contact angle

Receding contact angle

Armstrong et al. *under review*

Predicting Contact Angle

from oil cluster distribution & $p_c(S_w)$

→ SCA009 (Tuesday, 9:30)

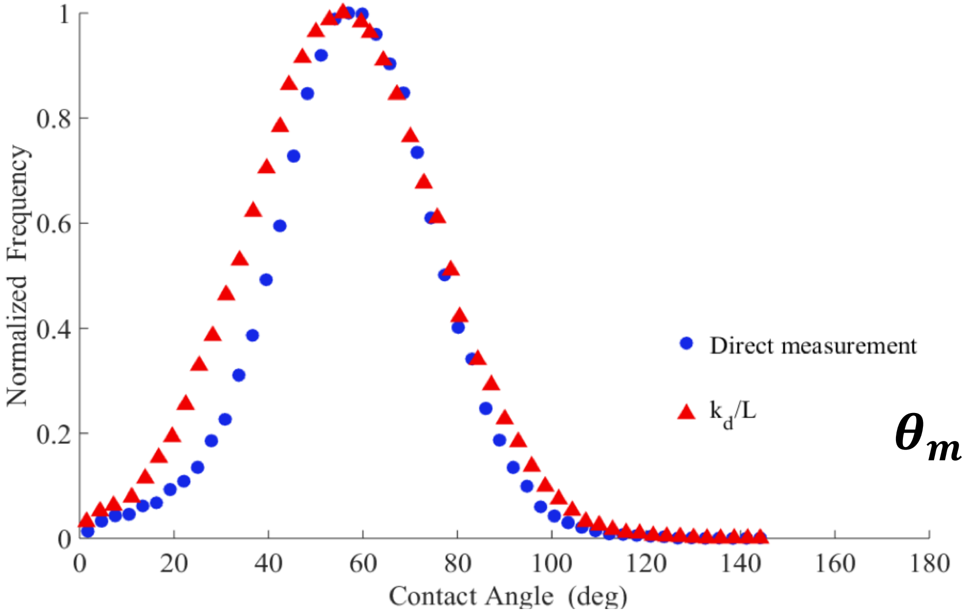

$$\theta_{macro} = \frac{\kappa_d}{4N_c}$$

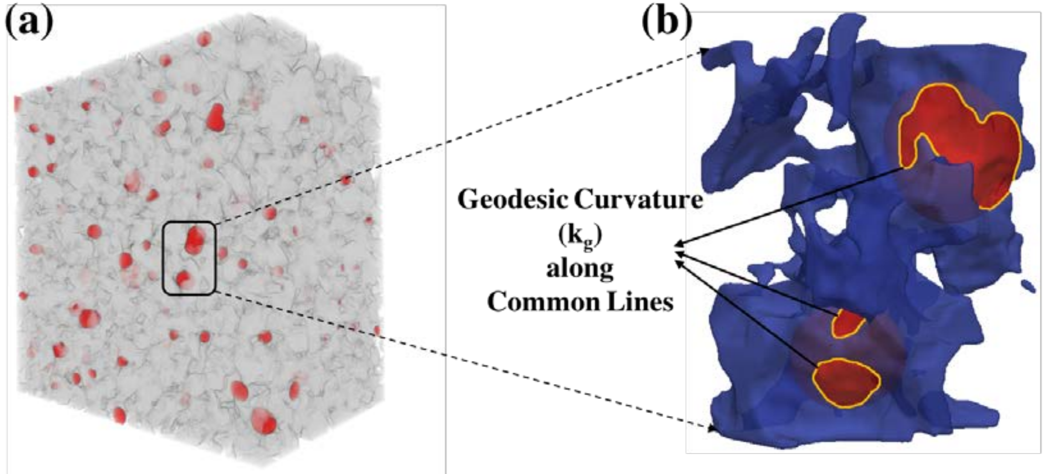

Armstrong et al. *under review*

Sandstone rock

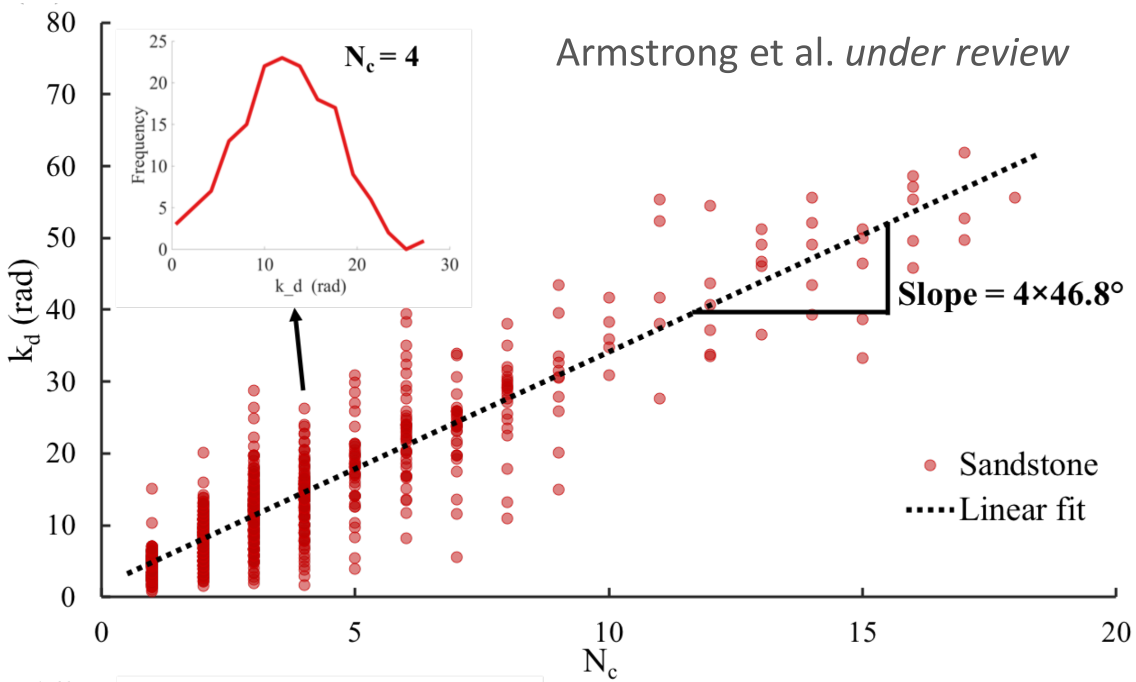

Sintered glass

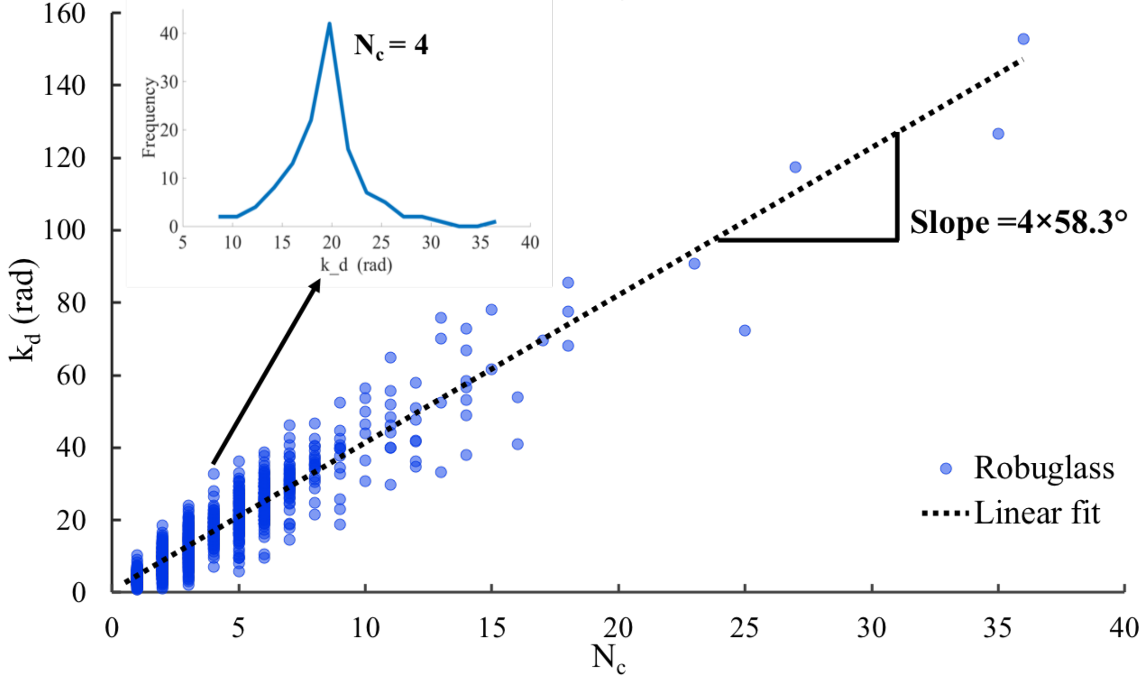

Minerology, Wettability and Topology

QEMSCAN DATA, Pore-Scale Minerology

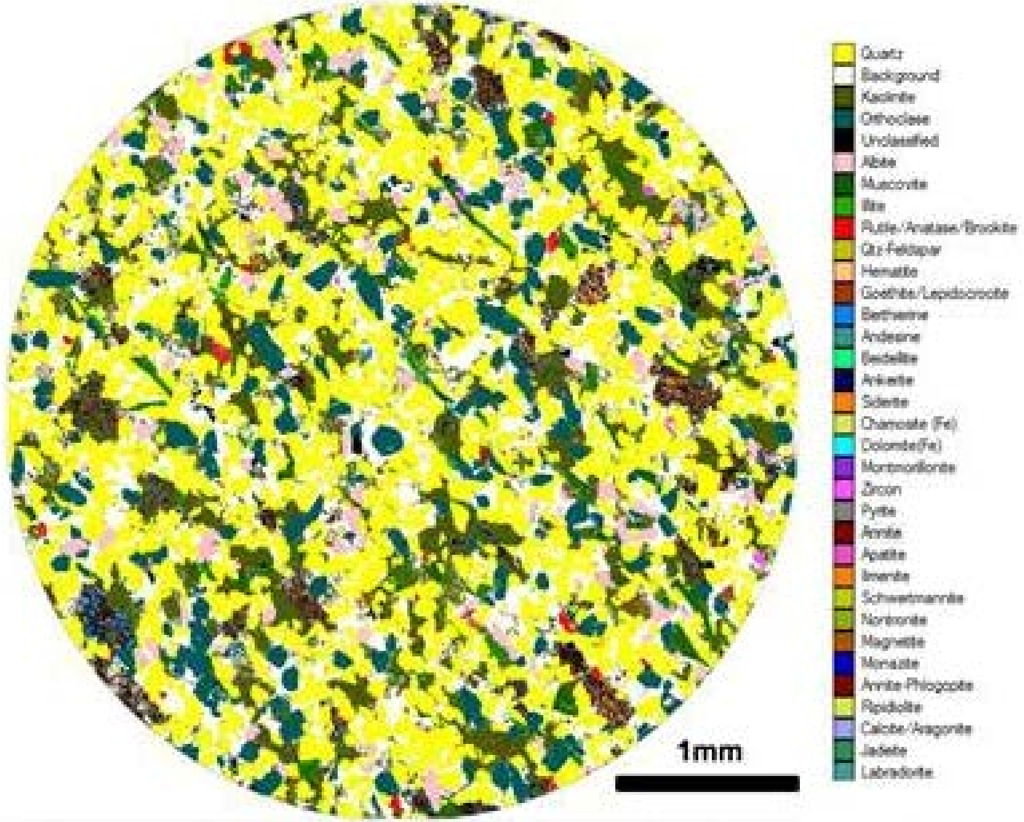

Euler characteristic quantifies impact of wettability on the connectivity of the oil phase

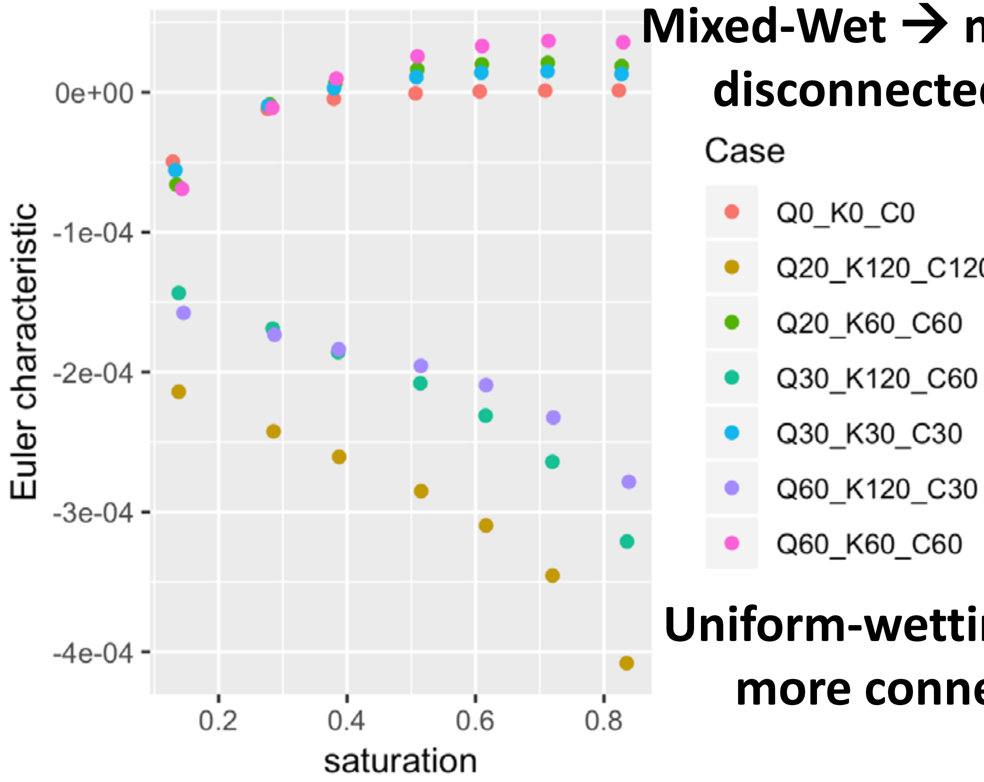

Mixed-Wet → more disconnected clusters

Uniform-wetting → more connected

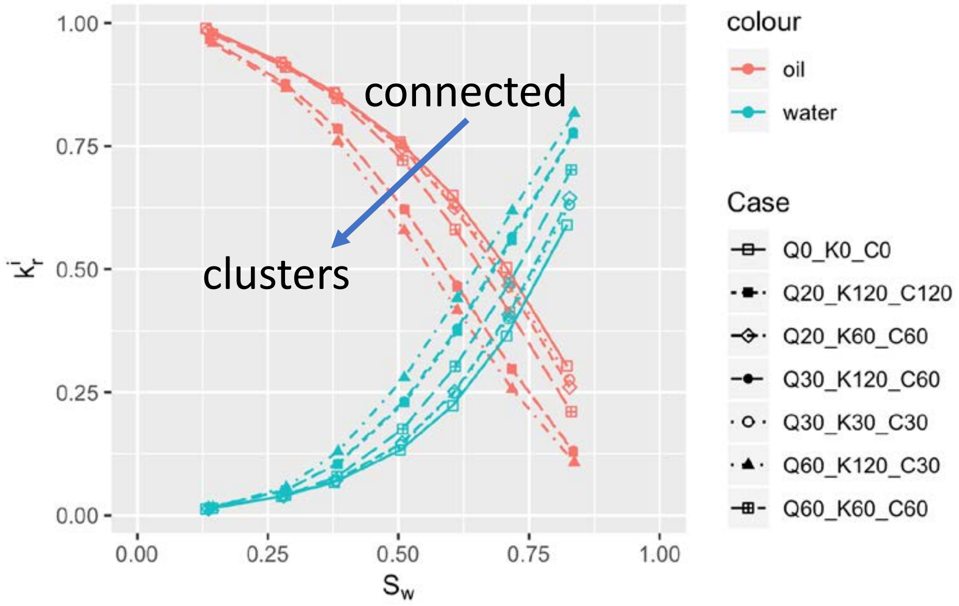

Fractured Porous Media

Original works of Adler (Fractured Porous Media)

PRL, Scholz et al. 2012

Dimensionless Density, ρ’
A measure of the connectivity of the fracture network

Fracture Network

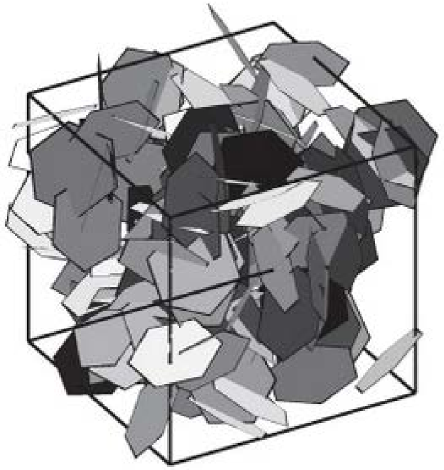

2D Porous Structures

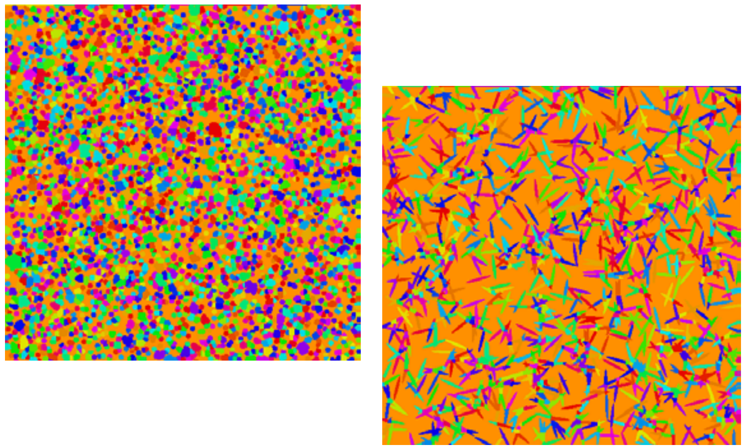

Permeability

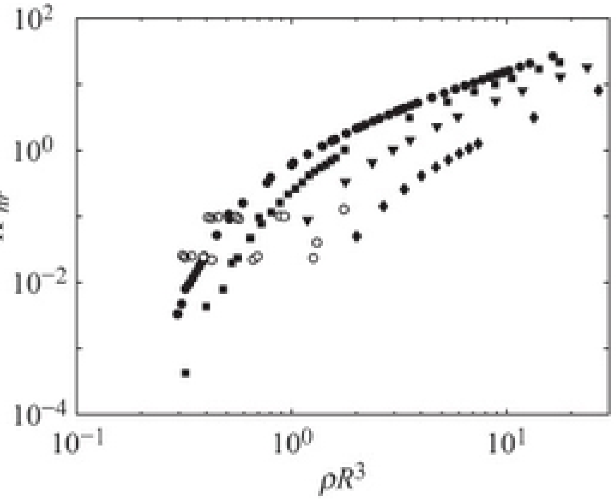

Fracture density x volume

Collapse on single curve

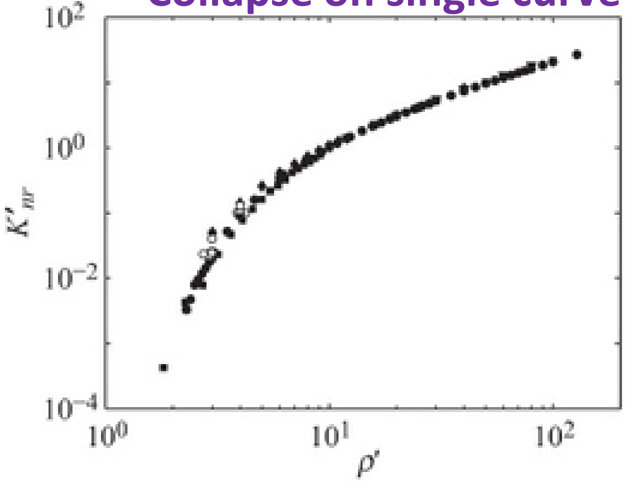

Excluded volume

Single Permeability Curve

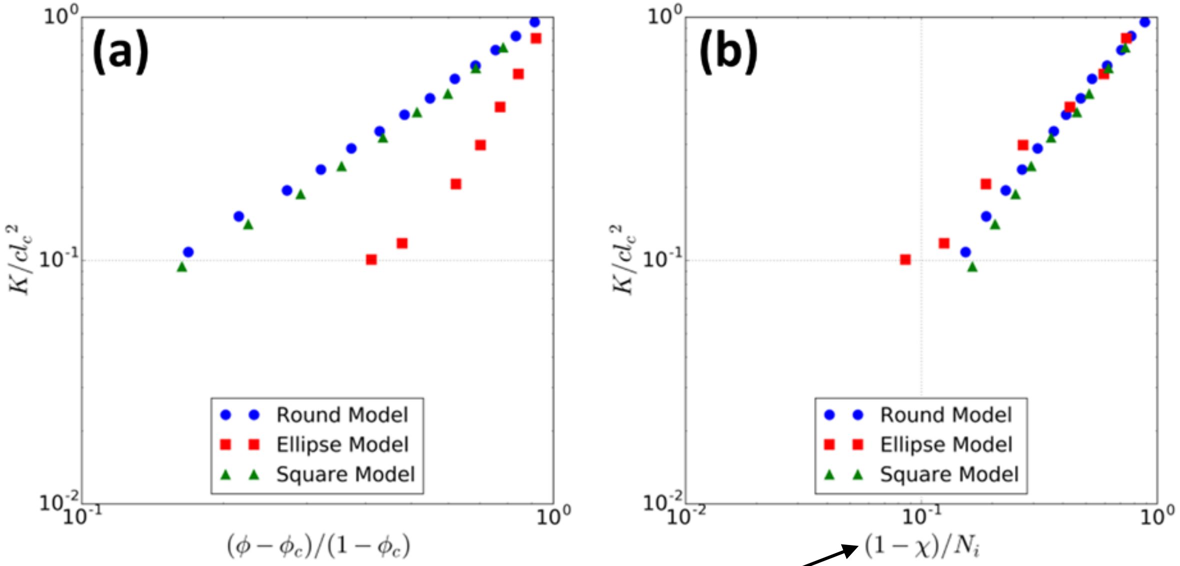

Number of Loops, $B_1 = [(\rho'/2)-1]\rho'$

[LOOPS + OBJECTS] / OBJECTS

Conclusions

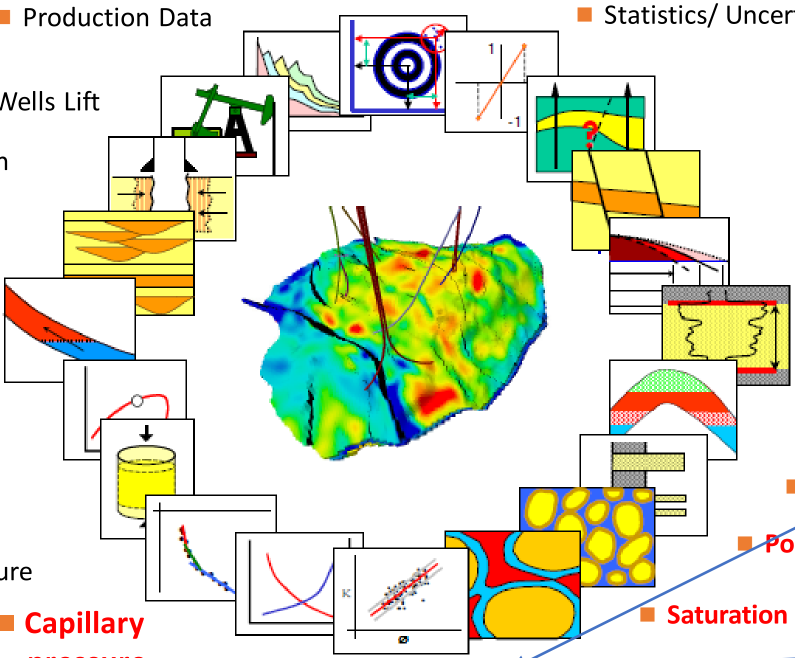

- Production Data
- Wells Lift
- Vells: Skin
- ity
- quifer
- id PVT
- ssibility
- oir pressure
- Statistics/ Uncertainty handling
- Prediction between wells
- Structure
- Reservoir Area
- Gross thickness
- Fluid distribution/contacts
- Net sand
- **Porosity**
- **Saturation**
- **Permeability**
- **Relative permeability**
- **Capillary pressure**

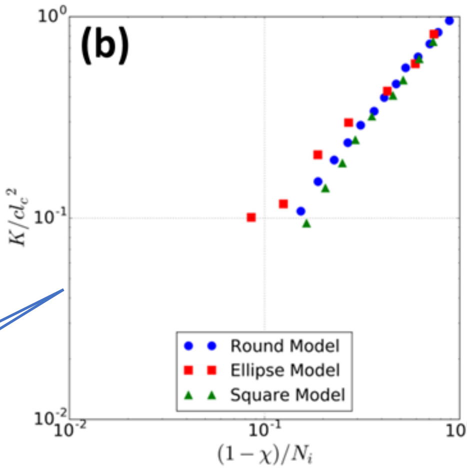

Pc hysteresis

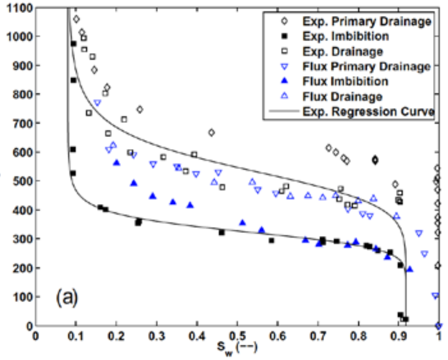

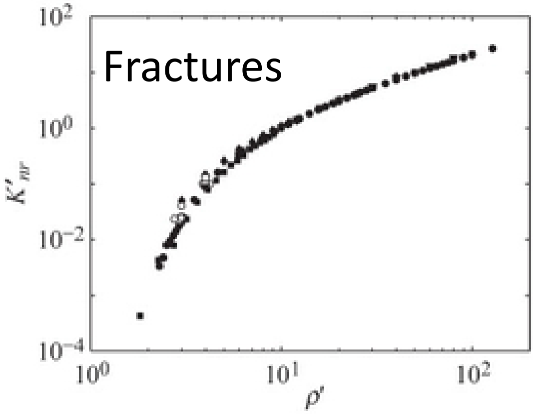

wettability

Relperm hysteresis

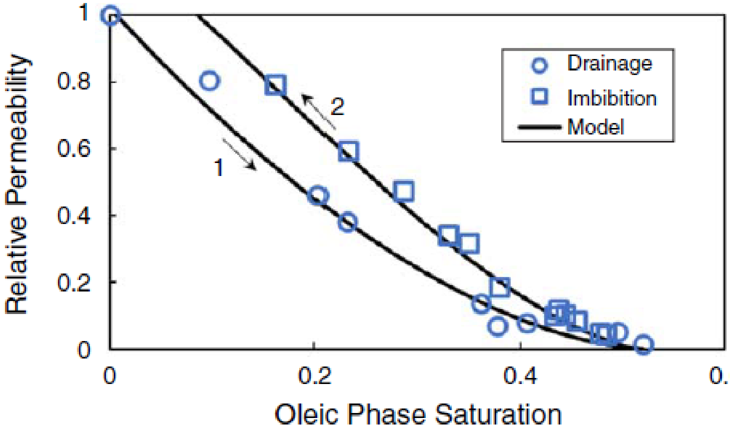

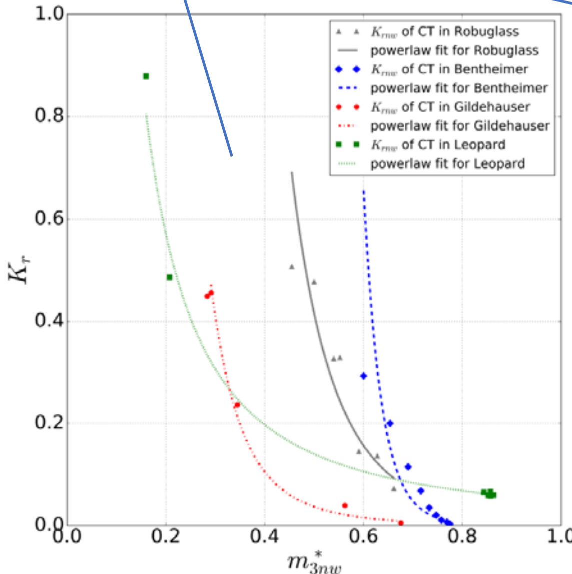

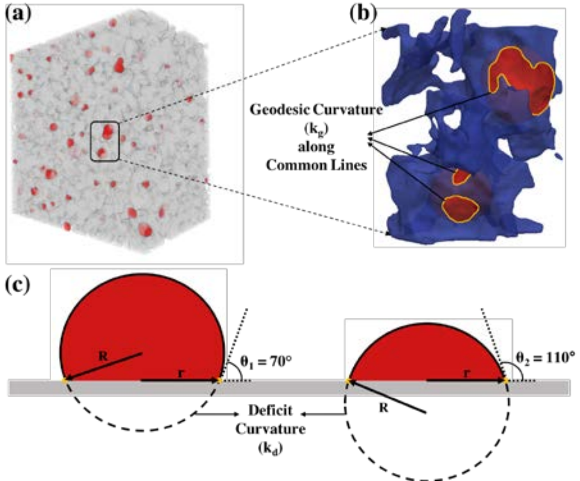

Key Literature

Review Papers and Textbooks

- Porous Media Characterization Using Minkowski Functionals: Theories, Applications and Future Directions Transport in Porous Media, 2018 *in press* doi:10.1007/s11242-018-1201-4
- J. Ohser, F. Mücklich, Statistical analysis of microstructures in materials science, Wiley, 2000.
- Klaus R. Mecke, Dietrich Stoyan, Statistical Physics and Spatial Statistics. The Art of Analyzing and Modeling Spatial Structures and Pattern Formation, Lecture Notes in Physics, Springer, 2000.

Research Papers

- C. H. Arns, M. A. Knackstedt, K. Mecke, 3D Structural Analysis: Sensitivity of Minkowski Functionals. Journal of Microscopy 240, 181-196, 2010.
- H.J. Vogel, U. Weller, S. Schlüter, Quantification of Soil Structure Based on Minkowski Functions, Computers & Geosciences 36, 126-1251, 2010.
- Herring et al. Advances in Water Resources 62, 47-58, 2013.
- S. Schlüter, S. Berg, M. Rücker, R. T. Armstrong, H.-J. Vogel, R. Hilfer and D. Wildenschild, Pore scale displacement mechanisms as a source of hysteresis for two-phase flow in porous media Water Resources Research 52(3), 2194-2205 2016.
- J. E. McClure, R. T. Armstrong, M. A. Berrill, S. Schlüter, S. Berg, W. G. Gray, C. T. Miller A geometric state function for two-fluid flow in porous media, Phys. Rev. Fluids 3(8), 084306, 2018.
- Z. Liu, A. Herring, A. Sheppard, C. Arns, S. Berg, R. T. Armstrong, Morphological characterization of two-phase flow using X-ray microcomputed tomography flow-experiments, Transport in Porous Media 118(1), 99-117, 2017.

Backup

2-Phase Flow in Porous Media

Single-phase

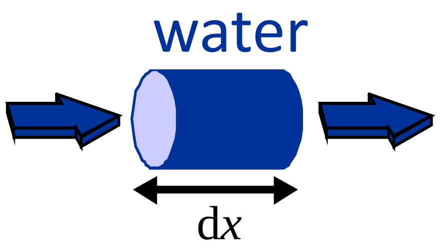

Darcy's law

$$v_{Darcy} = -\frac{K}{\mu}\frac{dp}{dx}$$

Phenomenological extension of Darcy's law i.e. not a law anymore

Multi-phase

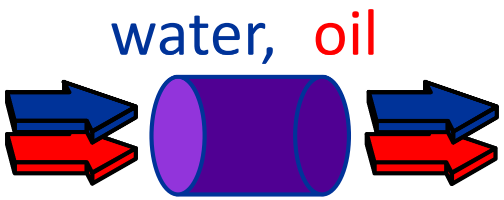

$$v_i = -k_{r,i}\frac{K}{\mu_i}\frac{dp_i}{dx}$$

$$k_{r,i} = k_{r,i}(S_w)$$

$$p_c = p_o - p_w = p_c(S_w)$$

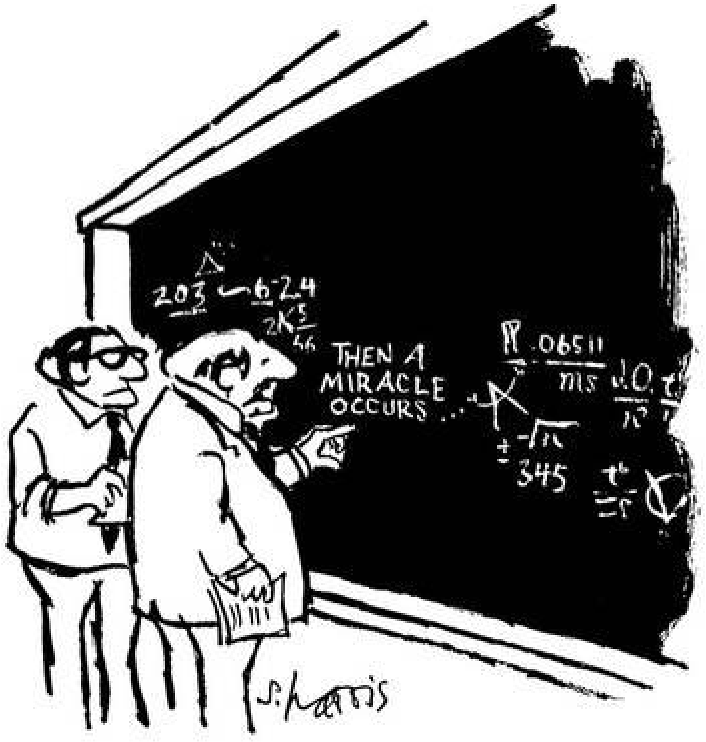

"I think you should be more explicit here in step two."

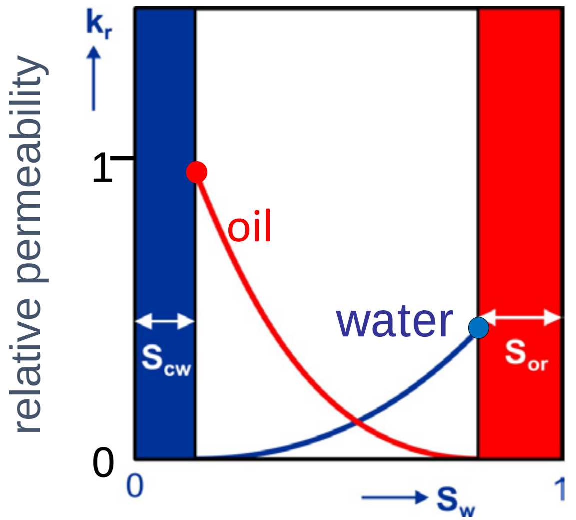

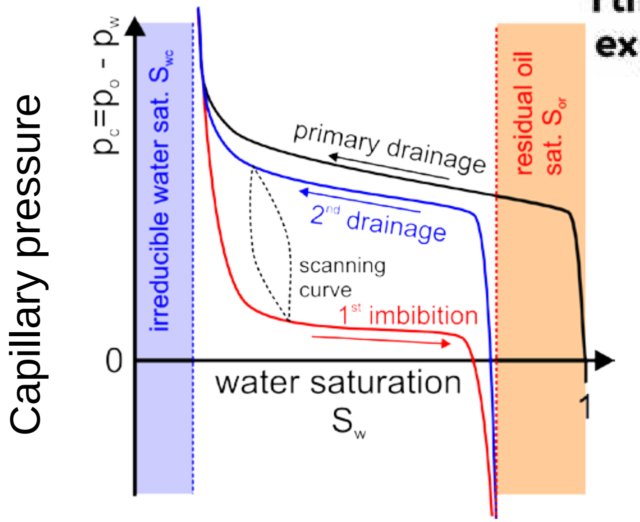

So far this has been sufficient, but

When trying to augment SCAL by Digital Rock, it is important to

- correctly classify the problem

And it becomes inevitable to understand what relative permeability actually is, i.e. face the

- Upscaling from Pore to Darcy Scale challenge

More conceptually.

The State Variables of Capillarity

Integral Geometry

Hadwiger's theorem: unique characterization of 3D objects by 4 Minkowski functionals

m_0 = volume (saturation

$$M_0^n = \lambda(\Omega_n) = \int_{\Omega_n} dr$$

m_1 = interfacial area

$$M_1^n = \lambda(\Gamma_n) = \int_{\Gamma_n} dr$$

m_2 = mean curvature (cap. pressure)

$$M_2^n = \int_{\Gamma_n} \left(\frac{1}{R_1} + \frac{1}{R_2} \right) dr$$

m_3 = integral curvature = $2\pi\chi$

$$M_3^n = \int_{\Gamma_n} \frac{1}{R_1 R_2} dr \ .$$

McClure et al. Phys. Rev. Fluids, 2018

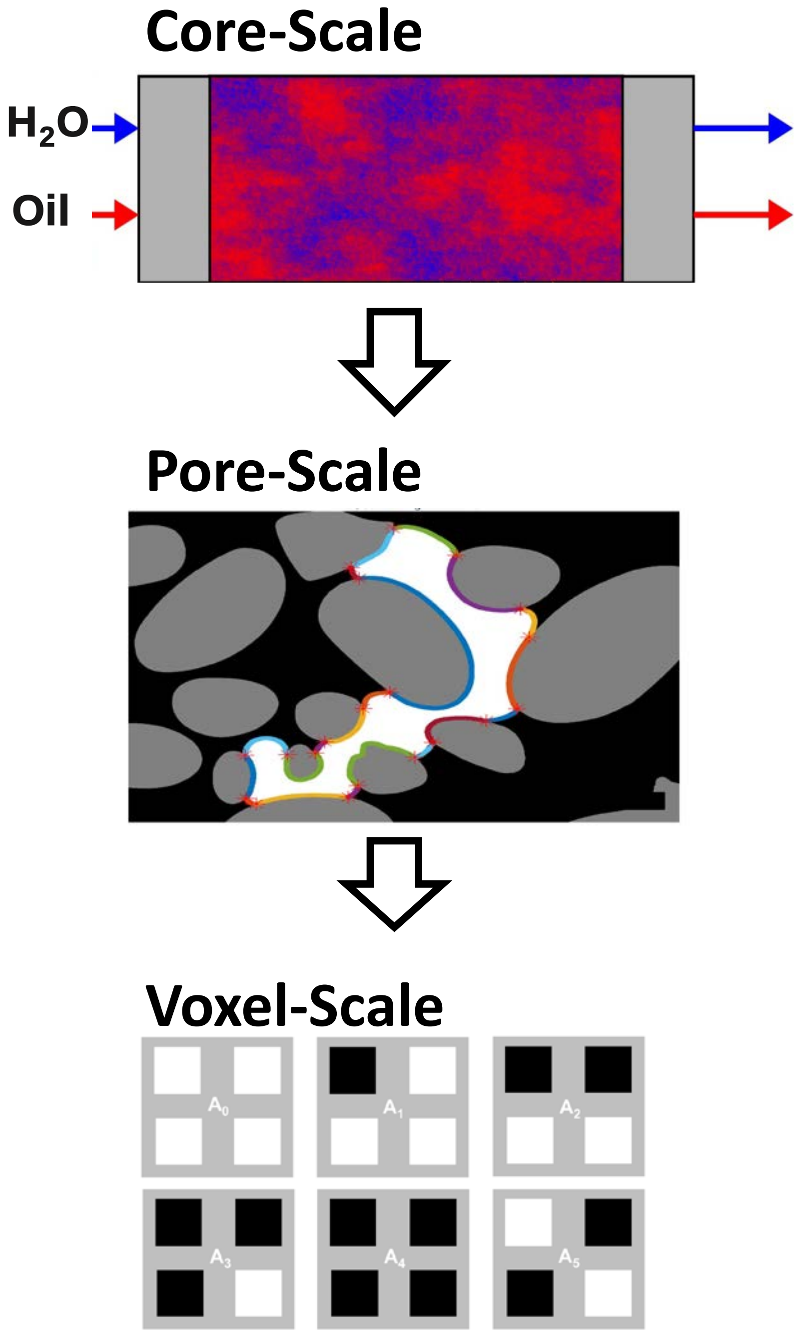

Capillary Pressure vs. Saturation

Capillary Pressure

$$P^c = \gamma J_w^{wn}$$

- P_c-S_w is essentially a geometric definition (or statement)
- Saturation does not uniquely define the geometrical state
- Steiners formula suggests that all four MF are required for a unique definition

MF in terms of macro-scale parameters

$$M_0^n = \epsilon^n V$$

$$M_1^n = (\epsilon^{wn} + \epsilon^{ns})V$$

$$M_2^n = (J_w^{wn}\epsilon^{wn} + J_s^{ns}\epsilon^{ns})V$$

$$M_3^n = \chi^n$$

Cluster Dynamics Introduces Topological Changes

[Rücker et al., GRL, 2015]

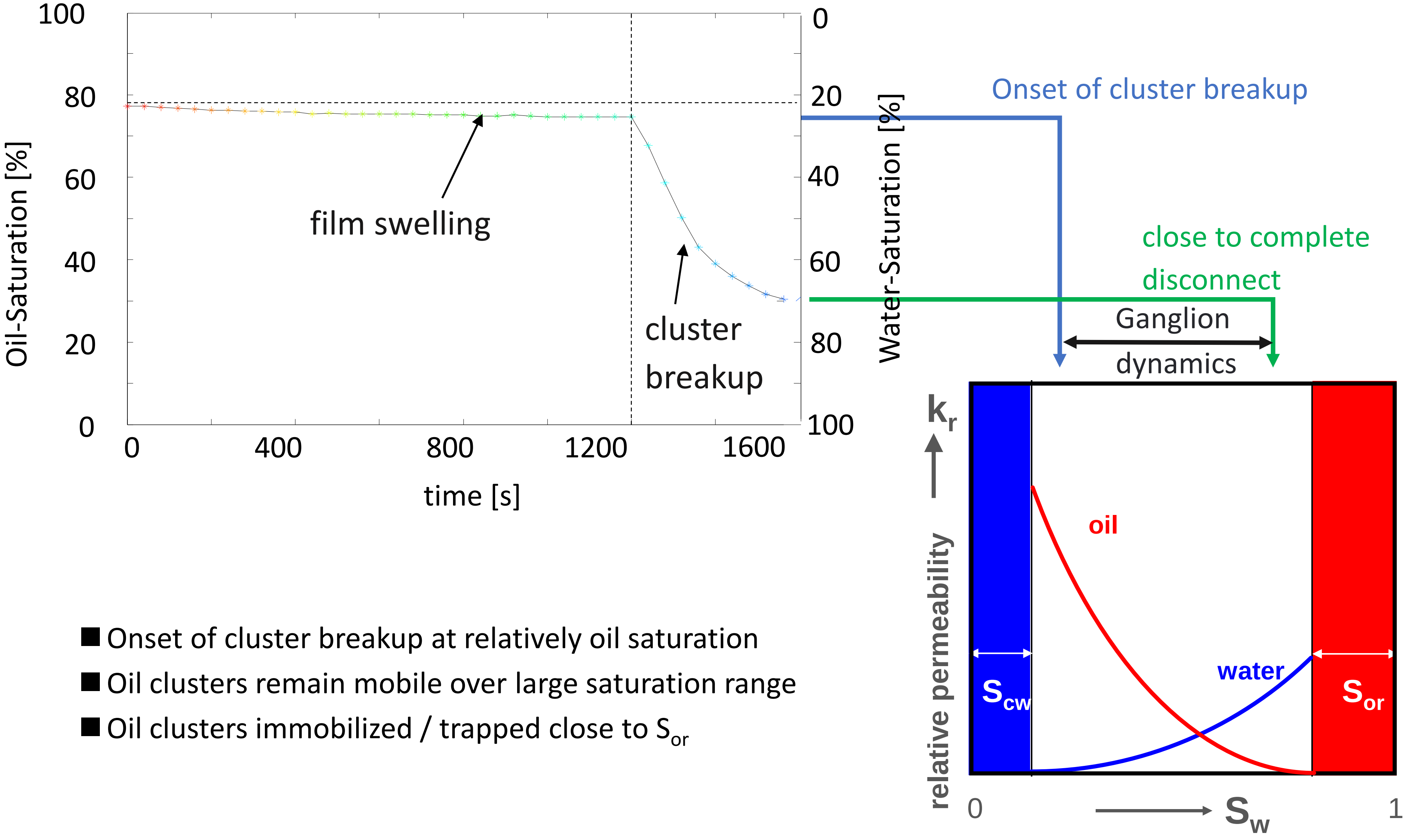

film swelling

cluster breakup

Onset of cluster breakup

close to complete disconnect

Ganglion dynamics

- Onset of cluster breakup at relatively oil saturation
- Oil clusters remain mobile over large saturation range
- Oil clusters immobilized / trapped close to S_{or}

Co-existence of connected pathway flow and ganglion dynamics over most of the mobile saturation range

Characterization of Flow Regimes: Phase Diagrams ...

Independent Variables: regions

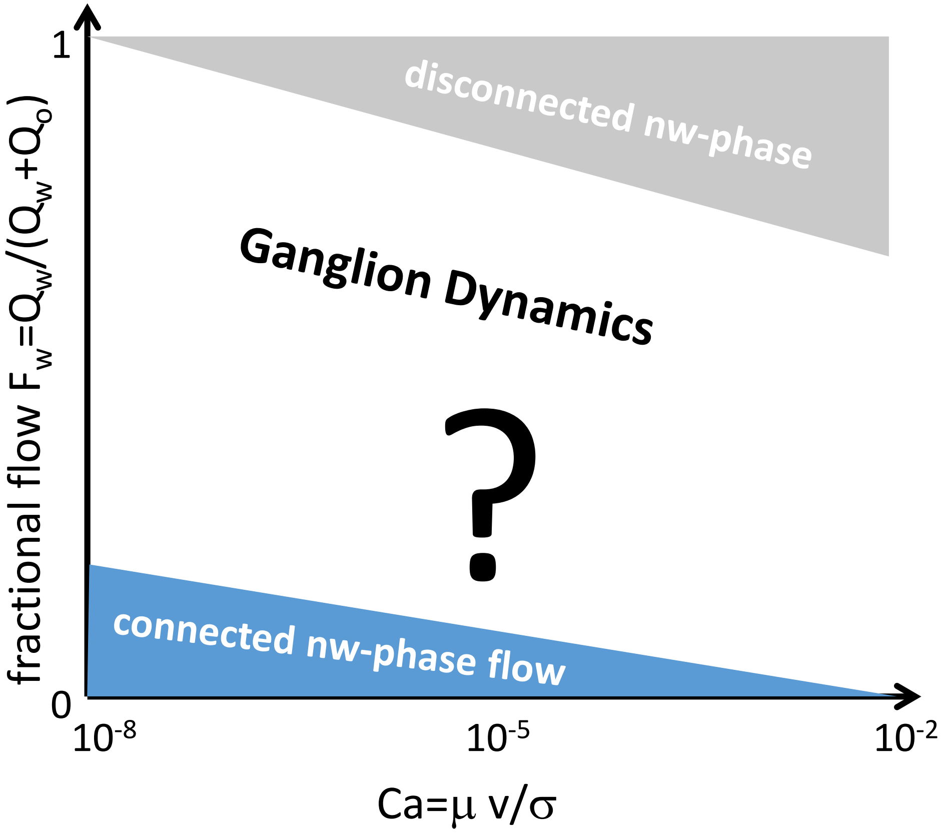

classical

Dependent Variables: trajectories

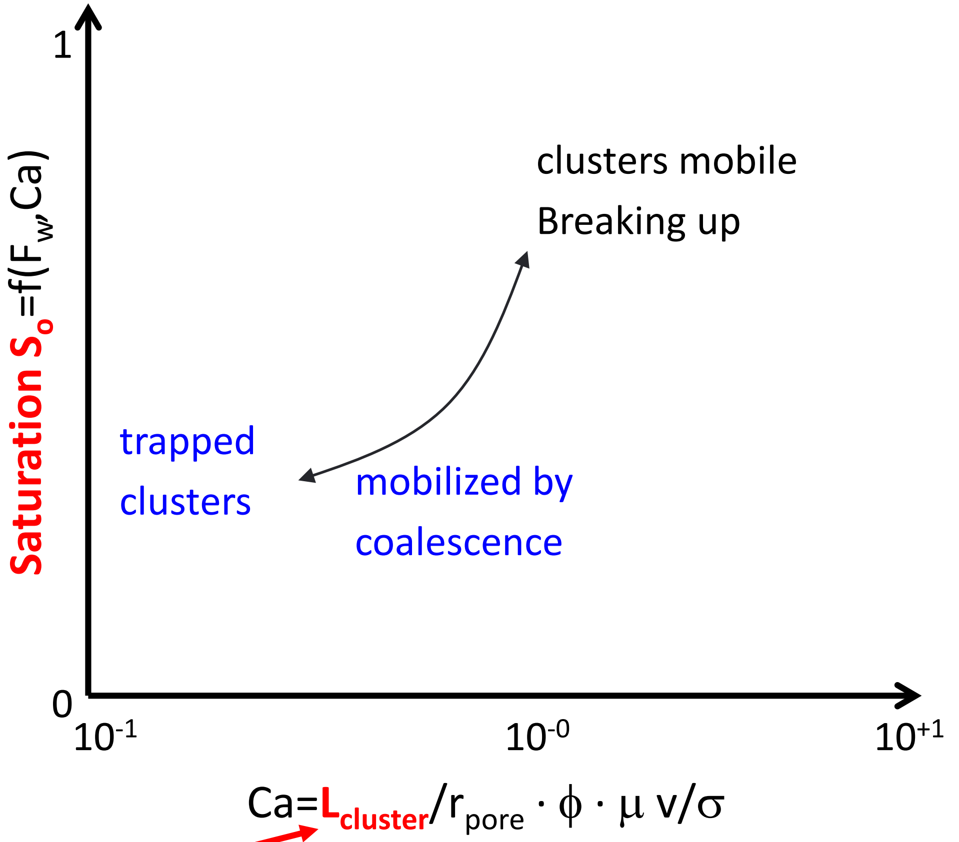

Cluster based [Armstrong, 2014]

State variables

(at the time we did not know yet that we should have used A_{nw})

Clusters: Growing and Coalescence → χ **de**creases

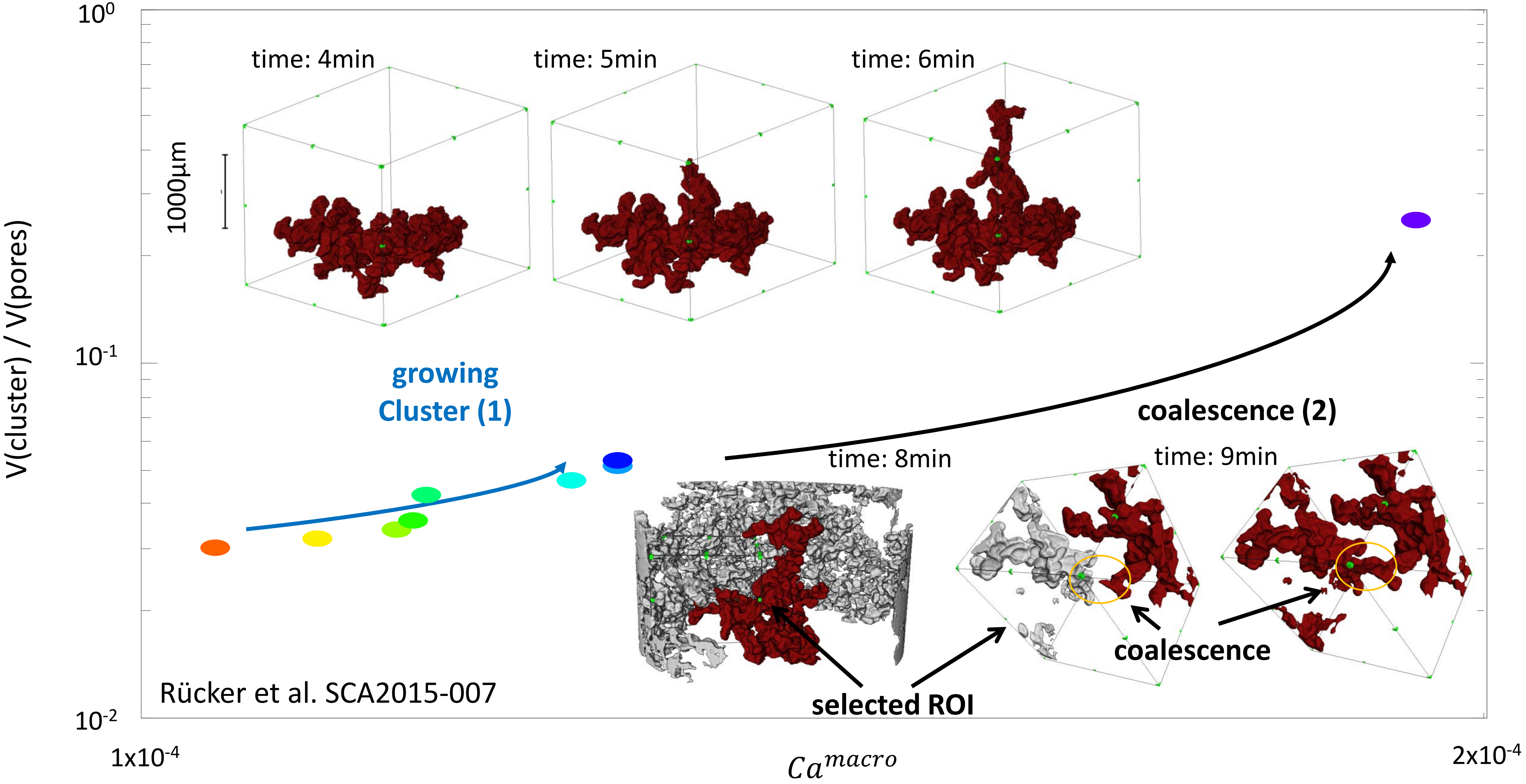

Rücker et al. SCA2015-007

Clusters: Break-up by Snap-off → χ **in**creases

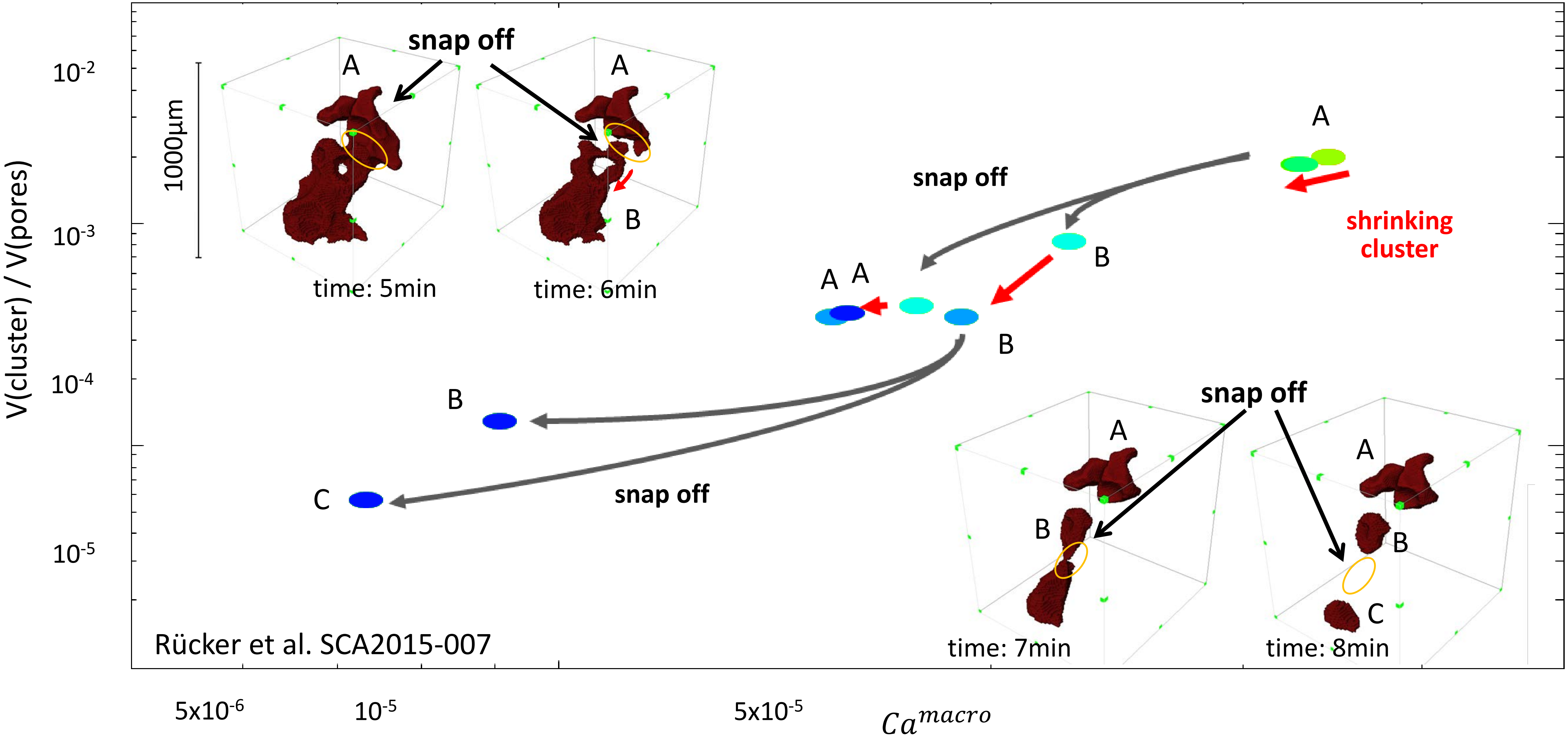

Rücker et al. SCA2015-007

Characterization of Flow Regimes: Phase Diagrams ...

Connected pathway flow

time: 3min

time: 5min

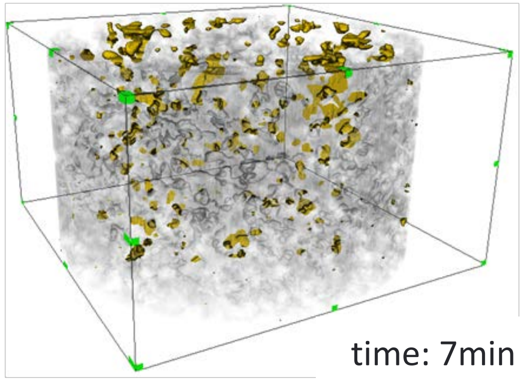

time: 7min

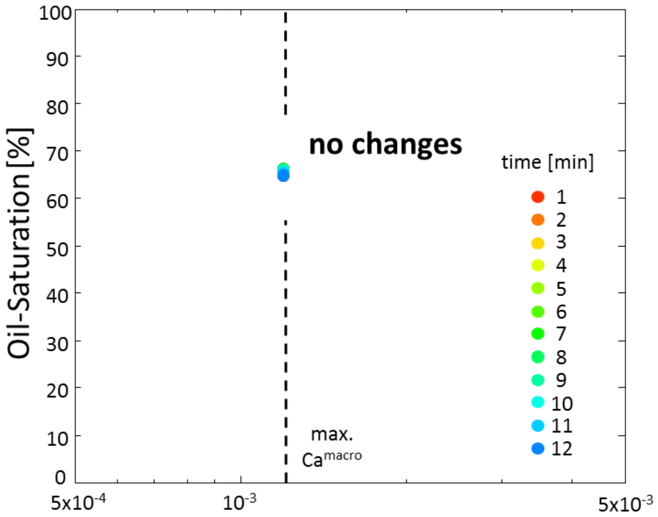

Ganglion dynamics

time: 6min

time: 7min

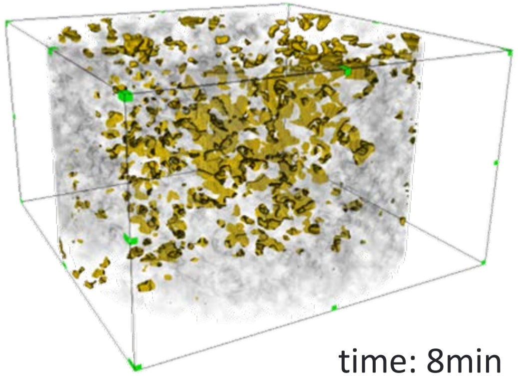

time: 8min

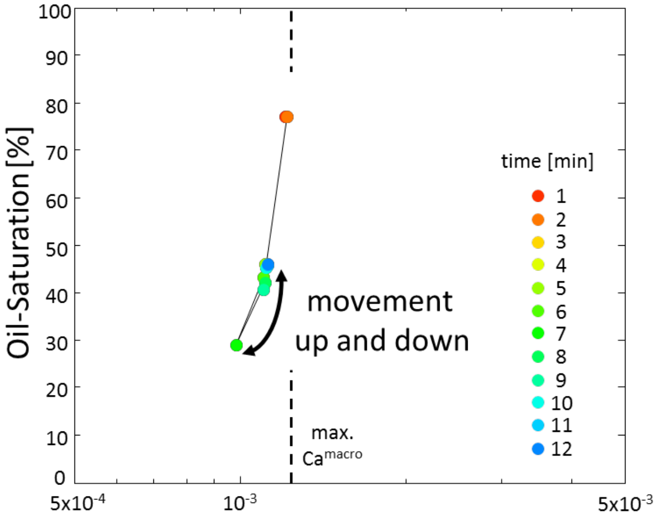

$$Ca_o^{macro} = \frac{l^{cl}}{r^p}\varphi\frac{\mu_w v}{\gamma_{wnw}},$$

Rücker et al. SCA2015-007

Application: Validation of Pore Scale Simulation

Can we obtain imbibition relative permeability from a quasi-static approach ?

morphological approach Becker, J. et al. 2007 ; Hilpert, M. et al. 2001 ; Vogel, H. J. et al. 2005

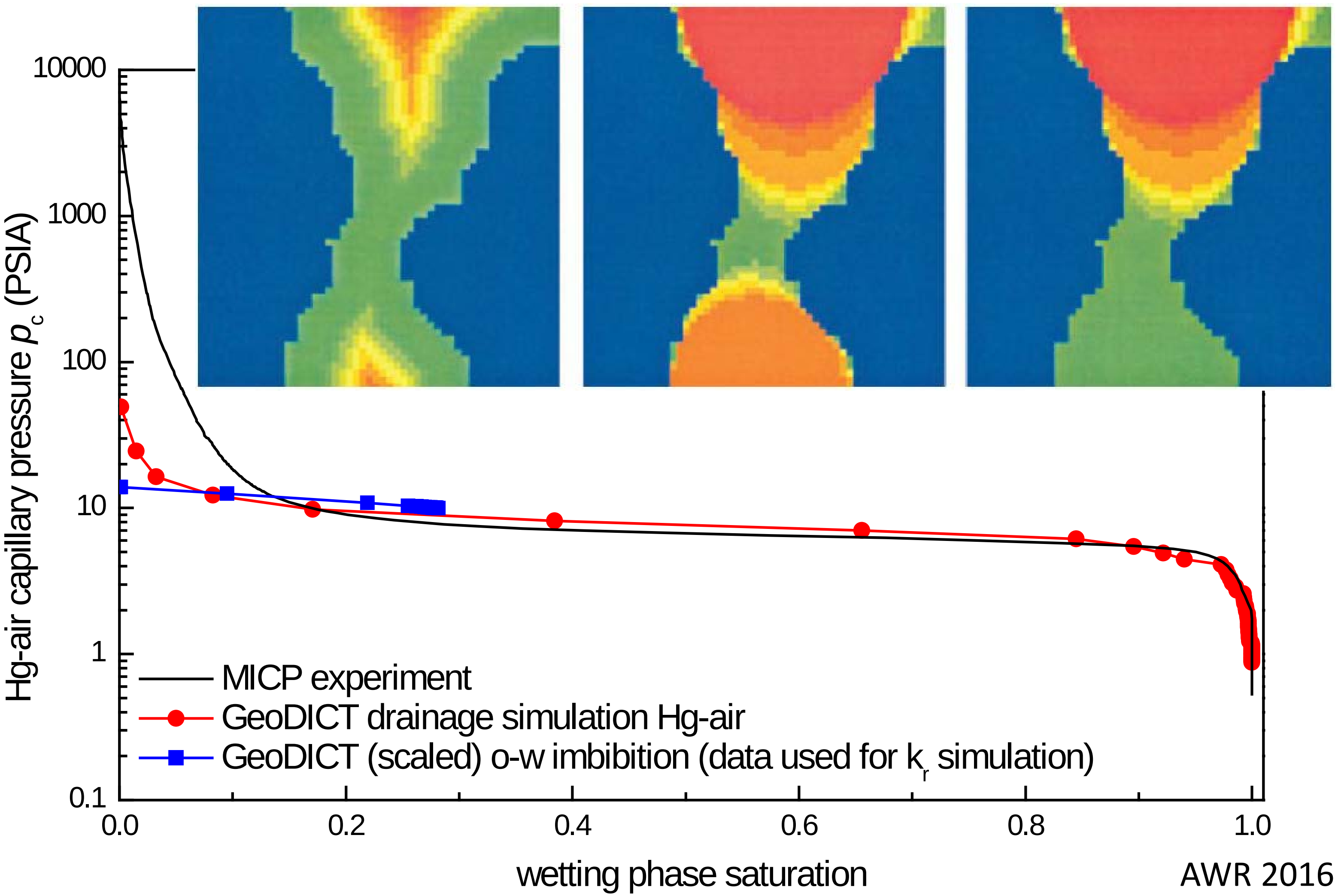

AWR 2016

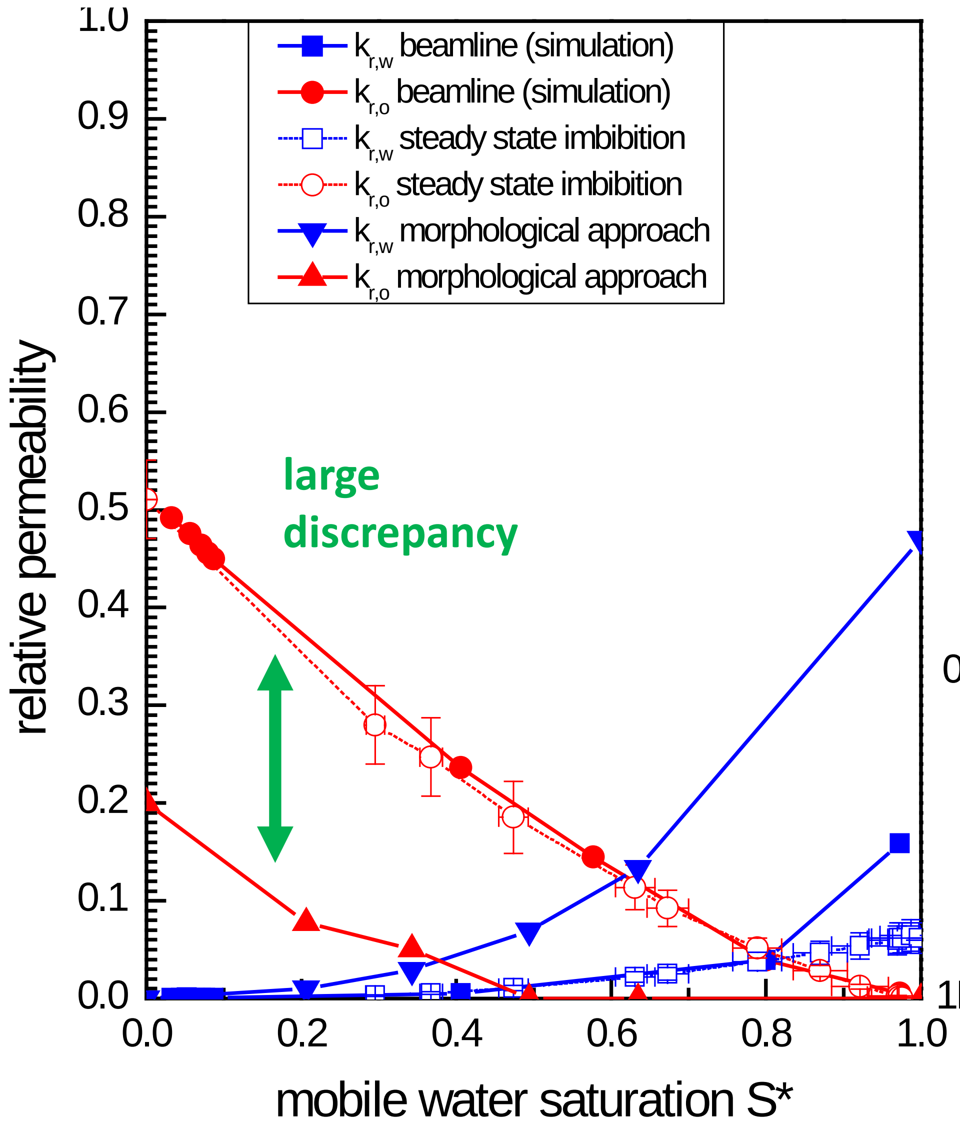

Influence of Wettability on Topology

Dynamic Connectivity → [PNAS, Reynolds et al. 2017]

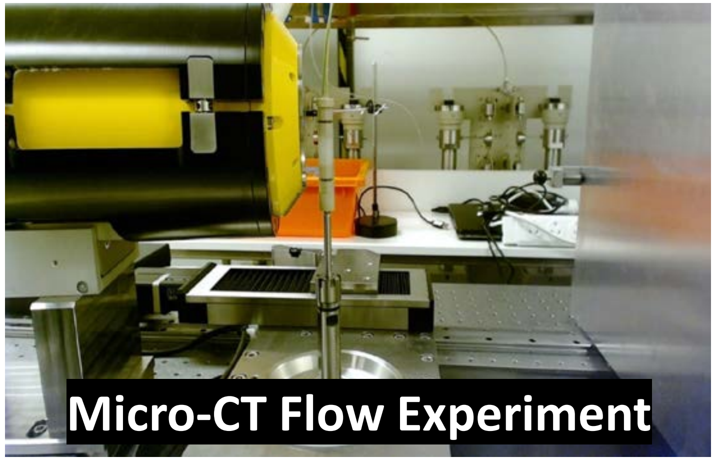

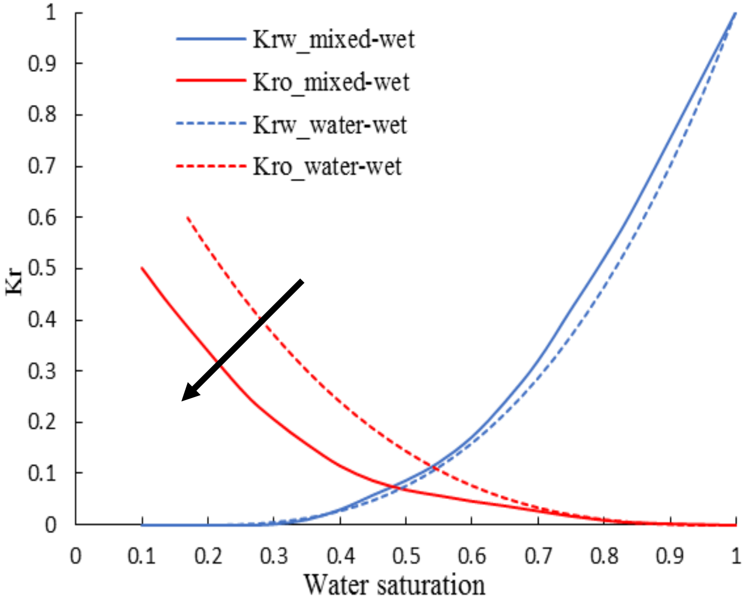

Power Associated with Flow

$$\mathcal{P}_i = \frac{dW}{dt} = -\boldsymbol{q_i} \cdot \nabla p \approx \frac{\mu_i q_i^2}{K_i}$$

Surface Energy of WP/NWP Interface

$$\text{(Surface energy) } E = \frac{\sigma}{l}$$

Tested Two Different Wettabilities

Water Wet: I = 0.72
Mixed-Wet = -0.11

Propensity of Interface Creation

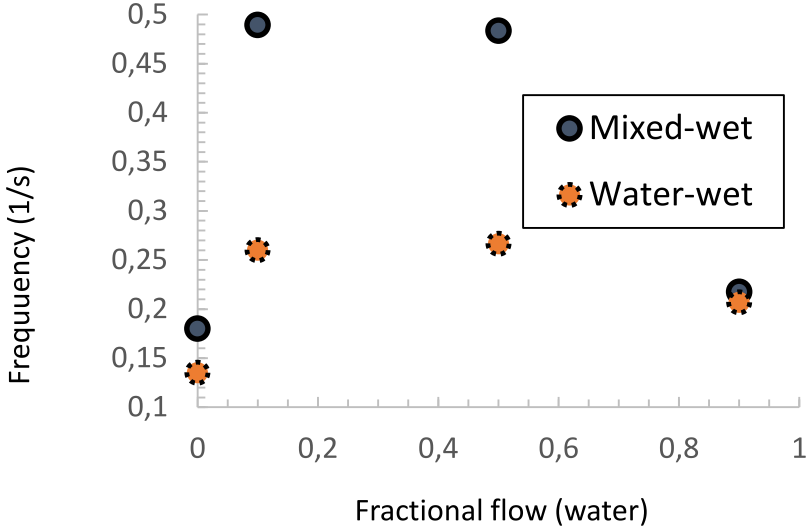

Generation of Unknown Phase